UNIVERSITY OF CALIFORNIA, SAN DIEGO

The influence of density-dependent aggregation characteristics on the population biology of benthic broadcast-spawning gastropods: Pink abalone (*Haliotis corrugata*), red abalone (*Haliotis rufescens*), and wavy turban snails (*Megastraea undosa*)

A Dissertation submitted in partial satisfaction of the
Requirements for the degree Doctor of Philosophy

in

Marine Biology

by

Cynthia Aileen Button

Committee in charge:

Professor Paul K. Dayton, Co-Chair
Professor James J. Leichter, Co-Chair
Professor Grant Deane
Professor David Holway
Professor Laura Rogers-Bennett

2008

INFORMATION TO USERS

The quality of this reproduction is dependent upon the quality of the copy submitted. Broken or indistinct print, colored or poor quality illustrations and photographs, print bleed-through, substandard margins, and improper alignment can adversely affect reproduction.

In the unlikely event that the author did not send a complete manuscript and there are missing pages, these will be noted. Also, if unauthorized copyright material had to be removed, a note will indicate the deletion.

ProQuest LLC
789 East Eisenhower Parkway
P.O. Box 1346
Ann Arbor, MI 48106-1346

The Dissertation of Cynthia Aileen Button is approved, and it is acceptable in quality and form for publication on microfilm.

Co-Chair

Co-Chair

University of California, San Diego

2008

DEDICATION

This dissertation is dedicated to the memory of Dr. Mia J. Tegner whose passion for science-directed conservation and management has inspired much of the following work.

EPIGRAPH

Oh, some folks boast of quail on toast
Because they think it's toney,
But I'm content to owe my rent
And live on abalone.
Oh! Mission Point's a friendly joint,
Where ev'ry crab's a crony,
And true and kind you'll ever find
The clinging abalone.

He wanders free beside the sea,
Where'er the coast is stony;
He flaps his wings and madly sings—
The plaintive abalone.
By Carmel Bay, the people say,
We feed on lazzaroni
On Boston beans and fresh sardines,
A toothesome abalone.

Some live on hope, and some on dope
And some on alimony;
But my tom-cat, he lives on fat
And tender abalone.
Oh! some drink rain and some champagne,
Or brandy by the pony;
But I will try a little rye
With a dash of abalone.

Oh! some like jam, and some like ham,
And some like macaroni;
But bring me a pail of gin
A tub of abalone.
He hides in caves beneath the waves,—
His ancient patrimony;
And so 'tis shown that faith alone
Reveals the abalone.

The more we take the more they make
In deep-sea matrimony;
Race suicide cannot betide
The fertile abalone.
I telegraph my better half
By Morse or by Marconi;
But if the need arise for speed,
I send an abalone.

Jack London, Abalone Song

TABLE OF CONTENTS

LIST OF ABBREVIATIONS

A1 ..... Intermediate-Sized Pink Abalone Adults (100-153mm)
A2 ..... Large Pink AbaloneAdults (>153mm)
AIC ..... Akaike Information Criterion
ARMP ..... Abalone Recovery and Management Plan
AS ..... Aggregation Size
AS_c ..... Critical Aggregation Size
BIC ..... Bayesian Information Criterion
CDFG ..... California Department of Fish and Game
CMR ..... Capture-Mark-Recapture
CJS ..... Cormack-Jolly-Seber Method
FAO ..... Food and Agricultural Association
FR ..... Fort Ross, California
HML ..... Hopkins Marine Laboratory, Monterey, California
IUCN ..... International Union for the Conservation of Nature
J ..... Pink Abalone Juveniles (<50mm)
KM ..... Kendall-Moran Distance Estimation Method
L95 ..... Lower 95% Confidence Interval
LDRE ..... Logistic Dose-Response Equation
Map-AS ..... Aggregation Size from Transect Mapping Method
MLS ..... Minimum Legal Size
MLS_C ..... Commercial Minimum Legal Size
MLS_R ..... Recreational Minimum Legal Size
MSD ..... Minimum Spawning Density
NOAA ..... National Oceanic and Atmospheric Administration
NN ..... Nearest Neighbor Distance
NN-AS ..... Aggregation Size from Nearest-Neighbor Method
nRMSE ..... Normalized Root Mean Squared Error
OC ..... Ocean Cove, California
PL ..... Point Loma, California
QAIC ..... Quasi-AIC
SA ..... Pink Abalone Subadults (50-100mm)
SIO ..... Scripps Institution of Oceanography
SMI ..... San Miguel Island, California
SMI-SE ..... San Miguel Island, southeast region
SMI-SW ..... San Miguel Island, southwest region
SSR ..... Sum of Squared Residuals
TRP ..... Total Reproductive Potential
TS ..... T-Square Distance Estimation Method
TTF ..... Time to Reach the Fishery
U95 ..... Upper 95% Confidence Interval
VDSP ..... Van Damme State Park, California
VMR ..... Variance-to-Mean Ratio

LIST OF FIGURES

CHAPTER 1

CHAPTER 2

CHAPTER 3

CHAPTER 4

CHAPTER 5

LIST OF TABLES

CHAPTER 1

CHAPTER 2

CHAPTER 3

CHAPTER 4

ACKNOWLEDGEMENTS

"Our passions are the winds that propel our vessel, our reason is the pilot that steers her; without the winds she would not move, without the pilot she would be lost." This old French proverb captures the spirit of every marine scientist I have ever met. We are driven by our passion for continually learning about the wonders of nature, and for the goal of bettering our world for future generations. The value of positive mentorship in guiding our efforts cannot be overstated. I am extremely fortunate to be surrounded by brilliant people whose passion for their work and their way of life is an inspiration. I would like to extend my deepest thanks to all those who have inspired, mentored, and supported me as I advanced through these initial stages of my scientific career.

It has been amazing to have Paul Dayton and Jim Leichter as co-advisors for the last six years. I am honored to be Jim's first graduate student and one of Paul's last. Their strengths are extremely complementary to each other. I have gained broader perspectives on science, natural history, and scientific careers because of the diversity of their mentorship. Paul has taught me that no matter how many times you look through a microscope at a pile of sand, you will always find something you never saw before. And, that is the true joy of marine ecology. He also encouraged me to form collaborations with fishermen and fisheries scientists, through which I have gained important perspective on how resource management and utilization can interact to create either a positive or negative relationship between fishermen and scientists. Jim has taught me how to think critically about my work, to really analyze the questions I am asking before I begin the work. Above all, I appreciate Jim's encouragement to always try new things

and to visit new places because it is through experience that you gain understanding. Thank you both for expanding my mind and my horizons.

My committee members, Laura Rogers-Bennett, Russ Lande, Grant Deane, and David Holway represent an amazing wealth and diversity of knowledge. I am deeply grateful for the time and interest they invested in my work over the years. Their feedback, advice, and encouragement have improved my research and my dissertation tremendously.

Laura Rogers-Bennett wins my most valuable committee member award, and has acted as an honorary advisor to me since the day we met five years ago. She is a true scholar, a patient mentor, and a keen collaborator. Whenever I called Laura for advice, she never rushed our conversations. We always ended our calls with more questions than we had started with, but we also had a better understanding of the approach needed to answer those questions. Laura's support of my work led to the inclusion of the aggregation surveys with the California Department of Fish and Game red abalone surveys in northern California and at San Miguel Island. She also coordinated my involvement with Henry Fastenau's scientific diving class, which was instrumental in collecting aggregation data at two of my sites. I owe a lot of my success to Laura's support and guidance throughout my graduate career.

Russ Lande has also been a positive guiding influence on my work. He tutored me in population demography and stochastic population modeling. His advice was always seemingly prescient; he would answer questions that I didn't know I had at the time, but the answers would be with me when I needed them. I am very grateful for the time he served on my committee.

In addition to my committee of advisors, I have a staggering number of people to thank for their enthusiastic *voluntary* help with my graduate work, even when it meant swimming in circles for hours in the cold upwelling waters off Point Loma, or the even colder waters in northern California. Ian Taniguchi and Pete Haaker from the California Department of Fish and Game are the most amazing abalone hunters I have had the opportunity to see in action. They brought in 30 abalone each to my one when they first helped me start the tagging study of the Point Loma pink abalone population. I am extremely grateful for their willingness to simultaneously collaborate with and mentor me at such an early stage in my graduate career.

I am also privileged to have found support and advice from individuals within the California benthic invertebrate fishing industry. Pete Halmay and Dave Rudie have been extremely supportive of creating dialogue between fishermen, scientists, and conservationists in San Diego. Their efforts of finding common ground among these diverse points of view are noble and are crucial for the future of our coastal marine resources. I am proud to consider each of them a friend and mentor. Through my research at San Miguel Island, I have also had the pleasure of working with Chris Voss and Jim Marshall. All of my interactions with them have been positive and informative. I can learn more about the fishing industry and the history of the abalone populations from talking to a fisherman over beer than I can learn in six years of reading books. My warmest thanks to all of those fishermen I shared beers with offshore of San Miguel Island one blustery evening in September.

When I signed up to do a project requiring a lot of scuba diving, I only thought I knew what I was getting myself into. Fortunately, I had a lot of help from volunteer

divers. I learned as much or more from them as they did from me. In particular, I want to recognize Maiko Kasuya (My first dive buddy dedicated to the abalone project, and an excellent sounding board), Kristin Riser (I swear she has gills!), Jonathan Shaeffer (What can't this guy do??), Scott Mau (Invaluable), Robert Todd (My most fanatical, but trustworthy dive buddy), Joe MacDonald (Always entertaining), Benjamin Pister (Um... cake, please!), Cleridy Lennert-Cody (It's perfectly normal to talk stats while bobbing in a small boat), Damien Cie (Your site, or mine?), and Miriam Goldstein (Don't forget the candied ginger!). These individuals were part of the core group of people upon which I relied for help in the field at the Point Loma survey locations. A bunch of other SIO divers were able to help out sporadically as well. They helped fill many of the gaps in my diving schedule when the core dive buddies weren't available – Caty Gonzalez, Ken Seel, Aurelien Ponte, Rich Walsh, Christian MacDonald, Kate Hanson, Erdem Karakoylu, Andrew Thurber, Sarah Glaser, Talina Konotchick, Mike Wilson, Jason Murray, Megan McKenna, Christine Whitcraft, Dana Gulbranson, Morgan Richie, Melissa Omand. My dive buddies endured 10-hour days with sometimes cold, rough waters and bouncy hour-long boat rides to and from the pier. But, other times, we were rewarded with >50 foot visibility, sightings of a juvenile black sea bass, or an octopus pretending to be a little white sponge on the underside of a rock. Thank you to all of you who kept smiling through the rough bits, and shared the wonderful experiences we had while we "worked" in the kelp forest.

During the red abalone population surveys, I was helped by divers from SIO, the California Department of Fish and Game, the UC Davis Scientific Diving Class, and members of the Abalone Advisory Group. From SIO, I need to thank Rich Walsh, Joe

MacDonald, and Miriam Goldstein who travelled many hours in the car in anticipation of seeing vast fields of red abalone. From the California Department of Fish and Game, Laura Rogers-Bennett, Dave Dann, Jason Herum, Kristin Hubbard, Christy Juhasz, Ian Taniguchi, Jerry Kashiwada, John Harreld, Dennis Davenport, Sönke, Kevin Joe, Pete Haaker, Dennis McKiver, Jeff Heitzenrater, Spencer Gilbert, and Kristine Barsky strengthened my research tremendously by helping me measure aggregation characteristics from Fort Bragg to San Miguel Island. Particular thanks to Ian Taniguchi and Derek Stein for coordinating the trips to San Miguel Island and making sure there was room for my dive buddy and me.

From the 2007 UC Davis scientific diving class, Colleen Young, Jessica Lund, Sean Graven, Neils Cooper, Kristin Aquilano, Brad Howard, Olen Dick, Keith Blackwood, Cipriano Santos, Stephan Armfield, Jonathan Schram, Jay Ault, and Ashley McDonough measured aggregation characteristics at Hopkins Marine Reserve and at Fort Ross. Many thanks to Henry Fastenau for allowing me to use his class of very competent divers to get more data!

I have also had many very fine high school, undergraduate, and post-baccalaureate helpers in the lab. Many thanks to William Hicks, Caty Gonzalez, Calvin Lee, Caitlin Allen, Kailey Banks, Courtney Prodor, Astrid Solorzano, and Maya Peters for your time, enthusiasm, and support. I had a blast molding you into geeky marine biologists!

I am lucky to be a member of two labs at SIO that are comprised of some truly brilliant yet slightly wacky scientists (professors, not excluded). My heartfelt thanks and warmest wishes to Ed Parnell, Kristin Riser, Nacho Vilchis, Jonathan Shaeffer, Ryan

Darrow, Megan Ferguson, Jeff Riffell, Andrea Lawless, Kim Whiteside, Darcy Taniguchi, Maiko Kasuya, Mike Murray, Tonya Huff, Bonnie Becker, Miriam Goldstein, Marco Hatch, Damien Cie, Christian Anderson, Talina Konotchick, Kate Hanson, and Sam Pritchard. I love that we are not an exclusive lab, but that we adopt many honorary members – Ben Pister, Becca Fenwick, Christine Whitcraft, Pat McMillan, John McGowan, Kate Allen, Marcel Croon, Andrew Thurber, Geoff Cook, and Celli Hull. You have all helped make my graduate experience extraordinary. Sapo Malagong, Sam Ho-Chin, Ellen B. Scripps, Hobe, Archi Bachter, Lily, Diesel, Joe, Lucy, and Nickel and Dime also helped keep things interesting in the hallway. My friends and fellow graduate students at SIO helped me to understand the diversity of marine science. Thanks to Sarah Glaser, Melissa Soldevilla, Serena Moseman, Melinda Simmons, Becca Fenwick, Kristen Gruenthal, Alejandra Prieto-Davo, Erin Gontang, Lisa Munger for sharing your research and your insights with me. This is the hardest part, to express in words what you have meant to me. Thank you!

Throughout my time at Scripps, Dawn Huffman, Denise Darling, Becky Burrola, Alice Zheng, Sharon Williams, Josh Reeves, Ryan Eddings, Lawrence Bailey, and many others have worked behind the scenes to make sure that all goes smoothly for me both academically and financially. Eddy Kisfaludy, Christian MacDonald, and Rich Walsh have also provided endless support. For that, I am extremely grateful.

Funding for this research was provided by California Sea Grant, the UC Marine Council Coastal Environmental Quality Initiative, the Edna Bailey Sussman Fund, the Mia Tegner Memorial Fund, a Halliday Field Research grant, the Hicks Foundation, and

Ellis “Poo” Wyer. I would like to thank all of these organizations and individuals for their generous assistance.

Chapters 2 through 5 were prepared as separate papers to submit for publication in peer-reviewed journals, co-authored by Laura Rogers-Bennett. The reader may encounter some redundancy of the information presented among those chapters. The text of Chapter 2 is in preparation for submission to the journal Ecological Applications. The text of Chapter 3 is in preparation for submission to the journal Marine Ecology Progress Series. Chapter 4 is in preparation for submission to the journal Ecological Applications. The text of Chapter 5 is in preparation for submission to the journal Ecological Modeling. The dissertation author was the primary investigator and author for each of these papers.

VITA

1995 – 1996	Water Quality Researcher Polluted Waters Project Puget Soundkeeper Alliance Seattle, Washington
1999	NSF Research Experience for Undergraduates Fellow International Kuril Island Project University of Washington, Seattle
2000	B.S., Zoology (Marine Emphasis) University of Washington, Seattle
2000, 2001	Teaching Assistant, Marine Zoology and Botany Friday Harbor Laboratories, University of Washington
2000 – 20002	Research Assistant Friday Harbor Laboratories, University of Washington
2006	Teaching Assistant, Marine Biology University of California, San Diego
2008	M.S., Marine Biology Scripps Institution of Oceanography University of California, San Diego
2002 – 2008	Ph.D., Marine Biology Scripps Institution of Oceanography University of California, San Diego

FIELDS OF STUDY

Major Field: Marine Biology

Studies in Biological Oceanography
Professors Paul Dayton and James Leichter

Studies in Fisheries Ecology
Professor Laura Rogers-Bennett

ABSTRACT OF THE DISSERTATION

The influence of density-dependent aggregation characteristics on the population biology of benthic broadcast-spawning gastropods: Pink abalone (*Haliotis corrugata*), red abalone (*H. rufescens*), and wavy turban snails (*Megastraea undosa*)

by

Cynthia Aileen Button

Doctor of Philosophy in Marine Biology

University of California, San Diego, 2008

Professor Paul K. Dayton, Co-Chair

Professor James J. Leichter, Co-Chair

The population growth rates of benthic broadcast-spawning species may be limited at low densities due to extreme reductions in fertilization rates. I investigated the influence of aggregation characteristics on the low-density population dynamics by incorporating aggregation-influenced fecundity estimates into a demographic matrix model for both pink (*Haliotis corrugata*) and red abalone (*H. rufescens*). I measured

aggregation-level characteristics in populations representing a broad range of densities and spatial dispersions in order to characterize the relationships between population density, nearest-neighbor distances, and aggregation sizes.

Average aggregation sizes were strongly correlated with population density, such that lower-density populations contained smaller aggregations. The relationship between nearest-neighbor distances and population density was nonlinear, such that distances increased rapidly as the population density decreased below a threshold level. The effect of aggregation size on fecundity translates into a rapid decline in population growth below a threshold average aggregation size. The magnitude of the depensation effect may be amplified when additional factors influencing fertilization success (i.e. nearest-neighbor distances) are considered.

The results of a four-year study of a pink abalone population near San Diego, California, indicate that the population is partially recovered as defined by the California Department of Fish and Game Abalone Recovery and Management Plan. However, the average population growth rate estimate was 1.070 yr^{-1} for high fertilization success conditions, and 0.902 yr^{-1} for low fertilization success conditions. Based on the average nearest-neighbor distances measured in this population (>5 meters), the expected fertilization success rate is low. This finding suggests that, in the absence of an external larval supply, this population may be declining.

This work provides important baseline information on aggregation characteristics that was previously unavailable for the California populations of pink and red abalone, and wavy turban snails (*Megastraea undosa*). The matrix models illustrate how the aggregation-level characteristics may be incorporated into a formal population model in

order to predict the critical aggregation size for that population. The results may be used to review the recovery of abalone stocks and to analyze the effectiveness of future management and recovery schemes.

CHAPTER 1.

Introduction to the Dissertation

The creation of sustainable management plans and stock-rebuilding strategies is a growing concern for fisheries scientists. An estimated 50% of the worldwide fisheries in the Food and Agricultural Organization's (FAO) database are designated as over-exploited (Garcia and Newton 1997; Mace 1997; Beverton 1998) and 25% of the major single-species fisheries have collapsed since 1950 (Mullon, Freon et al. 2005). The percentage of collapses has remained steady for the last half century, indicating no improvements in our abilities to successfully maintain fisheries at sustainable levels. The economic and cultural impacts of these collapses on local communities can be devastating. In addition, the ecological impact of a fisheries collapse is unknown until after the loss has occurred. The potential recovery period for these populations is also not easily predicted. As a consequence, fisheries biologists have received criticism from fishers, conservationists, and scientists for applying overly-simplistic models to complex biological systems without incorporating uncertainty into the population forecasts (Garcia 2005). As more fisheries collapse, we are faced with an increasing number of populations that are currently at very low densities. We need to study these populations to learn about low-density population dynamics and how to avoid future collapses in similar fisheries.

Many shellfish species in California's kelp forests may be particularly subject to population declines below a threshold density due to an extreme reduction in fertilization success. Once this lower population limit is reached, the possibility of recovery without

intervention is unlikely. The effect of reduced mating success due to critically low population density was first introduced by Allee (1931). The reduction in fertilization success is likely exacerbated in species with limited mobility, such as with many benthic broadcast-spawning invertebrate species (e.g. abalone). Therefore, fisheries population models for these species need to incorporate density-dependent processes acting at low population levels in order to avoid harvesting below this threshold density.

The sensitivity of benthic invertebrate species to over-fishing may be further exacerbated by their high economic value. According to the National Oceanic and Atmospheric Administration (NOAA), benthic invertebrates comprised approximately 50% of the California state fishery income for 2006, while only representing 12% of the total fished biomass (Table 1.1). The economic value of the benthic invertebrate fisheries ($3,508/ metric ton) is an order of magnitude higher than the California market squid fishery *Loligo opalescens* ($548/ metric ton) and "other" fisheries (vertebrates, pelagic invertebrates, and algae) ($436/ metric ton). The high economic value of commercial benthic invertebrate species challenges fisheries managers to balance economic and conservation priorities.

SIGNIFICANCE OF THE STUDY ANIMALS

Abalone provided a substantial fishery for over eighty years in California, culminating in the depletion of the five major southern California commercial species by 1997 (Rogers-Bennett, Haaker et al. 2002). Figure 1.1 illustrates the serial depletion and ultimate collapse of the fisheries prior to1997. A devastating combination of disease and over-exploitation reduced population levels to well below the current theoretical minimum spawning density (2,000 ha^{-1}) (California Department of Fish and Game 2002).

Between 1950 and 1997, the economic value of commercial abalone rocketed from approximately $0.45 per pound ($1029 / metric ton) to over $25 per pound ($55,115 / metric ton) (Figure 1.2). The extreme wholesale market value of the abalone during this time provided tremendous motivation for continued collection of the abalone. Even a small number of individuals would give the fisher a substantial economic boost.

Despite the damage to the southern California abalone stocks, red abalone (*Haliotis rufescens*) stocks north of San Francisco remain at relatively high densities. The resilience of this population seems to be due to a management scheme that allows only free-divers to collect abalone, inadvertently creating a depth refuge for individuals below approximately 8.4m (Karpov, Haaker et al. 1998). However, the temptation to poach abalone from illegal depths or from small pockets of higher-density populations in southern California remains high due to the inflated value of abalone on the market (Figure 1.2) (Hauck and Sweijd 1999).

In the early 1990's, the wavy turban snail (*Megastraea undosa*) was targeted as a potential abalone substitute in the U.S. market. The wavy turban snail is a large herbivore, reaching basal diameters up to 150 mm, and living in densities of up to 24,000 ha^{-1}. The range of this species is limited to the region between Pt. Conception and Baja California Sur, where it is common from the low intertidal zone to depths of approximately 35 m. Landings for this fishery have remained low for the last decade in California due to the lack of a US market for the fishery (Figure 1.3), however the Mexican fishery for this species has been growing since the 1980's. Little is published about the life history of this species, however recent descriptions of its ecology and larval biology suggest a strong similarity to abalone life-history traits. Like abalone, this species

broadcast spawns lecithotrophic larvae with a short planktonic period, on the order of a few days to a week (Guzmán del Próo, Reynoso-Granados et al. 2003). This similarity to abalone suggests that these populations may be similarly susceptible to reduced population densities.

OBJECTIVES OF THE DISSERTATION

The primary purpose of this dissertation is to investigate the influence of aggregation characteristics on the low-density population dynamics of abalone and other benthic broadcast-spawning gastropods. I examined methods of measuring aggregation-level characteristics that are appropriate for monitoring both high- and low-density populations of benthic broadcast-spawning invertebrates (Chapter 2). The aggregation-level characteristics provide insight into depensatory processes that may influence the population dynamics of these species at low densities. When applied to a high-density population of a fished species, the data will provide important baseline information should that population decline. The data may also be used to monitor the continued health of the population to avoid a rapid failure of the fishery.

To test the efficiency of these population monitoring techniques, I conducted a four-year population study of a low-density pink abalone (*Haliotis corrugata*) population (Chapter 3 and Chapter 4) and an intermediate-density wavy top turban snail population in the Point Loma kelp forest near San Diego, CA. In order to increase the effectiveness and impact of this research, I formed partnerships with scientists at the California Department of Fish and Game (CDFG). Through these collaborations, I was able to extend the application of these techniques to multiple red abalone populations throughout California (Chapter 5). These populations ranged in density from high to low, which

allows examination of density-dependent effects on aggregation characteristics. The results of this work will be used to better review the recovery of abalone stocks, to develop a management plan for the wavy turban snail before the local fishery increases landings, and to analyze the effectiveness of future management and recovery schemes. In addition, this research will provide important baseline data on these populations with which to compare future monitoring results.

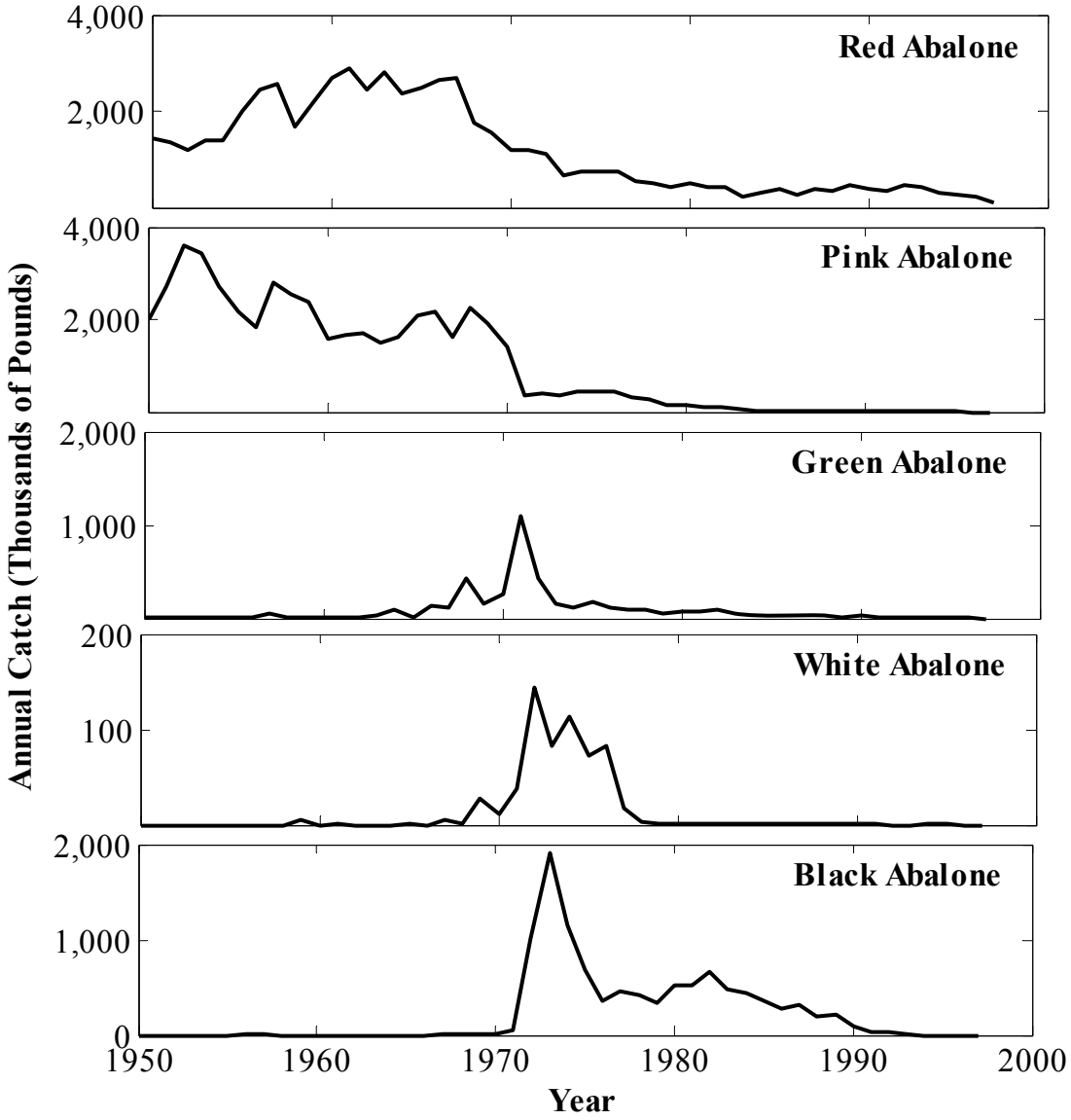

Figure 1.1 Serial depletion of five California abalone species. From the top down – red abalone (*Haliotis* rufescens), pink abalone (*H.* corrugata), green abalone (*H. fulgens*), white abalone (*H. sorenseni*), and black abalone *(H. cracherodii*). Data are available at the NOAA website http://www.st.nmfs.gov/st1/commercial/landings/annual_landings.html.

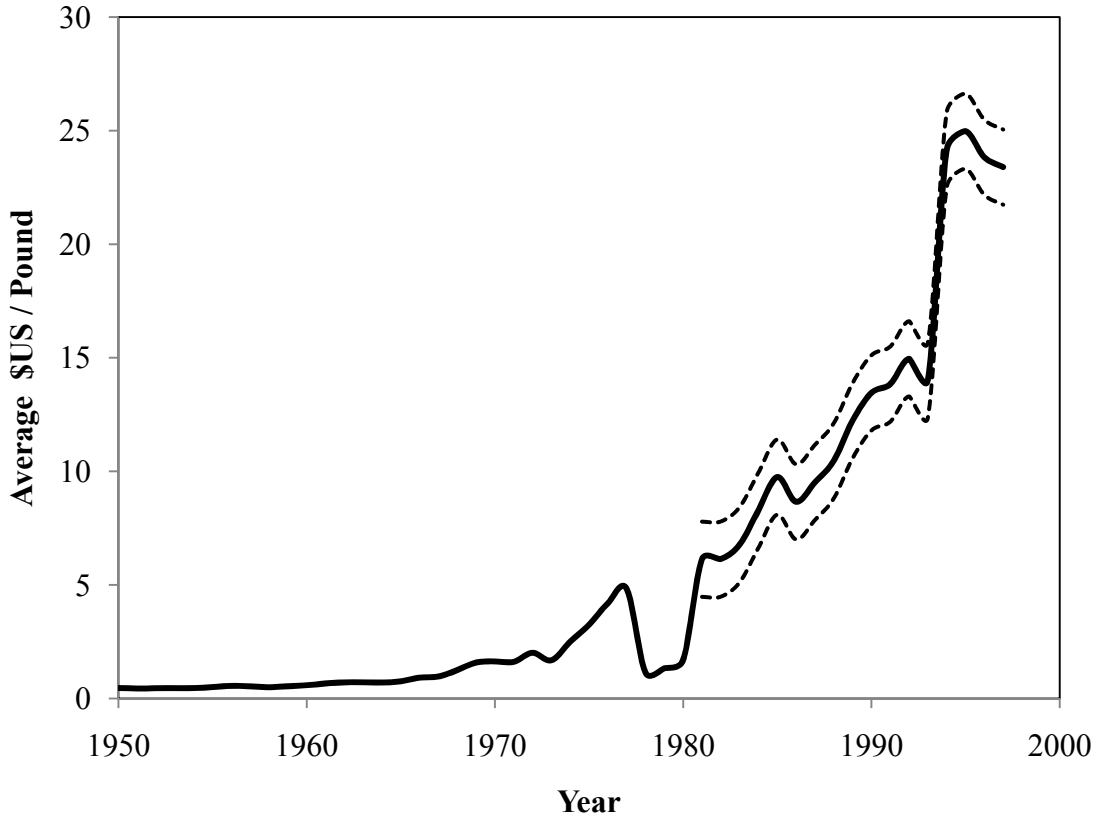

Figure 1.2 California commercial abalone average annual economic value (1950-1997). Data are available at the NOAA website http://www.st.nmfs.gov/st1/commercial/landings/annual_landings.html. The solid line is the average commercial value per pound in US dollars. Prior to 1981, abalone landings were not separated by species in this database. The dashed lines indicate the 95% confidence intervals around the average price per pound for five species of abalone (Red, Pink, Green, Black, and White Abalone).

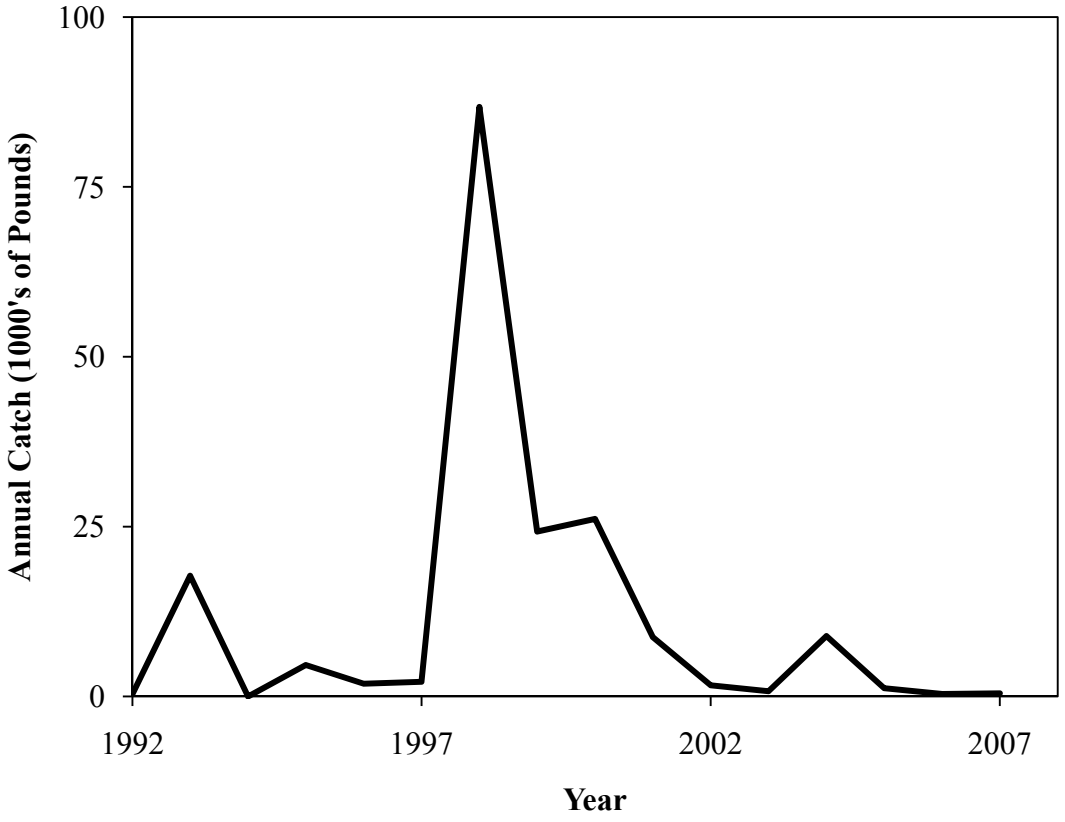

Figure 1.3 California commercial landings for the wavy turban snail, 1992-2007. Data are available at the NOAA website http://www.st.nmfs.gov/st1/commercial/landings/annual_landings.html.

Table 1.1 Annual commercial landings statistics for California fisheries in 2006. Data are available at the NOAA website http://www.st.nmfs.gov/st1/commercial/landings/annual_landings.html. "Other" fisheries include vertebrates, algae, and pelagic invertebrates (other than squid).

Fishery	Metric Tons	% Tonnage	Value	% Value	Value / Ton
Benthic Invertebrates	18,510	12	$64,929,198	50	$3,508
Squid	49,175	32	$26,958,513	21	$548
Other	87,292	56	$38,018,923	29	$436
TOTAL	154,976	100	$129,906,634	100	n/a

REFERENCES

Allee, W.C. (1931). *Animal Aggregations*. The University of Chicago Press, Chicago: 431 pp.

Beverton, R. (1998) Fish, fact and fantasy: A long view. *Reviews in Fish Biology and Fisheries*, **8**(3), 229-249.

California Department of Fish and Game (2002). *Draft Abalone Recovery and Management Plan*. California Department of Fish and Game, Marine Region, Sacramento, CA.

Garcia, S.M. (2005) Fishery science and decision-making: Dire straights to sustainability. *Bulletin of Marine Science*, **76**(2), 171-196.

Garcia, S.M., C. Newton (1997) Current situation, trends and prospects in world capture fisheries. In: M. Duke (Ed). *Global trends : fisheries management : Proceedings of the Symposium Global Trends, Fisheries Management*. American Fisheries Society, Seattle, WA: 3-27.

Guzmán del Próo, S.A., T. Reynoso-Granados, et al. (2003) Larval and early juvenile development of the wavy turban snail, *Megastraea undosa* (Wood, 1828) (Gastropoda: Turbinidae). *Veliger*, **46**(4), 320-324.

Hauck, M., N.A. Sweijd (1999) A case study of abalone poaching in South Africa and its impact on fisheries management. *Ices Journal of Marine Science*, **56**(6), 1024-1032.

Karpov, K.A., P.L. Haaker, et al. (1998) The red abalone, *Haliotis rufescens*, in California: Importance of depth refuge to abalone management. *Journal of Shellfish Research*, **17**(3), 863-870.

Mace, P.M. (1997) Developing and sustaining world fisheries resources: The state of the science and management. In: D.A. Hancock, D.C. Smith, A. Grant & J.P. Beumer (Eds). *Developing and sustaining world fisheries resources: The state of the science and management: The Second World Fisheries Congress*. CSIRO, Brisbane, Australia: 1-20.

Mullon, C., P. Freon, et al. (2005) The dynamics of collapse in world fisheries. *Fish and Fisheries*, **6**(2), 111-120.

Rogers-Bennett, L., P.L. Haaker, et al. (2002) Estimating Baseline Abundances of Abalone in California for Restoration. *California Cooperative Oceanic Fisheries Investigations Reports*, **43**, 97-111.

CHAPTER 2.

The Use of Nearest-Neighbor Distance Methods to Estimate Population Density and Aggregation Characteristics of Populations Susceptible to Allee Effects

ABSTRACT

This study is the first to examine the accuracy of the T-Square (TS) and Kendall-Moran (KM) plotless density estimation techniques over a broad range of densities and spatial distributions, in natural populations, with realistic sample sizes for time-limited field studies. I explored the usefulness of these distance-based population surveys for assessing population density and aggregation characteristics in populations susceptible to Allee effects at low densities. Densities estimated by the TS and KM methods were compared to densities determined directly by transect surveys for ten populations of three benthic broadcast-spawning gastropods (*Haliotis corrugata, H. rufescens,* and *Megastraea undosa*). The surveyed populations represent a broad range of population densities (0.01 – 1.1 m^{-2}) and spatial distributions. The difference between the transect- and distance-based density estimates increases as the spatial distribution becomes more aggregated. The linearly increasing bias in the density estimates is well-predicted by the variance in count survey data, and by the transect density, but not by the distance-based indices of aggregation. The results of this study suggest that the TS and KM methods may only be appropriate for assessments of low-density populations which also tend to have lower variances. Distance-based methods also provide valuable information on smaller-scale spatial characteristics that may influence population dynamics at low densities. The average nearest-neighbor distances were well-predicted by a power

function of the transect densities with a negative exponent. Likewise, average aggregation sizes were well-predicted by the transect densities with a positive linear function. Understanding the shapes of the relationships between population-level and aggregation-level characteristics reveals the influence of population density on the aggregative behavior of these species. For species whose persistence at low densities relies on aggregative behavior, the combination of transect- and distance-based surveys provides valuable information for long-term monitoring.

INTRODUCTION

Monitoring programs for over-exploited species frequently begin after populations have declined to low abundances and are designed to assess the efficacy of or need for recovery efforts. With fisheries collapses worldwide (Mullon, Freon et al. 2005), the number of low-density populations that require assessment is increasing. These populations are often patchily distributed in space and are difficult to census with precision using standard survey methods. Transect or quadrat surveys may insufficiently sample low-density populations unless the survey area is very large. This increased monitoring effort poses difficulties when the surveyors are time-limited in the field (e.g. subtidal or intertidal locations) or if the cost of increasing the number of survey days is prohibitive (Krebs 1999).

In addition to quantifying population abundance over time, surveys of low-density populations should address the influence of possible Allee effects. At low densities, populations subject to an Allee effect may decline rapidly due to reductions in successful cooperative-hunting, predator-avoidance tactics, or reproduction. These mechanisms all require aggregative behavior to persist at low-densities in order to sustain positive

population growth. Therefore, aggregation-level characteristics (i.e. nearest-neighbor distances and aggregation sizes) should be included in surveys of populations susceptible to depensatory declines that may undermine recovery efforts. For the reasons stated above, low-density populations pose unique challenges to conservation biologists designing appropriate survey protocols.

For estimating densities of stationary or relatively slow-moving species, such as plants or benthic invertebrates, nearest-neighbor distance methods are often used as a lower-cost, flexible alternative to transect methods (Cottam and Curtis 1949; Byth 1982; Engeman, Sugihara et al. 1994). The distance-based methods use one or more distance measurements to infer the density and spatial distribution of the population, including measurements of random-point-to-closest-individual distances and individual-to-nearest-neighbor distances. The data obtained for these plotless density estimation techniques can also be used to describe aggregation characteristics in the population (*see Chapter 4 and 5*). Because populations tend to be aggregated in space, distance-based survey methods need to be robust to deviations from a random spatial distribution.

Distance-based methods of estimating density have twice been applied to high-density abalone populations in Australia with differing degrees of success. Officer et al. (2001) simulated distance sampling of a high-density natural abalone population (>3 abalone m^{-2}) to test the performance of a density estimator originally described by Diggle (1975). The authors concluded that this density estimation technique, which required only one measurement per sample, was accurate with sample sizes greater than 300 measurements. McGarvey et al. (2005) tested the accuracy of two distance-based methods (Diggle 1975; Byth 1982) applied to two high-density natural abalone

populations (0.62 - 1.25 abalone m^{-2}). These authors reported that both methods consistently underestimated the true densities by 18-55 percent with sample sizes ranging from 22-30 sets of distance measurements. Neither study explored the use of either the KM or TS protocols that were shown to be more robust to aggregated distributions (Engeman, Sugihara et al. 1994) and that may be more straightforward to implement in field studies.

The purpose of this paper is twofold: 1) to present survey methods used to assess low- and high-density populations of three species of broadcast-spawning benthic gastropods in California (*Haliotis corrugata, H. rufescens,* and *Megastraea undosa*), and 2) to compare the efficacy of the KM and TS density estimation techniques against the standard transect method for natural populations across a range of densities (~0.01 – 1.1 abalone m^{-2}). The three gastropod species chosen for this study are slow-moving, broadcast-spawning species that may be subject to reduced fertilization success at low densities if aggregations are not maintained (Belmar-Pérez, Guzmán del Próo et al. 1991; Shepherd and Brown 1993; Babcock and Keesing 1999; Botsford, Campbell et al. 2002). They occur in similar habitats over a broad geographic range within California. In addition, the populations have experienced different historical fishing pressures – overfished, recently fished, sustainably fished, and impacted by sea otter predation (Table 2.1) (California Department of Fish and Game 2001; California Department of Fish and Game 2002).

METHODS

Populations

Ten population surveys were performed from May-October of 2005-2007 (Table 2.1). Five red abalone populations were surveyed in 2007 over a broad geographic range within California. Three are located north of San Francisco within the range of a recreational skin-diving-only fishery – Van Damme State Park (VDSP), Ocean Cove (OC), and Fort Ross (FR). These are high-density populations that are closely monitored and actively managed by the California Department of Fish and Game. The population located near the Hopkins Marine Laboratory (HML) in Monterey Bay is protected from human-induced fishing mortality, but is subject to intense sea otter predation. The San Miguel Island (SMI) population has been protected from fishing since 1997.

Pink abalone (2006 – 2007) and wavy turban snail (2005-2007) populations were surveyed in the Point Loma (PL) kelp forest near San Diego, California (Figure 2.1). The pink abalone population has been protected from fishing since 1997. The wavy turban snail population has only recently been fished in small numbers (thousands of pounds per year) since the early 1990's (California Department of Fish and Game 2001). The population abundance of this species does not seem to be impacted by this fishery based on comparisons of current densities with historic densities for Point Loma (Dr. Paul Dayton, *unpublished data*).

Sampling Methods

Population surveys were conducted by scuba divers using distance-based methods. The PL populations were surveyed by scientific divers from Scripps Institution of Oceanography (SIO). The data from VDSP, OC, and SMI were collected primarily by

CDFG personnel (scientists and wardens) and SIO divers whereas the FR and HML data were collected primarily by students of the University of California, Davis, scientific-diving class.

Transect Surveys

The locations of the transect surveys within each study site were determined randomly. The size and number of transects surveyed at each location differed by study site. The total transect area at each site is given in Table 2.1. For each transect, the number of individuals was recorded and divided by the transect area to calculate the density for that transect. The density estimate for each study site was calculated by averaging the transect densities by the number of survey locations.

Distance-Based Surveys

The TS protocol requires two distance measurements be recorded (Figure 2.2) – the distance from a random waypoint to the nearest individual (x), and the distance from that individual to its nearest neighbor within a half circle pointing away from the initial random point (y). The second distance measurement for the KM protocol must be the distance from the first individual to its nearest neighbor in any direction. In rare cases, the second TS distance measurement (y) may not represent the distance to the true nearest neighbor of the first individual. In those cases, a third measurement is recorded (z) to accommodate the KM data requirements.

Density estimation using the TS data was obtained by the following equation (Krebs 1999):

$$\widehat{N}_{TS} = n^2 / \{2 \sum(x_i) [\sqrt{2} \sum(y_i)]\} \quad (2.1)$$

where $\widehat{N}_{TS}$ is the T-Square density estimate and n is the number of measurement pairs.

The standard error of the estimate is calculated for the reciprocal of the $\widehat{N}_{TS}$ estimate:

$$SE\left(1/\widehat{N}_{TS}\right) = \left\{\left[8\left(\bar{y}^2 s_x^2 + 2\bar{x}\bar{y}s_{xy} + \bar{x}^2 s_y^2\right)\right]/n\right\}^{0.5} \quad (2.2)$$

where,

$$s_x^2 = \{\sum x_i^2 - (\sum x_i)^2/n\}/(n-1) \quad (2.3)$$

$$s_y^2 = \{\sum y_i^2 - (\sum y_i)^2/n\}/(n-1) \quad (2.4)$$

$$s_{xy} = \{\sum x_i y_i - (\sum x_i)(\sum y_i)/n\}/(n-1) \quad (2.5)$$

In addition to these asymmetric errors, a normal approximation of the standard error was calculated for the TS data using the delta method to allow comparison with the transect errors.

$$\sim SE\left(\widehat{N}_{TS}\right) = SE\left(1/\widehat{N}_{TS}\right)\left|\ln\left(1/\widehat{N}_{TS}\right)\right| \quad (2.6)$$

The significance of the differences in the transect and TS density estimates was tested using a Z-test:

$$Z = \left(\widehat{N}_T - \widehat{N}_{TS}\right)/\sqrt{\left(\sim SE\left(\widehat{N}_{TS}\right)\right)^2 - \left(SE\left(\widehat{N}_T\right)\right)^2} \quad (2.7)$$

If *Z* is less than -1.96 or greater than +1.96, then the density estimates are significantly different with $\alpha = 0.05$.

The density estimate for the KM protocol ($\widehat{N}_{KM}$) is calculated based on the total searched area in each location (A_i) – the area of the two circles searched minus the intersection of the circles (Kendall and Moran 1963; Engeman, Sugihara et al. 1994):

$$\widehat{N}_{KM} = \{[\sum(p_i)] - 1\}/\sum A_i \quad (2.8)$$

where p_i is the number of individuals within the area A_i,

$$A_i = \pi x_i^2 + \pi z_i^2 - x_i^2\{\theta - \sin\theta\cos\theta\} - z_i^2\{\varphi - \sin\varphi\cos\varphi\} \quad (2.9)$$

and,

$$\theta = \cos^{-1}(1 - z_i^2(2x_i^2)^{-1}) \tag{2.10}$$

$$\varphi = \cos^{-1} z_i(2x_i)^{-1} \tag{2.11}$$

The 95% confidence intervals for the $\widehat{N}_{KM}$ estimate were obtained by finding the 2.5 and 97.5 percentiles of 10,000 fixed-*xy* bootstrap samples.

Aggregation Surveys

In order to quantify aggregation sizes in the population, we counted the number of individuals within a 2.5 m radius of the nearest individual to the initial random point in the survey. The minimum aggregation size is therefore equal to one. We chose the 2.5 m radius based on *in situ* results of fertilization success with increasing distance from a conspecific described by Babcock and Keesing (1999) for *H. laevigata* in South Australia. The negative exponential equation approximating the probability curve is

$$F = e^{-bd} \tag{2.12}$$

where, F is the probability of fertilization, d is the distance between nearest neighbors, and $b \sim 0.4$. The spatial scale of this equation (where fertilization probability is equal to e) is defined as $d \sim 1 / b = 2.5$ meters. This means that within 2.5 m of another abalone, the expected fertilization probability is greater than 0.37, increasing rapidly as the distance decreases. Aggregation size data were collected during all of the surveys except for the 2005 and 2006 wavy turban snail population surveys.

In addition to aggregation sizes, we calculated indices of aggregation for each survey, using the T-Square index of dispersion described by Hines and Hines (1979),

$$h = \{2n(2\sum x_i^2 + \sum y_i^2)\} / \left\{\left(\sqrt{2}\sum x_i + \sum y_i\right)^2\right\} \tag{2.13}$$

Eberhardt's test of randomness based on the point-to-nearest-neighbor distances (Krebs 1999), and the variance-to-mean-ratios of the transect densities and the aggregation sizes. These indices describe the deviation from randomness in the spatial distribution of the populations, so they may correlate with the differences between the average transect and plotless density estimates.

The error associated with the average density estimates was calculated by subtracting the plotless density estimate from the average transect density.

$$\Delta N_{TS} = \widehat{N}_T - \widehat{N}_{TS} \tag{2.14}$$

$$\Delta N_{KM} = \widehat{N}_T - \widehat{N}_{KM} \tag{2.15}$$

The absolute value of these errors divided by the average transect density gives the normalized root mean squared error for each population. These results can then be compared with the previous studies examining the performance of these density estimators.

Regression Analysis

Bootstrap regression analyses were performed to assess the predictability of the average aggregation characteristics based on the average transect densities. We also examined the influence of aggregation on the accuracy of the plotless density estimates by comparing ΔN_{TS} and ΔN_{KM} to the transect density and to the indices of aggregation and variability in the data. In addition, we examined the relationships between the best predictor variables of these density differences (Table 2.3 and Table 2.4). To determine the 95% confidence intervals of the regression parameters and the coefficients of determination (R^2), we performed fixed-*xy* bootstrap parametric regression analyses. For

each of 20,000 bootstrap samples, we randomly chose 10 pairs of data and performed a least squares fit (in Matlab® by Mathworks, Inc.). Confidence intervals for the fit parameters were calculated by the percentile method. For linear fits, the probability that the regression had a negative slope was determined by the proportion of bootstrap samples that resulted in R less than zero.

RESULTS

Summary statistics for the transect densities, nearest-neighbor distances, and aggregation sizes are given in Table 2.2. The pink abalone population had the lowest average density (0.01 – 0.02 individuals / m^2), largest average nearest-neighbor distances (>5 m), and smallest average aggregation sizes (1.6 – 2.0 individuals). The red abalone populations north of San Francisco had the highest densities (0.69 – 1.11 individuals / m2), smallest average nearest-neighbor distances (≤ 1.00 m), and largest average aggregation sizes (8.7 – 14.3 individuals). The two southern red abalone populations surveyed had intermediate densities (0.13 – 0.14 individuals / m2), average nearest-neighbor distances (1.74 – 1.84 m), and average aggregation sizes (3.9 individuals). The wavy turban snail population also had intermediate densities (0.19 – 0.43 individuals / m2), average nearest-neighbor distances (0.89 – 1.23 m), and average aggregation sizes (5.0 individuals).

Average nearest-neighbor distances and aggregation sizes were highly correlated with the average transect density estimates (Figures 2.3, 2.4; Tables 2.3, 2.4). The relationship between transect densities and the nearest-neighbor distances was well-predicted by a power function ($y = \alpha x^{\beta}$) with a negative exponent. The average aggregation size increased linearly with the average transect density.

For all ten populations, the density estimates from the transect and TS data were not significantly different. The errorbars for the TS estimates are large (Figure 2.5), making any differences in the mean estimates statistically indiscernible. Both plotless density estimation techniques produced biased average estimates for high-density, high-variablity populations (Figure 2.5). The KM average estimates were consistently lower than the transect averages, ranging from 1% to 90% nRMSE. The TS estimates ranged from 22% to 75% nRMSE, at times over-estimating density compared to the transect averages. The greatest congruence between the plotless and transect density estimates was seen in the results from the wavy turban snail surveys and the low-density pink abalone survey in 2007 (Figure 2.6).

The results of the regression analyses examining the best predictor variables for the differences in the density estimates are given in Tables 2.3 and 2.5. The best predictor of ΔN_{TS} and ΔN_{KM} is the variance of the transect densities (Figure 2.7), followed by the variance-to-mean ratio of the transect densities (Figure 2.8) and the average transect density (Figure 2.9). The variance of the aggregation sizes is also highly correlated with the difference in the average density estimates (Figure 2.10) due to a high correlation with the transect variances and variance-to-mean ratios (Figures 2.11 and 2.12). The transect density was also strongly positively correlated with the variance of the transects (Figure 2.13). Neither the T-Square index of dispersion (h) nor the Eberhardt Test of randomness (E) showed a strong correlation with the differences in the average density estimates. In nearly all cases, ΔN_{TS} and ΔN_{KM} increased as the variability in the data increased (i.e. the slope of the regression was positive).

DISCUSSION

Spatial Complexity of Natural Populations

This study is the first to examine aggregation characteristics and the efficiency of using distance-based density estimation techniques over a broad range of densities and spatial distributions, in natural populations, and with realistic sample sizes for time-limited field studies. The small-scale spatial distributions of the surveyed populations have been influenced by different external pressures, some of which may impact aggregative behavior in non-random ways. For example, scuba-based fishing preferentially selects large aggregations over solitary individuals (Hart and Gorfine 1997). This practice may decrease the variance of the group sizes encountered. In contrast, sea otter predation results in the persistence of individuals only inhabiting deep crevice habitat. Thus, habitat complexity may play a stronger role in the spatial distribution of the HML abalone population than the populations exposed to human fishing (Hines and Pearse 1982; Micheli, Shelton et al. 2008). The wavy turban snail shows much less habitat affinity (Parnell, Dayton et al. 2006) and is much more mobile than either abalone species. These characteristics could potentially introduce more randomness into the spatial distribution of this species. Such locally-specific and species-specific spatial dynamics are difficult artificially construct without sufficient field data.

Efficacy of Density Estimation Methods

Although transects and quadrats remain the most accurate methods for estimating the density of a population (Engeman, Sugihara et al. 1994), the results of this study suggest that the TS and KM plotless methods may also be effective at estimating

population density under certain circumstances. The TS and KM methods are most effective for populations with lower spatial variability (i.e. less aggregation) (Figures 2.7, and 2.8). This result is expected based on the statistical assumption of a random spatial distribution that is central to the plotless estimation theory. However, the results of this study also suggest that these methods are appropriate for low-density populations (Figure 2.6) because of the lower spatial variability associated with low-density populations (Figure 2.11).

Interestingly, the differences in density estimates are predicted by the variance of the count data, but are not well-predicted by the distance-based tests of spatial dispersion (Table 2.2). Neither the T-Square index of dispersion nor the Eberhardt's test of randomness adequately describes the variability of the surveyed populations. However, the variance of the aggregation sizes provides sufficient information on the spatial dispersion in the population to predict the difference in the density estimates (Figure 2.8). Thus, the plotless density estimate may be modified to better correspond with the transect estimate by incorporating additional aggregation survey data into the analysis.

The result that the variance of the aggregation sizes correlates well with the density estimate differences is particularly unexpected because the aggregation sizes do not represent a true random sampling of the count data. The circular area defining the aggregation is always centered on an individual instead of a random point such that the minimum aggregation size is equal to one. Additionally, the central individual was chosen based on its proximity to the initial random point – a method that preferably selects either solitary individuals or individuals on the outer edge of an aggregation (Pielou 1959; Ripley 2004). These two factors may decrease the apparent variance in the

count data. Furthermore, the size of the area searched while characterizing the aggregation sizes is much smaller (~20 m^2) than the transect area (60-150 m^2). A change in quadrat or transect size is known to influence the apparent spatial dispersion in the population (Pielou 1960; Ripley 2004). Despite these biases in the estimates of the absolute variances of the populations, the relative variances across populations were apparently preserved in the aggregation size data for these populations.

Aggregation Data and Allee Effects

In addition to improving the plotless density estimates, the aggregation survey data also provide smaller-scale spatial information that may be relevant to populations susceptible to Allee effects. For the species surveyed by this study, the distances between neighboring broadcast-spawning individuals increased rapidly in populations with densities less than 0.15 individuals / m^2. The inflexion point along this curve may represent a critical density threshold, below which individuals may not maintain close enough distances to allow high rates of fertilization. The predicted average aggregation size at this low density level is less than four individuals. Given a 1:1 sex ratio, which is common in broadcast-spawning species, the probability that an aggregation will contain both males and females decreases rapidly in aggregations less than four (*see Chapter 4 and 5*). This decreased probability, in addition to the increased distances between individuals, may impact the reproductive potential of these aggregations (*see Chapter 5*). The biases associated with choosing the closest individual to the random point may result in a conservative estimate of the reproductive potential. The estimated average nearest-neighbor distance may be larger and the estimated average aggregation size smaller than the true average. In lower-density populations, these biases may be amplified by

potentially greater number of solitary individuals in the population, offering an even more conservative estimate as the population nears its critical density threshold.

Ideally, the survey method chosen for long-term population monitoring should perform equally well in high- and low-density populations. Neither of the plotless methods meets this criterion for density estimation due to the poor performance in high-density populations and the uncertainty associated with generalizing the correction factor to other species. For surveys of species reliant on aggregations at low densities, a combination of transect- and distance-based surveys may prove to be the most informative option over time. The two survey methods are complementary to each other in terms of the amount of effort required to accomplish each at different levels of population densities. Many plotless survey methods are quick and easy to perform in high-density populations, becoming progressively more taxing in less abundant populations. However, transect surveys are more time-consuming for high-density populations because of the larger number of individuals encountered. By combining the two survey methods, a greater diversity of data may be obtained for the population with only the allocation of effort between the two methods changing as population density changes.

ACKNOWLEDGEMENTS

This work was funded by California Sea Grant, the University of California Marine Council Coastal Environmental Quality Initiative, the Edna B. Sussman Fund, the Mia J. Tegner Memorial Fund, a Halliday Field Research grant, the Hicks Foundation, the Wyer Foundation, and the California Department of Fish and Game. I am grateful for permission to complete part of this work within the Hopkins Marine Reserve. Special

thanks to L. Rogers-Bennett, I. Taniguchi, and D. Stein for supporting the inclusion of the nearest-neighbor surveys on CDFG cruises. I am also grateful to H. Fastenau and the 2007 UC Davis scientific diving class for their careful data collection at Fort Ross and Hopkins despite the long surface swims. This work would not have been possible without the additional help of many volunteer divers from SIO, CDFG, and the San Miguel Island Abalone Advisory Group. Thanks to C. Anderson and H. Lyons for advice on statistical analyses and to E. Parnell, K. Hanson, C. Anderson, J. Leichter, D. Holway, and K. Riser for giving valuable feedback on earlier drafts of this chapter. The material in this chapter is in preparation to submission to the journal Ecological Applications, and was co-authored by Laura Rogers-Bennett. The dissertation author was the primary investigator and author of this paper

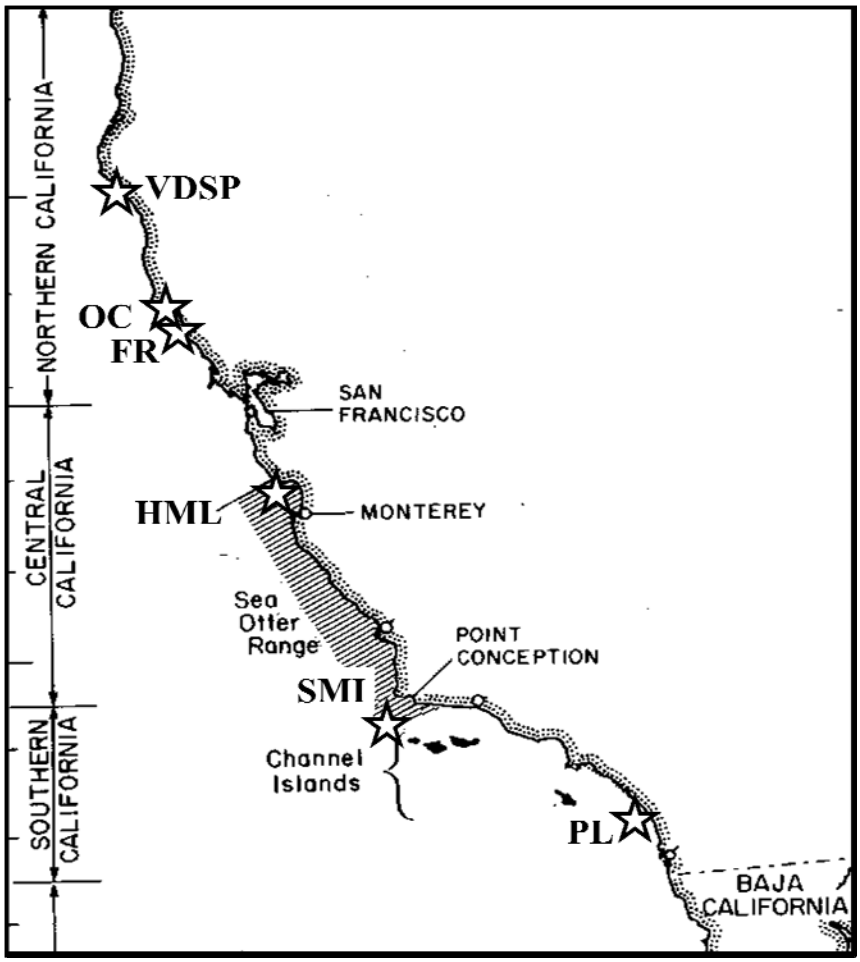

Figure 2.1 Locations of population surveys conducted. From north to south: VDSP - Van Damme State Park; OC - Ocean Cove; FR- Fort Ross; HML - Hopkins Marine Laboratory; SMI - San Miguel Island; PL – Pt. Loma.

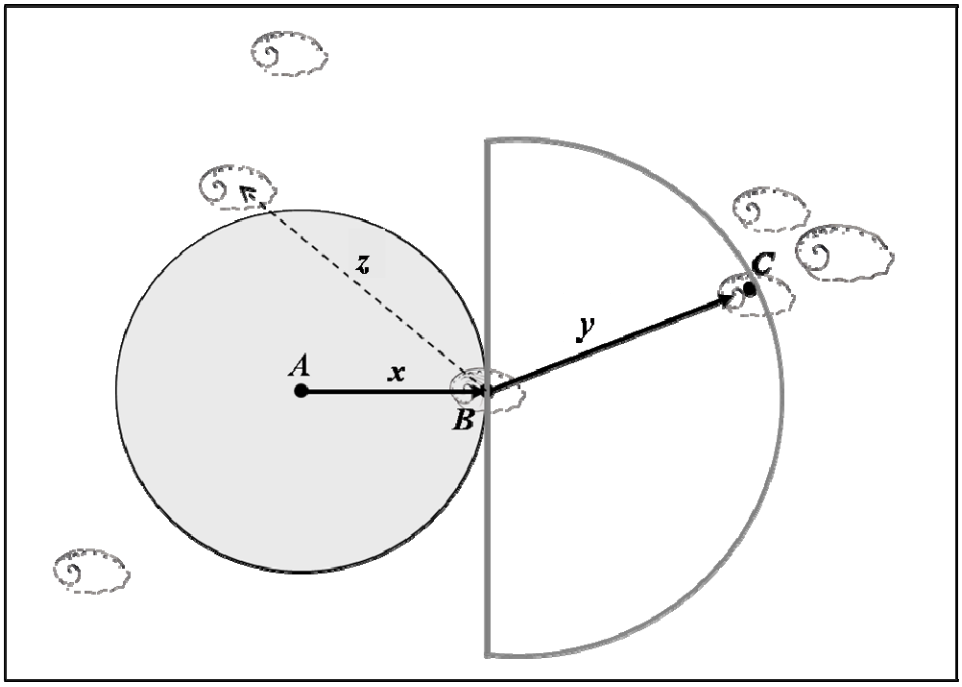

\

Figure 2.2 Diagram of T-square and Kendall-Moran nearest-neighbor sampling methods. The areas in the circle and half-circle represent the area searched for the T-Square sampling. *A*) The random starting point for the search, *B*) Nearest neighbor to *A*, *C*) Nearest neighbor to *B* in the direction away from *A*. *x* and *y* are the distances from *A*-*B* and from *B*-*C*, respectively. *z* is the distance to the true nearest neighbor of *B* if there exists an individual closer than *C*. (Figure adapted from Krebs 1999).

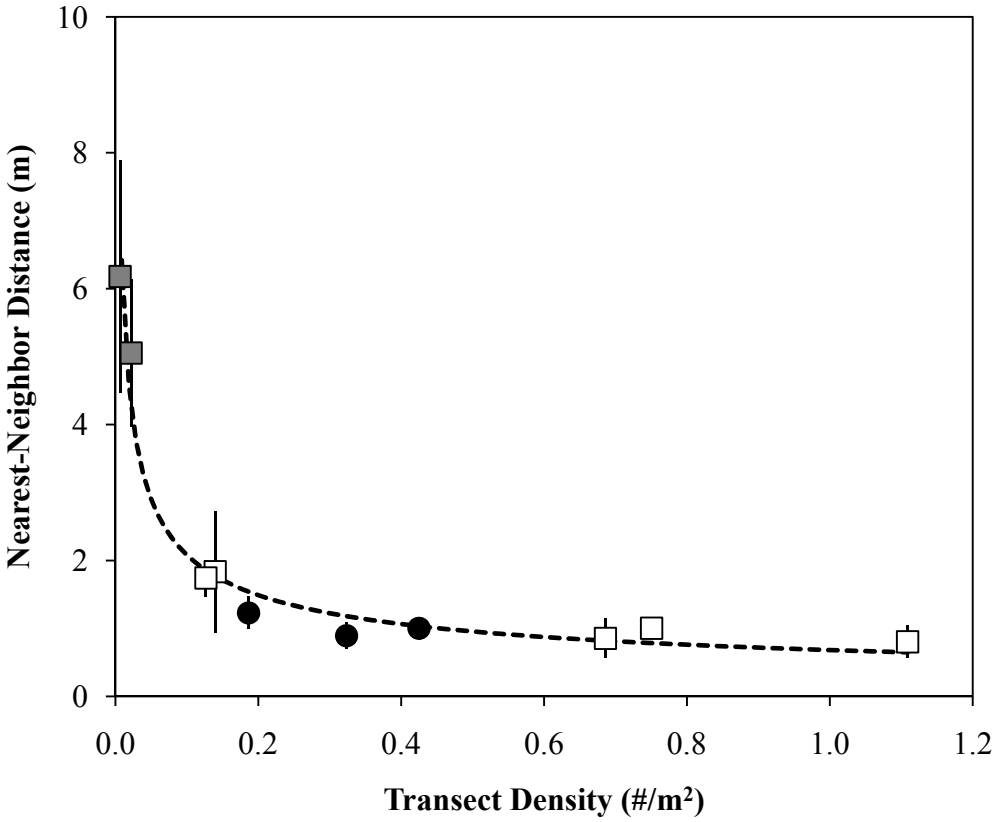

Figure 2.3 Regression of transect densities and nearest-neighbor distances. Error bars are standard errors. The best fit to the average data is a power function (dashed line). The gray squares represent the pink abalone estimates, the white squares represent the red abalone estimates, and the black circles represent the wavy turban snail estimates. $y = 0.6826\ x^{-0.4867}$; $R^2 = 0.9837$; p-value = 0.0000.

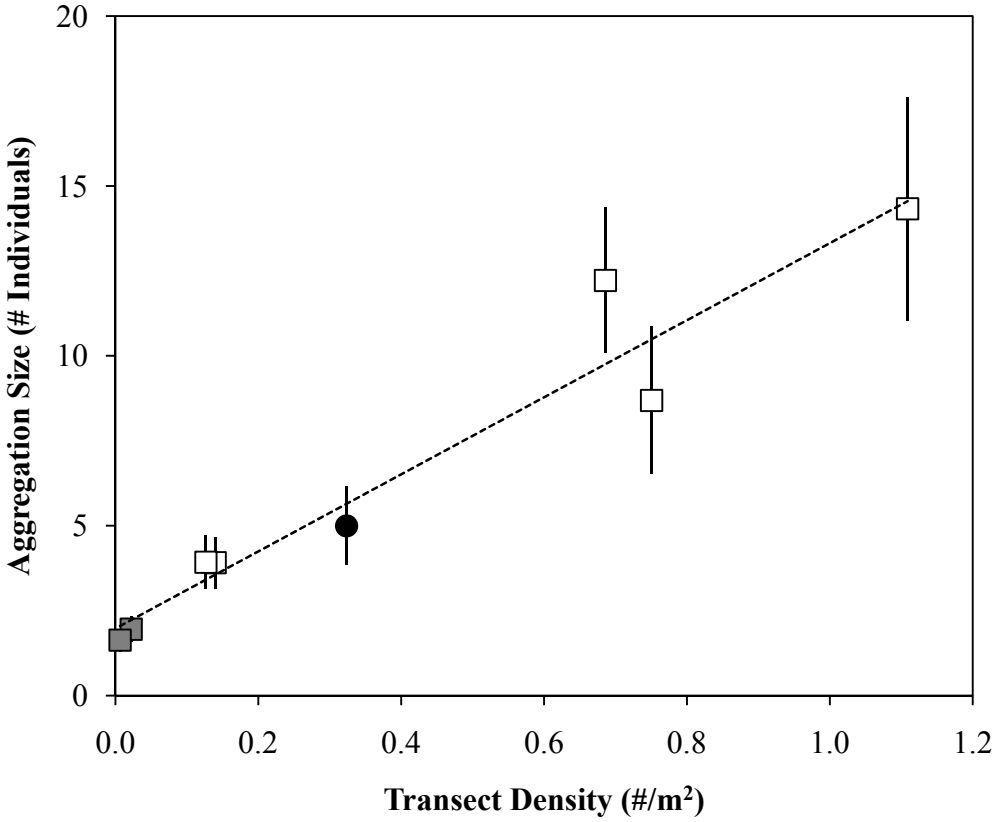

Figure 2.4 Linear regression of transect densities and aggregation sizes. The gray squares represent the pink abalone estimates, the white squares represent the red abalone estimates, and the black circle represents the wavy turban snail estimate. Error bars are standard errors.

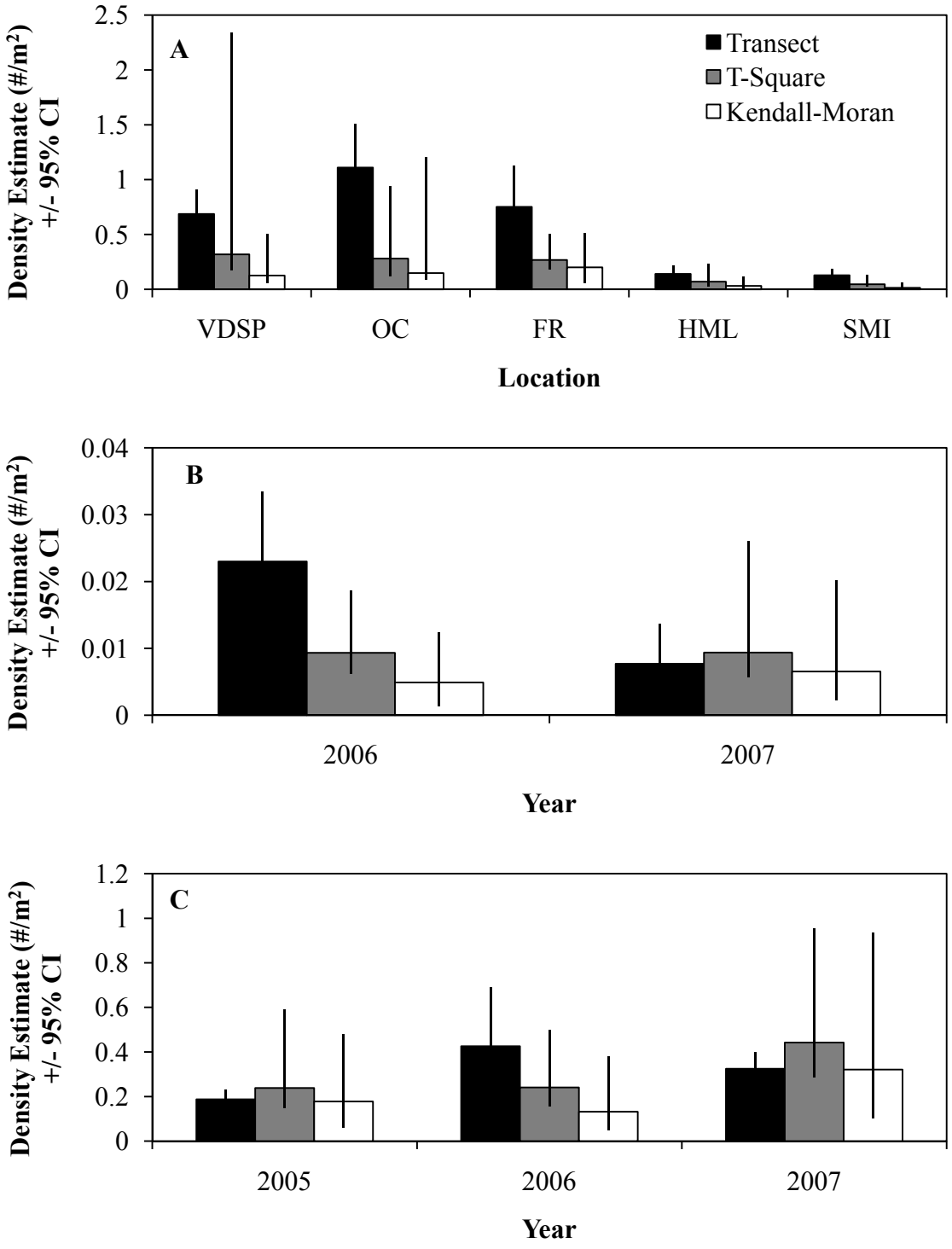

Figure 2.5 Density estimates +/- 95% confidence intervals for the transect, T-square, and Kendall-Moran protocols. A) red abalone 2007 population surveys, B) pink abalone Pt. Loma population surveys, C) wavy turban snail Pt. Loma population surveys. Location abbreviations are as in Figure 2.1.

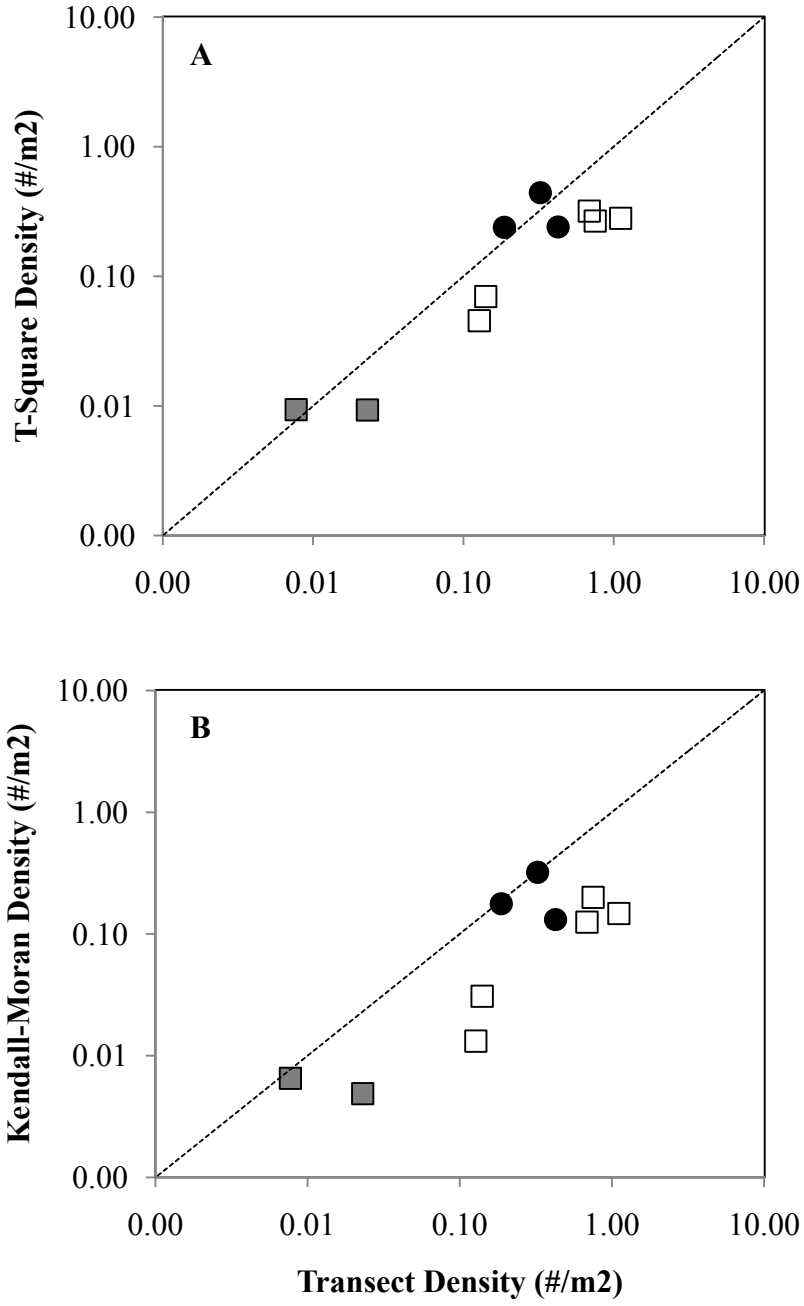

Figure 2.6 Comparison of the average transect density estimates with the A) average T-square densities and B) average Kendall-Moran densities. The gray squares represent the pink abalone estimates, the white squares represent the red abalone estimates, and the black circles represent the wavy turban snail estimates. The dashed diagonal line indicates unity of the density estimates.

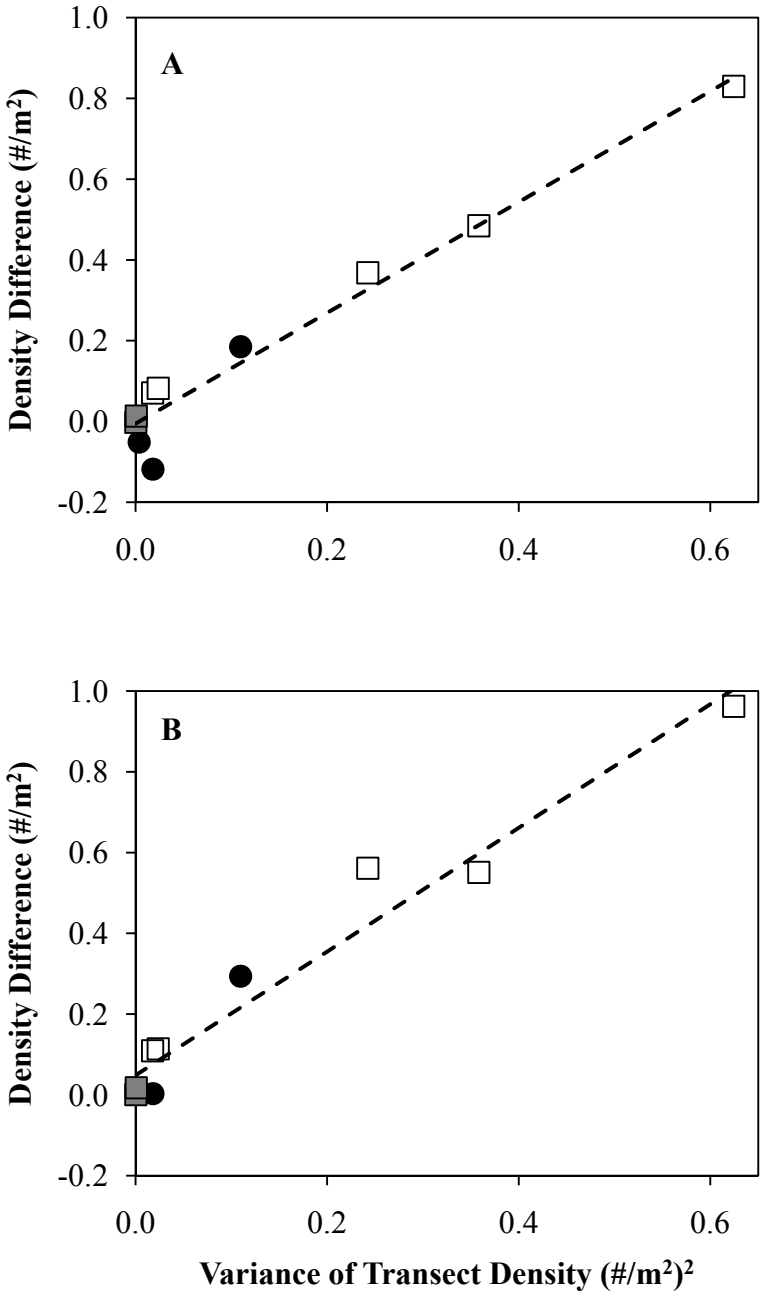

Figure 2.7 Linear regression of the transect density variances and the differences in the average density estimates. A) transect density minus T-square density, B) transect density minus Kendall-Moran density. The dotted line is a linear fit to the data. The gray squares represent the pink abalone estimates, the white squares represent the red abalone estimates, and the black circles represent the wavy turban snail estimates.

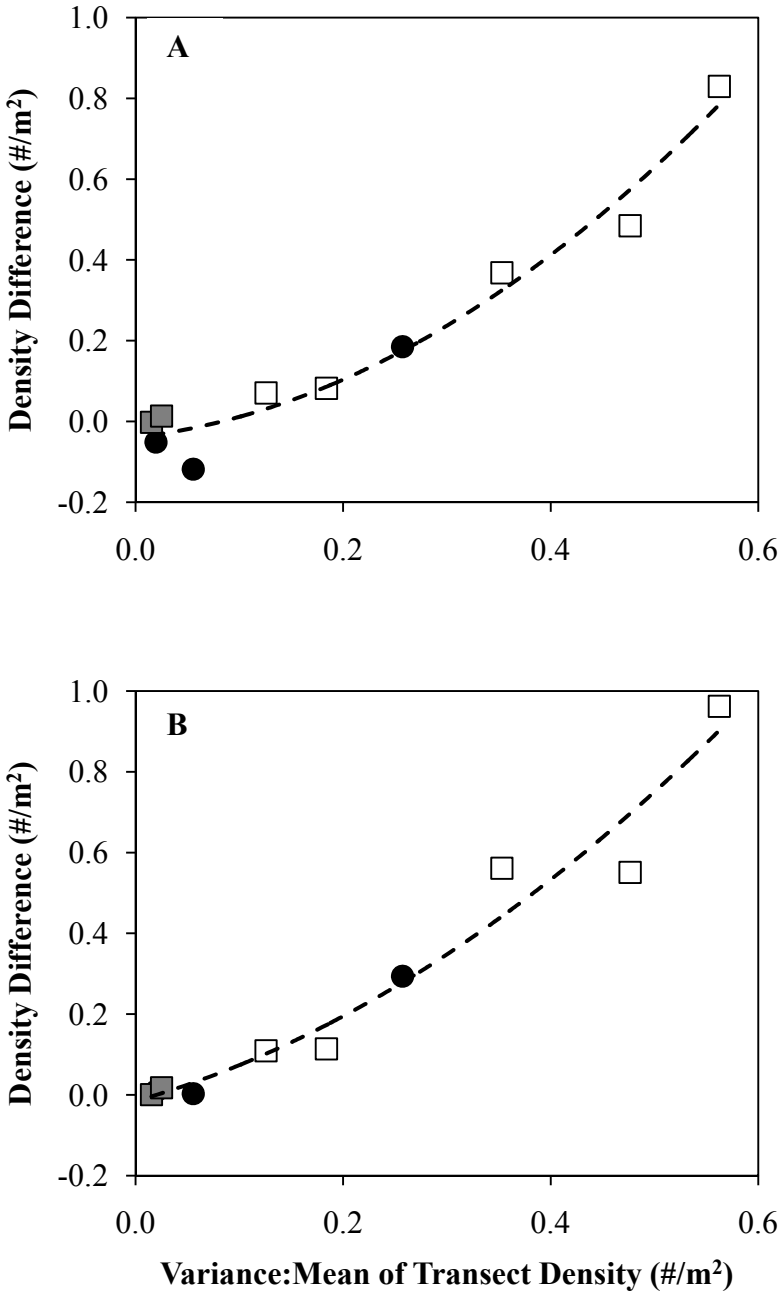

Figure 2.8 Regression of the transect variance-to-mean ratio and the differences in the average density estimates A) transect density minus T-square density, B) transect density minus Kendall-Moran density. The dashed line is a 2nd-order polynomial fit to the data. The gray squares represent the pink abalone estimates, the white squares represent the red abalone estimates, and the black circles represent the wavy turban snail estimates.

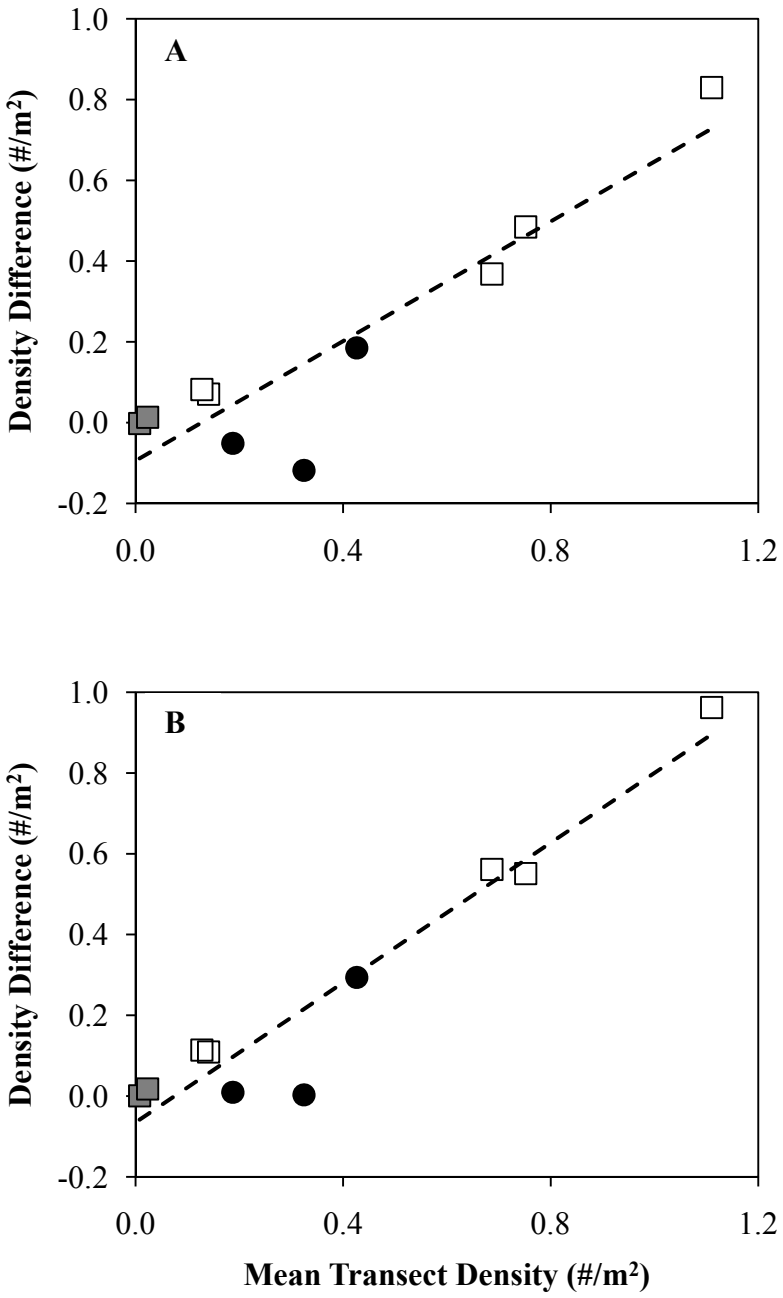

Figure 2.9 Regression of the average transect densities and the differences in average density estimates A) transect density minus T-square density, B) transect density minus Kendall-Moran density. The dashed line is a linear fit to the data. The gray squares represent the pink abalone estimates, the white squares represent the red abalone estimates, and the black circles represent the wavy turban snail estimates.

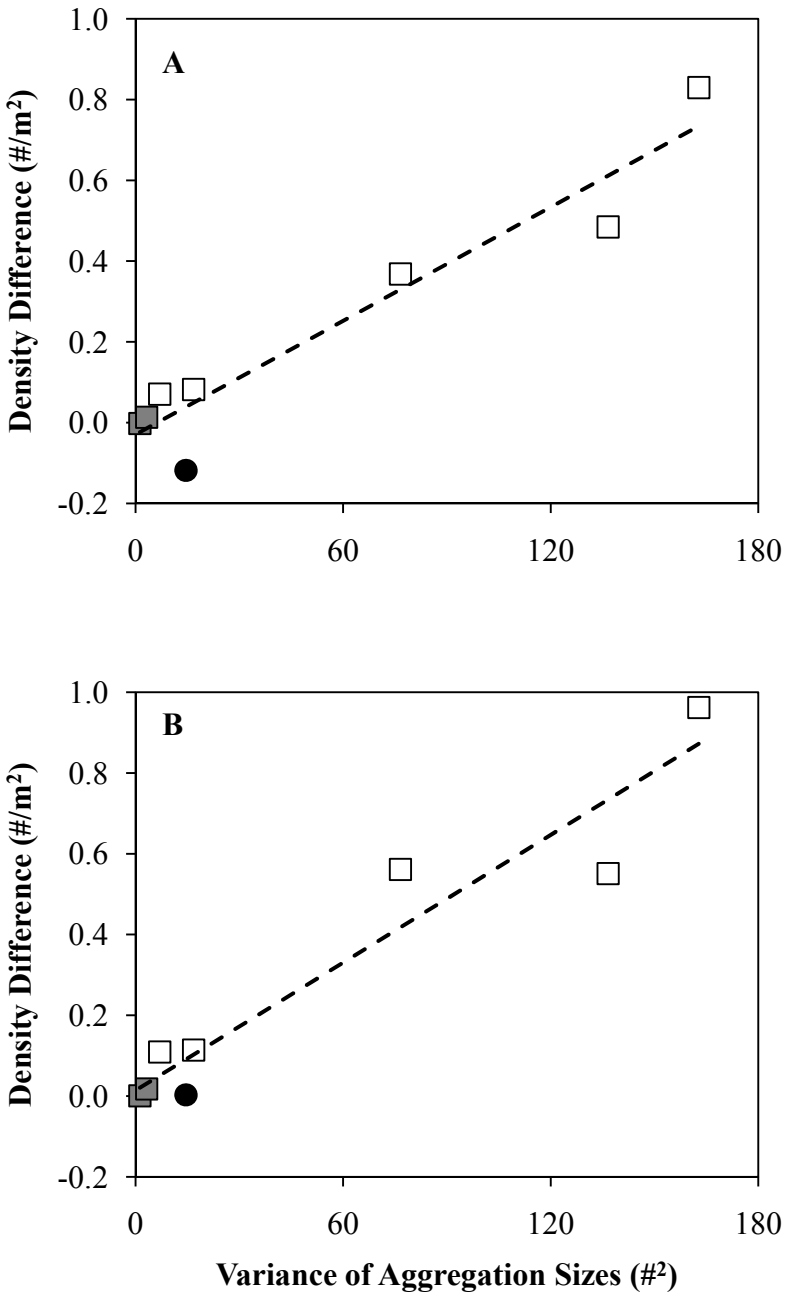

Figure 2.10 Regression of the variance of the aggregation sizes and the difference in the average density estimates A) transect density minus T-square density, B) transect density minus Kendall-Moran density. The dashed line is a linear fit to the data. The gray squares represent the pink abalone estimates, the white squares represent the red abalone estimates, and the black circle represents the wavy turban snail estimate.

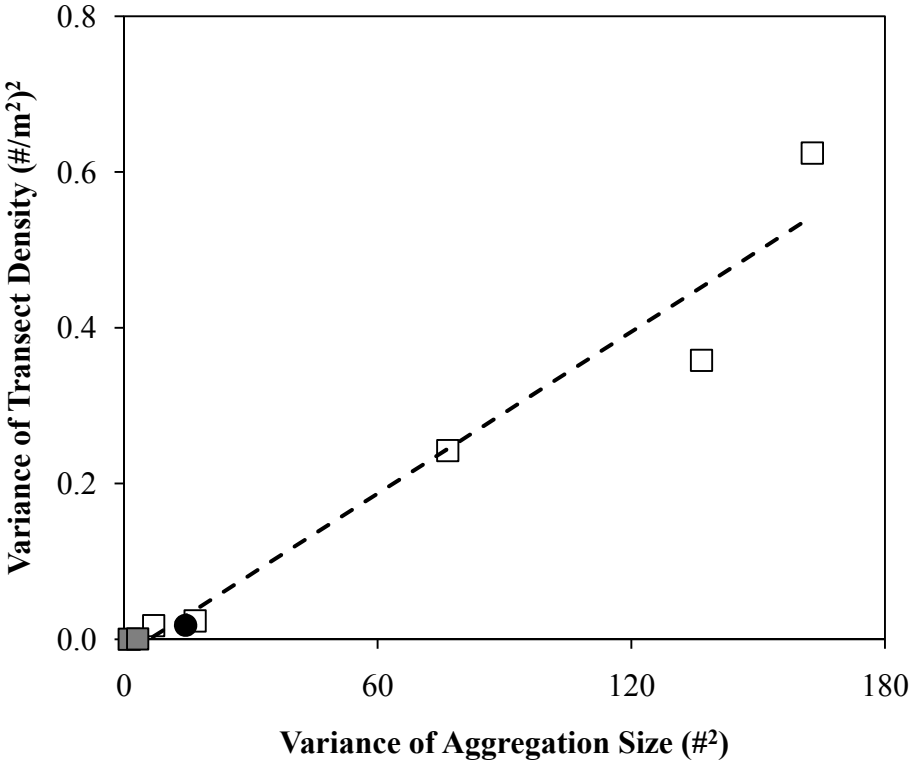

Figure 2.11 Regression of the variance of the aggregation sizes and the variance of the transect densities. The dashed line represents a linear fit to the data. The gray squares represent the pink abalone estimates, the white squares represent the red abalone estimates, and the black circle represents the wavy turban snail estimate.

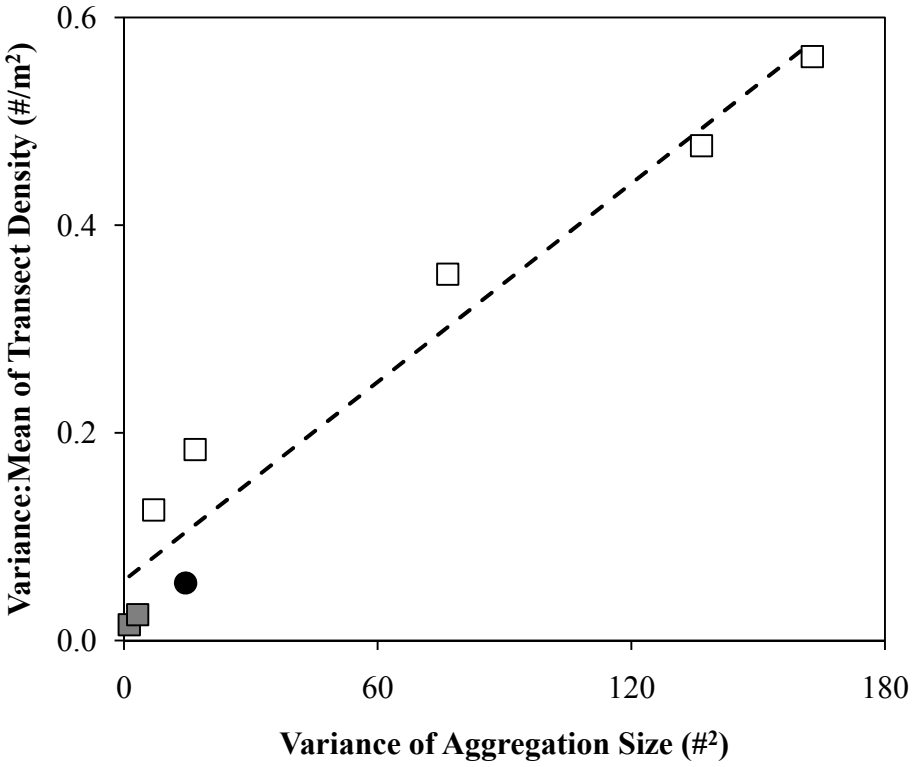

Figure 2.12 Regression of the variance of the aggregation sizes and the transect density variance-to-mean ratio. The dashed line represents a linear fit to the data. The gray squares represent the pink abalone estimates, the white squares represent the red abalone estimates, and the black circle represents the wavy turban snail estimate.

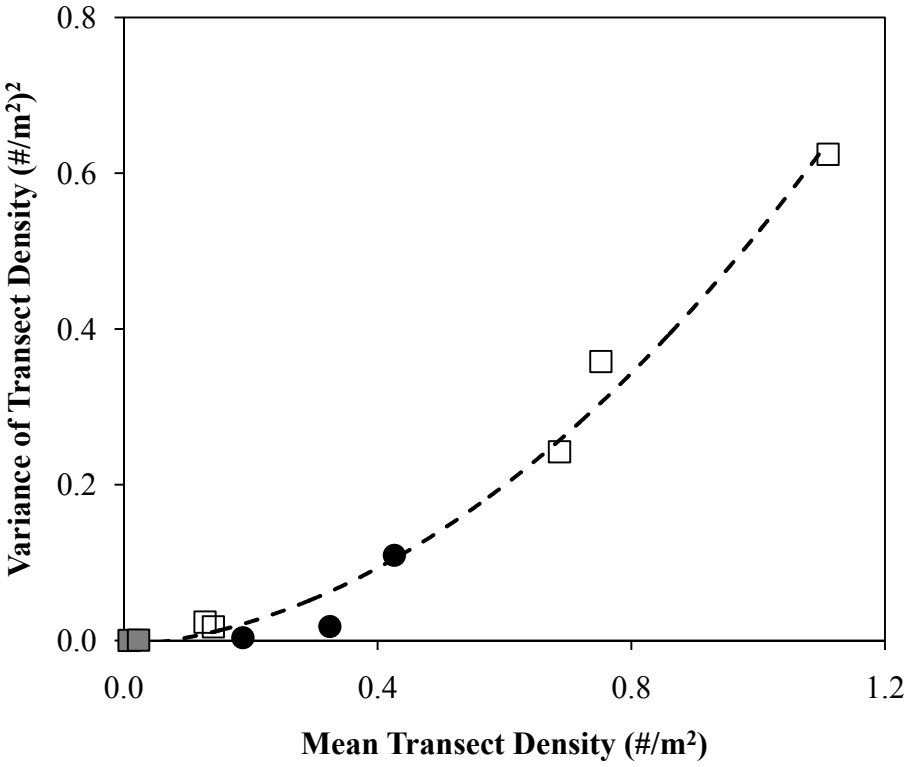

Figure 2.13 Regression of the average transect density with the transect variance. The dashed line represents a 2nd-order polynomial fit to the data. The gray squares represent the pink abalone estimates, the white squares represent the red abalone estimates, and the black circles represent the wavy turban snail estimates.

Table 2.1 List of population surveys including sample sizes and average transect densities for each species, location, and year. Location abbreviations are as in Figure 2.1. (T=Transect; TS=T-square; KM=Kendall-Moran)

			Sample Size			Total Transect	Transect Density	
Species	Location	Year	T	TS	KM	Area (m^2)	(#/m^2)	Fishing Pressure
Red Abalone	VDSP	2007	18	20	20	1080	0.69	Recreational
	OC	2007	15	15	14	900	1.11	Recreational
	FR	2007	10	29	28	395	0.75	Recreational
	HML	2007	12	12	12	475	0.14	Sea Otter
	SMI	2007	29	31	31	6480	0.13	Overfished
Pink Abalone	PL	2006	20	28	28	3000	0.02	Overfished
		2007	13	11	11	1950	0.01	
Wavy Turban Snail	PL	2005	6	14	14	720	0.19	Recent Small Fishery
		2006	6	26	26	642.5	0.43	
		2007	13	11	11	780	0.32	

Table 2.2 Summary statistics of transect densities, nearest-neighbor distances (NN distance), and aggregation sizes for each population. μ is the average value, σ is the standard deviation, and SE is the standard error. "--" indicates that no data were collected.

			Transect Density (#/m^2)			NN Distance (m)			Aggregation Size (#)		
Species	Location	Year	μ	σ	SE	μ	σ	SE	μ	σ	SE
Red Abalone	VDSP	2007	0.69	0.49	0.11	0.86	1.25	0.29	12.2	9.1	2.14
	OC	2007	1.11	0.79	0.20	0.80	0.88	0.24	14.3	12.8	3.29
	FR	2007	0.75	0.60	0.19	1.00	0.84	0.16	8.7	11.7	2.17
	HML	2007	0.14	0.13	0.04	1.84	3.08	0.89	3.9	2.6	0.76
	SMI	2007	0.13	0.15	0.03	1.74	1.45	0.27	3.9	4.2	0.78
Pink Abalone	PL	2006	0.02	0.02	0.01	5.05	5.73	1.08	2.0	1.8	0.38
		2007	0.01	0.01	0.00	6.18	5.68	1.71	1.6	1.1	0.34
Wavy Turban Snail	PL	2005	0.19	0.06	0.02	1.23	0.89	0.24	--	--	--
		2006	0.43	0.33	0.14	1.01	0.84	0.17	--	--	--
		2007	0.32	0.13	0.04	0.89	0.66	0.20	5.0	3.8	1.15

Table 2.3 Results of bootstrap linear regression analyses ($y = \alpha x + \beta$). N_T = transect density estimate; N_{TS} = T-Square density estimate; N_{KM} = Kendall-Moran density estimate; AS = aggregation size; h = h-statistic; ΔN_{TS} = Transect minus TS density estimates; ΔN_{TS} = Transect minus KM density estimates; σ^2 = variance; σ^2:μ = variance-to-mean ratio. $p(R<0)$ indicates the probability that the slope of the regression is negative. α, β, and R^2 are the values calculated for the true populations. For each parameter (α, β, and R^2), the bootstrap 95% confidence intervals are given. R^2 values in bold indicate a significant correlation at a 0.05 significance level. If the regression plot is available, the figure number is also given in this table (NA = Not Applicable).

Variable			95% CI			95% CI			95% CI			
x	y	α	lower	upper	β	lower	upper	R^2	lower	upper	p (R<0)	Figure
N_T	AS	11.333	8.7654	15.270	1.9592	1.3857	2.5627	**0.9371**	0.8298	0.9976	0.0000	2.6
σ_T^2	ΔN_{TS}	1.3772	1.2705	1.7820	-0.0056	-0.0605	0.0400	**0.9581**	0.7306	0.9965	0.0019	2.7
	ΔN_{KM}	1.5343	1.4137	2.4249	0.0478	0.0043	0.0953	**0.9557**	0.8886	0.9940	0.0002	
σ_{AS}^2	ΔN_{TS}	0.0047	0.0033	0.0057	-0.0309	-0.1161	0.0314	**0.9163**	0.6229	0.9992	0.0150	2.10
	ΔN_{KM}	0.0053	0.0037	0.0074	0.0136	-0.0429	0.0780	**0.9171**	0.7310	0.9943	0.0033	
N_T	ΔN_{TS}	0.7421	0.3453	0.9142	-0.0955	-0.2303	-0.0067	**0.8486**	0.2966	0.9795	0.0087	2.9
	ΔN_{KM}	0.8635	0.5934	0.9963	-0.0662	-0.1748	0.0020	**0.9234**	0.5771	0.9936	0.0039	
h	ΔN_{TS}	0.2851	-0.0213	0.5538	-0.3845	-0.8991	0.2278	0.3640	0.0029	0.9517	0.0362	NA
	ΔN_{KM}	0.3118	-0.0278	0.6135	-0.3626	-0.9394	0.2974	0.3499	0.0025	0.9431	0.0399	
E	ΔN_{TS}	0.2678	-0.0382	0.5528	-0.2852	-0.7226	0.2446	**0.3718**	0.0010	0.9654	0.0569	NA
	ΔN_{KM}	0.2845	-0.0630	0.6787	-0.2394	-0.7944	0.3482	0.3374	0.0006	0.9367	0.0815	
N_{TS}	ΔN_{TS}	0.5647	-0.4264	2.2125	0.0768	-0.0792	0.3159	0.0812	0.0002	0.8152	0.1754	NA
N_{KM}	ΔN_{KM}	0.6947	-0.8757	4.2469	0.1805	0.0022	0.4952	0.0488	0.0001	0.8507	0.2061	
σ_{AS}^2	N_T	0.0060	0.0047	0.0090	0.0822	0.0013	0.1854	**0.9252**	0.7894	0.9925	0.0002	NA
	σ_T^2	0.0034	0.0027	0.0040	-0.0205	-0.0409	0.0001	**0.9580**	0.9064	0.9985	0.0000	2.11
	σ_T^2:μ_T	0.0032	0.0028	0.0044	0.0587	0.0126	0.1091	**0.9493**	0.7836	0.9981	0.0001	2.12

Table 2.4 Results of bootstrap regression fit of a power function to the transect density and nearest-neighbor distances ($y = \alpha x^{\beta}$). N_T = transect density estimate (#/m^2); *NN* = nearest-neighbor distance (m).

Variable			95% CI			95% CI			95% CI		
x	*y*	α	lower	upper	β	lower	upper	R^2	lower	upper	Figure
N_T	*NN*	0.6826	0.5465	0.8169	-0.4867	-0.5663	-0.3657	**0.9837**	0.7606	0.9973	2.5

Table 2.5 Results of 2nd-order polynomial bootstrap regression analyses ($y = \alpha x^2+\beta x+\gamma$). N_T = transect density estimate; N_{TS} = T-Square density estimate; N_{KM} = Kendall-Moran density estimate; ΔN_{TS} = transect minus TS density estimates; ΔN_{TS} = transect minus KM density estimates; σ^2 = variance; σ^2:μ = variance-to-mean ratio. α, β, γ and R^2 are the values calculated for the true populations. For each parameter (α, β, γ and R^2), the bootstrap 95% confidence intervals are given. R^2 values in bold indicate a significant correlation at a 0.05 significance level. If the regression plot is available, the figure number is also given in this table.

Variable			95% CI			95% CI			95% CI			95% CI		
x	*y*	α	lower	upper	β	lower	upper	γ	lower	upper	R^2	lower	upper	Figure
σ_T^2:μ_T	ΔN_{TS}	2.0534	0.1048	4.6128	0.3120	-0.6650	1.2350	-0.0409	-0.1380	0.0180	**0.9596**	0.8692	0.9979	2.8
	ΔN_{KM}	1.6134	-1.3420	5.9347	0.7214	-0.6213	2.0220	-0.0161	-0.0871	0.0363	**0.9500**	0.8979	0.9992	
N_T	σ_T^2	0.4598	0.2919	0.9914	0.0700	-0.3126	0.2627	-0.0085	-0.0383	0.0290	**0.9837**	0.9458	0.9995	2.13

REFERENCES

Babcock, R., J. Keesing (1999) Fertilization biology of the abalone *Haliotis laevigata*: Laboratory and field studies. *Canadian Journal of Fisheries & Aquatic Sciences*, **56**(9), 1668-1678.

Belmar-Pérez, J., S.A. Guzmán del Próo, et al. (1991) Gonadic maturity and reproductive cycle of wavy turban snail (*Astraea undosa* Wood, 1828; Gastropoda: Turbinidae) in Bahia Tortugas, B. C. S. *Anales del Instituto de Ciencias del Mar y Limnologia Universidad Nacional Autonoma de Mexico*, **18**(2), 169-187.

Botsford, L.W., A. Campbell, et al. (2002). *Draft Abalone Recovery and Management Plan*. California Department of Fish and Game, Marine Region, Sacramento, CA.

Byth, K. (1982) On robust distance-based intensity estimators. *Biometrics*, **38**(1), 127-135.

California Department of Fish and Game (2001). *California's living marine resources: A status report*. California Department of Fish and Game: 592 pp.

California Department of Fish and Game (2002). *Draft Abalone Recovery and Management Plan*. California Department of Fish and Game, Marine Region, Sacramento, CA.

Cottam, G., J.T. Curtis (1949) A method for making rapid surveys of woodlands by means of pairs of randomly selected trees. *Ecology*, **30**(1), 101-104.

Diggle, P.J. (1975) Robust density estimation using distance methods. *Biometrika*, **62**(1), 39-48.

Engeman, R.M., R.T. Sugihara, et al. (1994) A comparison of plotless density estimators using Monte Carlo simulation. *Ecology*, **75**(6), 1769-1779.

Hart, A.M., H.K. Gorfine (1997) Abundance estimation of blacklip abalone (*Haliotis rubra*). II. A comparative evaluation of catch-effort, change-in-ratio, mark-recapture and diver-survey methods. *Fisheries Research (Amsterdam)*, **29**(2), 171-183.

Hines, A.H., J.S. Pearse (1982) Abalones shells and sea otters: Dynamics of prey populations in central California USA. *Ecology*, **63**(5), 1547-1560.

Hines, W.G.S., J.O. Hines (1979) The Eberhardt statistic and the detection of nonrandomness of spatial point distributions. *Biometrika*, **66**(1), 73-39.

Kendall, M.G., P.A.P. Moran (1963). *Geometrical Probability*. Griffin, London, England: 125 pp.

Krebs, C.J. (1999). *Ecological methodology*. Benjamin/Cummings, Menlo Park, Calif.: xii, 620 p. pp.

McGarvey, R., K. Byth, et al. (2005) Field trials and simulations of point-nearest-neighbor distance methods for estimating abalone density. *Journal of Shellfish Research*, **24**(2), 393-399.

Micheli, F., A.O. Shelton, et al. (2008) Persistence of depleted abalones in marine reserves of central California. *Biological Conservation*, **141**(4), 1078-1090.

Mullon, C., P. Freon, et al. (2005) The dynamics of collapse in world fisheries. *Fish and Fisheries*, **6**(2), 111-120.

Officer, R.A., M. Haddon, et al. (2001) Distance-based abundance estimation for abalone. *Journal of Shellfish Research*, **20**(2), 781-786.

Parnell, P.E., P.K. Dayton, et al. (2006) Marine reserve design: optimal size, habitats, species affinities, diversity, and ocean microclimate. *Ecological Applications*, **16**(3), 945-962.

Pielou, E.C. (1959) The use of point-to-plant distances in the study of the pattern of plant populations. *Journal of Ecology*, **47**(3), 607-613.

Pielou, E.C. (1960) A Single mechanism to account for regular, random and aggregated populations. *Journal of Ecology*, **48**(3), 575-584.

Ripley, B. (2004). *Spatial Statistics*. John Wiley & Sons, Inc., Hoboken, NJ: 252 pp.

Shepherd, S.A., L.D. Brown (1993) What is an abalone stock: Implications for the role of refugia in conservation. *Canadian Journal of Fisheries & Aquatic Sciences*, **50**(9), 2001-2009.

CHAPTER 3.

Modeling Vital Rates of a Pink Abalone (*Haliotis corrugata*) Population near San Diego, California

ABSTRACT

The results of this study provide important vital rate statistics, including mean growth and survival estimates and 95% confidence intervals, for a pink abalone population that may be recovering from an overfished status. Six functions fit to growth increment data were used to estimate the average age-at-maturity, the average time to reach the historic fishery minimum legal size (MLS), and the number of reproductive years before reaching the historic fishery MLS. In order to estimate the size-at-maturity for this population, I developed a non-lethal but effective method of determining the gender of mature abalone. I used this estimate of size-at-maturity and the historic MLS for this species to design a growth transition probability matrix. The transition probabilities were calculated based on the best-fit models to the growth increment data. The mean transition probabilities were similar regardless of the best-fit model used. Survival rates were estimated from mark-recapture data and compared across years, genders, and different levels of damage due to bar cuts to the foot.

The Point Loma pink abalone population near San Diego, CA, is characterized by slow growth with high survivorship (~0.77 yr^{-1}) in larger individuals. Annual growth increments were largest for the smallest individuals and growth rates dampened as the initial size of the animal increased. The overall shape of the predicted growth curve was dependent on the choice of data included in the analysis although the predictions from the

age-at-size analyses were similar regardless of model choice. The size-at-maturity was estimated to be 94mm. The average age-at-maturity was 8 – 9 years, and 24 – 29 years was the average time to reach the historic commercial MLS (159 mm). The sensitivity of the age-at-size estimates to ±10% parameter permutations increased as the size-of-interest increased. Survival rates in this population did not differ temporally, or between genders, but severe cuts to the foot did decrease the chance of survivorship.

INTRODUCTION

The pink abalone (*Haliotis corrugata*) is a large herbivorous gastropod that inhabits kelp-dominated high-relief rocky substrates. The geographic distribution of the pink abalone spans more than 1,300 km along the western coasts of the United States and México, from Point Conception in California to Isla Margarita in Baja California Sur. The vertical distribution ranges from 3 to 30 m depths, but population densities are greatest between 10 and 20 m (Cox 1962; Guzmán del Próo 1992). Fisheries for pink abalone closed in California in 1997 due to severe population declines (California Department of Fish and Game 2002), but the fishery in México is still active. Pink abalone, also known as the yellow abalone (abulón amarillo) in México, was the dominant species in the Mexican fishery before 1976, especially in the more productive central coast (Guzmán del Próo 1992).

Pink abalone are long-lived (20+ years), slow-growing, late-maturing (3-8+ years), but highly-fecund animals. They are relatively sedentary as adults, and rely on dense aggregations of spawning individuals for successful fertilization of gametes (Shepherd and Brown 1993; Babcock and Keesing 1999). Fertilization occurs externally to the animal, within the water column. The duration of the planktonic larval phase is

fairly short (5 – 8 days (Leighton 1974)), such that populations may be largely self-recruiting (Prince, Sellers et al. 1988; Tegner 2000). The strength of recruitment to the population is variable from year to year (Tegner 1989; Karpov, Haaker et al. 1998) and patterns in stock-recruitment curves are difficult to detect (McShane 1995). Catch-per-unit-effort indices for abalone fisheries exhibit hyperstability even when stocks are declining because of the aggregating behavior of individuals in the populations (Breen 1992; McShane 1994; Dowling, Hall et al. 2004). These life history-traits described above are correlated with a susceptibility to over-fishing in both marine fish and invertebrate species (Jennings, Reynolds et al. 1998; Sadovy 2001; Gascoigne and Lipcius 2004; Sadovy and Domeier 2005).

Estimating vital rates (i.e. growth, survival, and size-at-maturity) is important to determine appropriate size limits for exploitation or for determining the recovery potential of impacted populations. Overestimating growth or survival rates in the population may lead to growth over-fishing or to recruitment over-fishing (Troynikov and Gorfine 1998; Rogers-Bennett, Rogers et al. 2003). Growth over-fishing occurs when the minimum legal size (MLS) set for the fishery is too small to maximize the biomass of a cohort at the time it enters the fishery. The consequences of growth over-fishing are economic rather than biological. Recruitment over-fishing occurs when the MLS is too small to allow individuals to reproduce for a sufficient number of years prior to entering the fishery. This can significantly impact the potential for population growth. Consequently, accurate assessments of the average age-at-maturity and the average time to reach the fishery are critical for developing effective management strategies. Vital rates may also be used to develop a life-history based matrix population model that is

useful for identifying the potential effects of different fishing or recovery efforts on the population growth rate.

An understanding of the degree of variability (i.e. individual, temporal) inherent to the population is also important to incorporate into population dynamics models. Temporally stochastic rates may reduce the predicted long-run population growth rate relative to a deterministic model (Lande, Engen et al. 2003). The vital rates of abalone may vary as environmental conditions change (Day and Fleming 1992; Vilchis, Tegner et al. 2005). The availability and quality of food has been shown in laboratory studies to influence growth, mortality, and fecundity in abalone (Uki and Kikuchi 1982; Clarke and Creese 1998). Temperature changes also impact growth rates (Diaz, Re et al. 2006). In addition, mortality may depend on the density of conspecifics (Day, Gilmour et al. 2004) or the abundance of predators in the area (Tutschulte 1976; Beal and Kraus 2002). The relative impact of the variability in the vital rate estimates to the population growth rate and optimal size limits may be explored with sensitivity analyses.

The primary purpose of this study is to estimate vital rates, including the 95% confidence intervals of the mean estimates, for a pink abalone population in the Point Loma kelp forest near San Diego, California. This population is currently at low abundances, and the potential for recovery is unknown (*see Chapter 4*). In order to estimate the size-at-maturity for this population, I developed a non-lethal but effective method of determining the gender of mature abalone. I used this estimate of size-at-maturity and the historic MLS for this species to design a growth transition probability matrix. Six functions (Gaussian, Tanaka, Logistic Dose-Response, Ricker, Richards, and the von Bertalanffy Growth Curve) fit to growth increment data were used to inform the

growth transition probabilities and to estimate the average age-at-maturity, the average time to reach the historic fishery MLS, and the number of reproductive years before reaching the historic fishery MLS. The growth transition probability matrix is the foundation of a life-history based matrix population model for this population.

Survival rates were estimated from mark-recapture data and compared across years, genders, and different levels of damage due to bar cuts to the foot. When the abalone fishery was still open in southern California, pink abalone were reported to be particularly vulnerable to fishing-related mortality due to bar cuts (Burge, Shultz et al. 1975), and declines in the relative abundance of barely sub-legal abalone were attributed to bar-cut mortality (Tegner, Breen et al. 1989). The influence of bar cuts on the population growth rates would be useful to examine for fished populations that are potentially vulnerable to sub-legal bar-cutting. In addition, temporal variability and differences in vital rates between genders would influence the design of a matrix population model for this species.

METHODS

Study Area

The Pt. Loma kelp forest is one of the largest kelp forests in the world extending ~10 km along the coast of San Diego, CA (Dayton, Tegner et al. 1992). Within the central part of the kelp forest, I demarcated a 9-hectare area (300 m x 300m) which ranged in depth between 12 and 15 meters and contains substantial pink abalone habitat (Figure 3.1). Surveys of population- and aggregation-level characteristics were conducted concurrently with the tag-recapture study within this area (*see Chapter 4*). Tag locations were obtained by a random-number generation of latitudes and longitudes

within the 9-hectare area. The study area is characterized by a low-relief sandstone and mudstone substrate with scattered boulders and extensive ledge systems, and is dominated by Giant Kelp (*Macrocystis pyrifera)* with holdfasts often measuring over a meter in diameter. Clearings in the Giant Kelp are dominated by understory kelp species (*Laminaria*, *Pterygophora,* and *Eisenia*).

Sampling Methods

365 pink abalone were tagged over a nearly 3-year period (December 2003 – October 2006). Abalone were collected using commercially-made abalone irons and brought up to the boat for tagging. We recorded individual statistics including site location, size, and gender of each tagged animal. We also qualitatively assessed the level of damage to the foot of the abalone that may have occurred during the collection process as one of five categories – no damage (n = 240), light cut (to the foot) (n = 65), moderate cut (n = 26), severe cut (n = 28), and other (n = 6). Although dimensions of the damaged area were not measured, the differences among these categories were clear such that abalone could quickly be assigned to a category without doubt. A light cut was typically ~1 mm deep and resulted from the iron barely grazing the foot. Moderate cuts were deeper, enough to produce a small flap of the foot, approximately 1-3 mm deep. Moderate cuts were made when the abalone home scar, to which the foot conforms, was not entirely smooth. Severe cuts to the foot were typically much greater the 3 mm deep but did not penetrate into the body cavity.

The tagged abalone ranged in initial size between 23 mm and 184 mm. Abalone greater than ~80 mm were marked with numbered stainless steel washer tags wired through two adjacent respiratory holes in the shell with stainless steel wire. This tag

design has been used extensively for tag-recapture studies of abalone and has been shown to have no detectable effect on growth rates for red abalone (Haaker, Parker et al. 1998). Small numbered vinyl tags were applied to the shells of individuals smaller than 80mm with SuperGlue and coated with clear nail polish to add a protective layer to the tag. This smaller tag was meant to be temporary until the animal grew large enough that the stainless steel wire could be threaded through its respiratory holes. After the tagging process, all abalone were then physically replaced to suitable habitat at the same site by the scuba divers.

Subsequent visits to the tagging sites were conducted to obtain growth and survival estimates. Because the pink abalone at this location were relatively sedentary, I was able to re-encounter tagged animals by revisiting the original tagging locations each year. The timing of these visits was opportunistic between April and October of each year so that the intervals between encounters were not always equal to one year (Table 3.1). The duration of the census period also varied. I also frequently encountered tagged abalone while conducting the many other population surveys in the area. Whenever I saw a tagged abalone, I recorded the date, location, tag number, and size of the individual. Prior to 2006, I measured the re-encountered individuals while they were still attached to the substrate in order to minimize stress to the animal. However, this technique yielded poor precision in the growth rate estimates due to high measurement error. During the final years of the study (2006 and 2007), I removed the abalone from the substrate before measuring them while under water. All of the abalone measured in this way were replaced to the exact location from which I took them. For many of the

abalone, I measured the size five or more times in order to estimate the measurement error for this modified technique.

Modeling Techniques

Growth Estimation

In order to estimate the size-specific growth rate of individuals in this population, all growth increment data were standardized to annual increments by

$$\Delta L_{365} = \Delta L_t(365/t)$$

where ΔL_t is the measurement difference between the two census dates and t is the time at large in number of days. Only individuals with $t > 2/3$ year (243 days) were included in the growth study in order to avoid extrapolating the annual growth rates from much shorter time periods. Some abalone were encountered multiple times. In these cases, the growth rates were calculated for the longest period at large. The average time interval was 1.5 years and the maximum interval was 2.8 years.

Growth increments for small individuals (<80 mm) were unavailable from the tag-recapture data due to the limited detectability of this size class. To supplement the growth data, I measured 140 one-year-old pink abalone reared in the Southwest Fisheries Science Center facility from Point Loma pink abalone parents. These juveniles were maintained in ambient water temperature and fed an initial diet of diatoms cultured naturally from Point Loma algae (a mixture of fleshy red algae and kelp species).

I also included juvenile pink abalone growth data reported by Tutschulte (1976) for 150 additional animals ranging in initial size between 13mm and 94mm. Ninety-five of these abalone were maintained under laboratory conditions for one year and fed *Macrocystis pyrifera* blades. Thirty-six abalone were maintained in net cages at 9m

depth. A mixture of red algae and kelp species were placed in the cages periodically to provide food for these abalone. Nineteen abalone were marked and released to the wild and recaptured the following year. In all cases, tags were attached with wire through the respiratory holes and a small notch was made in the abalone shell that would serve as a reference point for measuring the growth increment the following year.

Because laboratory-reared animals are often considered to grow faster than animals in the wild, I performed an analysis of covariance (ANCOVA) on the growth data from Tutschulte (1976) to determine the appropriateness of including the laboratory-reared abalone in the growth rate analysis. The growth increment was the dependent variable with the initial size as a covariate and the three different treatments as the groups, or factors. The ANCOVA results showed no significant treatment effect ($F_{2,144}$ = 1.92; p = 0.1507), but the initial size of the abalone did have a significant effect ($F_{1,144}$ = 39.59; p = 0.0000). There was also a significant interaction effect between initial size and treatment ($F_{2,144}$ = 6.51; p = 0.0020).

I investigated the fit of six growth functions to the annual growth increment data (ΔL) versus the initial size (L_t) – Gaussian, Tanaka, Logistic Dose-Response, Ricker, Richards, and the von Bertalanffy Growth Curve (Table 3.2). The relative fit of these models to the pink abalone growth data was determined by ranking the Akaike Information Criterion (AIC) values (Akaike 1974). I also examined R^2 values, the sum of the squared residuals (SSR), and the Bayesian Information Criterion (BIC) as alternative methods for determining the best-fit model. In order to examine the influence of including laboratory-reared animals in the analysis, I fit these six growth models to two

sets of data – one set that included all available data (n = 366), and another set that included only those animals that had grown in non-laboratory conditions (n = 131).

For each of the datasets, the most parsimonious model with the least sensitivity to parameter permutations was chosen to inform the growth transition probability estimates. I calculated the mean and 95% confidence intervals of the transition probabilities based on the mean and 95% confidence intervals of the model parameter estimates. This method is more representative of an infinite probability distribution than the traditional method of using the relatively sparse growth data to inform the transition probabilities (Rogers-Bennett and Rogers 2006). The transition probabilities were calculated for a 4 x 4 stage-based matrix. The four stages in the model are 1) juveniles (25 – 50 mm), 2) subadults that are transitioning from an immature to a mature state (50 – 100 mm), 3) intermediate-sized adults (100 – 153 mm), and 4) large adults (153 + mm). The juvenile stage initiates after the abalone reaches 25 mm in order to be consistent with a red abalone matrix model for which the transition probability from egg to 25 mm was estimated (Rogers-Bennett and Leaf 2006). This estimate of first-year survival rate is unavailable for pink abalone populations. The range of sizes used for the subadult stage was determined based on the size-at-maturity results (*see below* and Figure 3.4). The division between the intermediate-sized and large adults was determined based on the historic minimum legal size for the recreational pink abalone fishery (MLS_R).

Size-at-Maturity Estimation

Size-at-maturity is an important demographic characteristic to determine for a population because of its influence on the net reproductive rate of individuals. An effective method for determining the size-at-maturity is to examine the maturity of egg

samples taken from histological sections of the gonad from multiple individuals across a broad range of sizes (Rogers-Bennett, Dondanville et al. 2004). This method requires sacrificing individuals but allows for differentiation of immature, mature, and necroptic (abnormal or senescent) eggs. Due to the low abundance of the local pink abalone population (*see Chapter 4*), the options for assessing the size-at-maturity were limited to non-lethal methods. I used the size at which gender determination was possible as a proxy for the size-at-maturity for the Point Loma pink abalone population.

The standard method of determining the gender of live abalone is to inspect the color of the gonad by pulling the foot away from the shell on the right posterior side of the abalone. When the abalone is gravid with gametes, this method is effective (*personal observation*). Male gonads are a creamy white color and female gonads are a dark green color. If the abalone contained few gametes (i.e. small gonad), the color of the gonadal area may be dark even if the animal were male due to the dark color of the digestive material located within the cylindrical gonad. When the gender determination based on visual inspection of the gonad color was inconclusive, I sampled the gonad with a 16-gauge syringe and examined the contents of the sample for either eggs or sperm. If the sample contained neither gamete type, I recorded that individual as immature.

Before applying the syringe sampling method to wild abalone, I tested the influence of the gonad-sampling method on the mortality of red abalone (*H. rufescens*) in the laboratory. On February 25, 2005, I tagged 27 red abalone housed at the University of California, Davis, Bodega Marine Laboratories using the tagging methods described above. I measured the lengths and weights of each abalone and determined the gender based on visual inspection of gonad color. I randomly chose nine of the abalone to

sample the gonad with a 25-gauge syringe, nine to sample with a 16-gauge syringe, and the remaining nine were not sampled with a syringe. The genders of the 18 sampled abalone were then determined by inspecting the samples for gametes. All of the abalone were returned to a flow-through seawater tank in ambient-temperature water for 75 days. No mortality resulted by the end of the 75 days. At the end of the experiment, all 27 abalone were dissected to assess the accuracy of the syringe method for determining gender. Only 64% of the genders determined by visual inspection of gonad color were consistent with the genders determined by dissecting the gonad whereas 89% of those sampled with a 25-gauge syringe and 100% of those sampled with a 16-gauge syringe were consistent.

In order to estimate the relationship between size and maturity in the Point Loma pink abalone, I determined the genders of 150 abalone in 2006 and 2007. I fit a generalized linear model with a binomial distribution to the data, where a positive gender identification was given a value of one and an immature individual was designated by a zero. The size at which 50% of the abalone were estimated to be mature was used as the size-at-maturity for this population. The equation that was fit to the data was:

$$P(L_i) = \frac{e^{(\beta_0+\beta_1 L_i)}}{1 + e^{(\beta_0+\beta_1 L_i)}}$$

where, P(L_i) is the probability of successful gender determination, L_i is the length of the abalone, and β_0 and β_1 are parameter estimates of the linear predictor.

Age-at-Size Estimation

The relationship between length and age was determined by iteratively solving the fitted growth functions, starting at a small initial size (0.01 mm). Using these size-at-age

curves, I estimated the average age-at-maturity (94 mm) and the average time to reach the minimum legal size in the historic recreational (MLS_R = 153 mm) and commercial fisheries (MLS_C = 159 mm). I tested the sensitivity of these estimates to changes in the model parameters by varying the parameters by ±10%.

Survival Estimation

Individual survival rates of tagged abalone were estimated with the Cormack-Jolly-Seber (CJS) approach available in Program Mark, a free software program designed for analyzing mark-recapture data (White and Burnham 1999; Cooch and White (eds.) 2008). The CJS approach allows for the simultaneous estimation of survival (φ) and recapture (p) probabilities in the population based on individual encounter histories. An encounter history is a series of zeros and ones describing the timing of sighting an individual throughout the study period. For example, the encounter history "10011" indicates that the individual was tagged initially in the first time period, not encountered during the next two time periods, but was re-sighted during the final two time periods. This example illustrates the need to estimate both survival and detectability in the data.

Individual encounter histories may also be categorized to allow for estimation of survival rates across treatments. To determine the effect of damage incurred during the tagging process on the subsequent survival of individuals, I divided the encounter histories (n = 342) into four groups, excluding individuals recorded with "other" damage. Because I did not re-encounter any tagged individuals smaller than 79 mm throughout the study, I also excluded these smaller individuals from the analysis (n = 17). In a separate analysis, I estimated the survival of males and females. I included in this analysis only those individuals for which I had positively determined their genders (e.g. sexually

mature individuals that were reproductive at the time of gender determination) ($n_{\female}$ = 114; $n_{\male}$ = 105). A third analysis was conducted to estimate the overall average survival rate for the population which treated all groups as equal (n = 314). For this analysis, any treatment group previously determined to differ in its survival rate (i.e. severely cut individuals) was excluded from the analysis. I also excluded individuals smaller than 79 mm and those with "other" damage.

I used the CJS method (Cormack 1964; Jolly 1965; Seber 1965) to fit a series of *a priori* survival (φ) and recapture (p) probability models to the encounter history data (Table 3.1). The set of candidate models was chosen based on the purpose of the analysis (Table 3.3). The basic set of four models tested the time-dependence of the survival and recapture probabilities. Five additional models tested the effect of the treatment group (G) on the probability estimates. Goodness of fit (GOF) tests for the most general, fully time-dependent model ($\varphi_t p_t$) in the candidate model set (Test2 and Test3 in program RELEASE) were performed to determine if the basic assumptions of the mark-recapture methods had been met. The four basic assumptions of the CJS method are:

1) Every individual has an equal probability of being encountered during census occasion (i).
2) Every marked individual has an equal probability of surviving to the next census occasion (i + 1).
3) Marks are not lost or overlooked.
4) The time interval between sampling is long relative to the sampling period.

The most critical of these assumptions are numbers 1 and 2, that all individuals have equal survival (Test2) and catchability (Test3) (Lebreton, Burnham et al. 1992; Krebs 1999; Cooch and White (eds.) 2008).

Violations of these assumptions may result in overdispersed data for the model. In such cases, a parameter describing the overall dispersion in the data, ĉ, may be used to adjust the rankings and relative weights of the candidate models. If the model describes the variance in the data well, then ĉ will be equal to one. If the value of ĉ is greater than three, the model may be inappropriate for the data (Cooch and White (eds.) 2008). The ĉ parameter was estimated by the median-ĉ simulation method in Program MARK. The quasi-AIC_c ($QAIC_c$) value is the model AIC value adjusted by the value of ĉ to accommodate overdispersion in the data. For all analyses, I report the survival and detectability estimates of the most parsimonious model as well as a weighted average of the best-fit models (i.e. those models with $QAIC_c$ weight values > 0).

RESULTS

Growth Estimation

Model Selection

Annual growth increments were calculated for seventy-six pink abalone from Point Loma, ranging in initial size between 91 mm and 178 mm (μ = 141.3 mm, σ = 18.8 mm). The measurement error (standard deviation of 5 to 10 measurements) associated with re-measuring individuals while under water ranged between 0.0 mm and 1.4 mm (μ = 0.4 mm, σ = 0.3 mm). The measurement error for growth increments was 0.6 mm. Additional measurement error is introduced by the process of estimating the annual growth increment for intervals not equal to one year (Day and Fleming 1992). This error

is not estimable without seasonal data on growth rates, but it is likely to be small in adult abalone because of the slower overall growth rates of adults. The average annual growth increment for these 76 abalone was 3.4 mm / year ($\sigma = 3.6$). A total of 140 abalone spawned on August 11, 2006 and reared under laboratory conditions was measured on November 16, 2007 (467 days old). The average annual growth increment estimated for these abalone was 22 mm ($\sigma = 2.3$ mm).

The relative ranks of the best-fit growth models were sensitive to the choice of data included in the analysis (Table 3.4). Excluding laboratory-reared individuals favored growth models with a linearly decreasing relationship between initial size and annual growth increments (Figure 3.2). The difference in the AIC values for the von Bertalanffy and Richards functions was 1.9, indicating that these two functions are essentially equivalent models for these data. In fact, the Richards function becomes the von Bertalanffy function when the parameter *n* is equal to -1. The mean estimate of this parameter for the analysis excluding laboratory data is -1.04 (Table 3.5).

Inclusion of the laboratory-reared abalone dampened the growth rates at smaller size classes such that the best-fit models for these data incorporated greater curvature in the fit than is possible with the simple von Bertalanffy function (Figure 3.3). The von Bertalanffy function was ranked number 5 with this analysis whereas it ranked number 1 when the laboratory data were excluded. The top four growth models (Logistic Dose-Response, Tanaka, Richards, and Gaussian) were equivalent ($\Delta AIC < 2$) according to the AIC values when all available data were included in the analyses (Table 3.4).

The Ricker function did not fit the data well regardless of which data were included in the analysis. This growth function failed by underestimating growth rates at

small initial sizes. Because of the negative R^2 value resulting from the fit to all of the available data, I discontinued consideration of this model fit for the estimates of age-at-size.

Growth Transition Probabilities

The best-fit models with the smallest sensitivities to parameter permutations for each dataset were the von Bertalanffy equation (non-laboratory conditions) and the Logistic Dose-Response equation (all data). The mean probability estimates in both matrices are very similar, differing by a maximum of 0.04 yr^{-1} (Table 3.6). The 95% confidence intervals differ between the two matrices to a greater extent (0.01 – 0.11 yr^{-1}).

Size-at-Maturity Estimation

The abalone used to determine the size-at-maturity ranged in size between 36 mm and 177mm. Eighty-eight percent of the animals were mature – 62 male, 70 female, and 18 immature abalone. Ten of the abalone were smaller than 100 mm. The smallest male abalone successfully identified was 88 mm. The smallest female was 94 mm. The largest sampled abalone with insufficient gametes for gender determination was 167 mm. This animal was sampled on June 18, 2007 which is the middle of the spawning period for pink abalone (April – November).

The generalized linear model fit to the data is shown in Figure 3.4. A summary of the fit results is given in Table 3.7. The size at which the genders of the abalone may be determined 50% of the time is 94 mm. This size was used as a proxy for the size-at-maturity in the age-at-size estimation analysis.

Age-at-Size Estimation

The results of the age-at-size calculations are shown in Tables 3.8 and 3.9. The sensitivity to parameter estimates increased as the size of interest increased, such that the greatest sensitivities were observed in the time to reach the MLS_C. Age-at maturity was the least sensitive to 10% permutations in the parameters for the models fit to the non-laboratory reared individuals (Table 3.8). The age-at-size estimates based on the Tanaka function were frequently the most sensitive to permutations in parameter estimates regardless of which data were included in the analysis.

Age-at-Maturity

The mean age-at-maturity estimation was not very sensitive to the model selected or to the choice of data inclusion in the analysis (Tables 3.8 and 3.9). The estimated age-at-maturity for non-laboratory reared individuals was 8 – 9 years for the 5 best-fit models and 7 – 9 years for the 5 best-fit models including all available data. The mean estimated age-at-maturity calculated from the Ricker function fit to the non-laboratory reared abalone was 17 years. Sensitivities in the results ranged from 1 year (Ricker – non-laboratory conditions) to 21 years (Tanaka – all data). The median of the sensitivity ranges across the six different models was 3 years for both datasets.

Time-to-Recreational-Fishery

The mean TTF-MLS_R was sensitive to the choice of data inclusion in the analysis (Tables 3.8 and 3.9). The estimated TTF-MLS_R for non-laboratory reared abalone was 21 – 22 years for the 5 best-fit models and 23 – 26 years for the 5 best-fit models including all available data. The mean estimate calculated from the Ricker function was 32 years for the non-laboratory reared data. Sensitivities in the results ranged from 4

years (Gaussian – non-laboratory conditions) to 49 years (Tanaka – all data). The median of the sensitivity ranges across the six different models for non-laboratory conditions was 18.5 years and 17.5 years for the 5 models fit to all available data.

Time-to-Commercial-Fishery

The results of the growth versus age analysis for the six models fit to the two datasets are illustrated in figures 3.5 and 3.6. The mean TTF-MLS_C was sensitive to the choice of data inclusion in the analysis (Tables 3.8 and 3.9). The estimated TTF-MLS_C for non-laboratory reared abalone was 24 years for the 5 best-fit models and 26 – 29 years for the 4 best-fit models including all available data. The von Bertalanffy growth curve fit to all of the data asymptoted prior to reaching 159 mm, so that no estimate of the time to fishery could be determined for this model. The mean estimate calculated from the Ricker function was 35 years for the non-laboratory reared data. Sensitivities ranged from 6 years (Logistic Dose-Response – all data) to 53 years (Tanaka – all data). The median of the sensitivity ranges across the six different models for non-laboratory conditions was 18.5 years and 23 years for the 4 models fit to all available data.

Time between Ages-of-Interest

The amount of time between ages of interest was somewhat consistent across the different models and between treatments. The estimated time between reaching maturity and entering the historic recreational fishery was 12 – 15 years (median: 13 years) for non-laboratory conditions and 14 – 25 years (median: 15 years) for all data. The estimated time between entering the historic recreational fishery and entering the historic commercial fishery was 2 – 3 years (median: 3 years) for non-laboratory conditions and 2 – 3 years (median: 2.5 years) for all data.

Survival Estimation

The range of initial sizes of tagged pink abalone used in the survival analyses was 79 – 187 mm although the number of animals included in each subset of the analyses differed (Table 3.10). The test of binomial dispersion in the data (median ĉ) showed some overdispersion (Table 3.10), so that QAIC values, weights, and deviances were used to rank the models and estimate weighted average survival rates (Table 3.11). In all three analyses (damage-specific, gender-specific, and total average survival), the difference in the QAIC values between the two best-fit models was greater than 2.0, indicating that the two models were not equivalent. However, the corresponding QAIC weights suggested that weighted averages across multiple models may be appropriate.

All of the best-fit candidate models included time as a factor influencing the recapture probabilities (Table 3.11). The recapture probability increased as the length of the census period increased. The lowest recapture probability (0.01) occurred during the 3rd census period in the winter of 2005 (census period = 9 days). The highest recapture probability occurred during the 2nd census period in the summer of 2004 (census period = 176 days). A regression of the relationship between census period length (x-axis) and recapture probability (y-axis) yielded a positive linear function of $y = 0.0033x + 0.0798$ ($R^2 = 0.8621$).

Effect of Damage to the Foot

Three of the nine candidate models for the damage analysis fit the data well enough to yield non-zero QAIC weights (Table 3.11). The QAIC value of the best-fit model ($\varphi_d p_t$) was 2.68 points less than the 2nd best-fit model ($\varphi_. p_t$), indicating that the data were not equally well described by both models. The 3rd best-fit model ($\varphi_t p_t$) had a

ΔQAIC value of 4.98 and a QAIC weight value of 0.06. Because this low-weighted model was the only one to include time as a factor influencing survival, the weighted average estimates of survival differed by only 0.03 yr^{-1} through time (Table 3.12). The average survival and recapture estimates calculated from the best-fit model and from the weighted averages of the three best-fit models differed by only as much as 0.07 (Table 3.12) because of the large differences in the weight factors for each model (Table 3.11).

Because the ΔQAIC for the 2nd best-fit model is greater than 2.0, I will report the results of the best-fit model in the text (*but see Table 3.12 for estimates based on the weighted averages*). Survival probabilities were similar for abalone with no damage to moderate damage (no damage: 0.74 ± 0.05 SE; light cut: 0.84 ± 0.07 SE; moderate cut: 0.86 ± 0.09 SE), but were much reduced for abalone with severe damage to the foot (0.52 ± 0.11 SE). The 95% confidence intervals around the average estimates reveal overlap in the range of estimated survival rates across groups (Table 3.12).

Gender Analysis

Three of the nine candidate models for the gender analysis fit the data well enough to yield non-zero QAIC weights (Table 3.11). The QAIC value of the best-fit model ($\varphi. p_t$) was 2.07 points less than the 2nd best-fit model ($\varphi_g p_t$), indicating that the data were not equally well described by both models. The 3rd best-fit model ($\varphi_t p_t$) had a ΔQAIC value of 5.06 and a QAIC weight value of 0.05. Because this low-weighted model was the only one to include time as a factor influencing survival, the weighted average estimates of survival differed by only 0.03 through time (Table 3.13). The average survival and recapture estimates calculated from the best-fit model and from the

weighted averages of the three best-fit models differed by only as much as 0.02 (Table 3.13) because of the large differences in the weight factors for each model (Table 3.11).

Because the ΔQAIC for the 2nd best-fit model is greater than 2.0, I will report the results of the best-fit model in the text (*but see Table 3.13 for estimates based on the weighted averages*). Survival probabilities were the same for females and males, and did not change through time (0.73 ± 0.05 SE).

Average Survival

Two of the four candidate models for the analysis including all non-severely cut individuals greater than 78 mm in length fit the data well enough to yield non-zero QAIC weights (Table 3.11). The QAIC value of the best-fit model ($\varphi. p_t$) was 4.63 points less than the 2nd best-fit model ($\varphi_t p_t$), indicating that the data were not equally well described by both models. The 2nd best-fit model was given a low QAIC weight value (0.09) and was the only model to include time as a factor influencing survival. The weighted average estimates of survival differed from the best-fit model estimates by only 0.04 through time (Table 3.14). The average survival and recapture estimates calculated from the best-fit model and from the weighted averages of the two best-fit models differed only by as much as 0.02 (Table 3.14) because of the large differences in the weight factors for each model (Table 3.11).

Because the ΔQAIC for the 2nd best-fit model is greater than 2.0, I will report the results of the best-fit model in the text (*but see Table 3.14 for estimates based on the weighted averages*). Survival probabilities were similar to those obtained by the gender analysis (0.77 ± 0.05 SE).

DISCUSSION

The results of this study provide important vital rate statistics, including mean estimates and 95% confidence intervals, for a pink abalone population that is potentially recovering from an overfished status (*see Chapter 4*). The Point Loma pink abalone population is characterized by slow growth with high survivorship of larger individuals. Annual growth increments were largest for the smallest individuals and growth rates dampened as the initial size of the animal increased. The overall shape of the predicted growth curve was dependent on the choice of data included in the analysis although the predictions from the age-at-size analyses were similar regardless of model choice. The size-at-maturity was estimated to be 94mm. The average age-at-maturity was 8 – 9 years (94 mm), and 24 – 29 years was the average time to reach MLS_C (159 mm). The sensitivity of the age-at-size estimates increased as the size-of-interest increased. Survival rates in this population did not differ temporally, or between genders, but severe cuts to the foot of the abalone did decrease the chance of survivorship in the field.

The estimated vital rates from this study were used to inform the development of a stage-based growth transition probability matrix which provides the foundation for a matrix population model (*see Chapter 4*) and population viability analysis (Morris and Doak 2002). The mean transition probabilities were similar regardless of which best-fit model was used to calculate the probabilities. The variability in the vital rate statistics may be used to develop a stochastic population model in order to predict the long-run growth rate and quasi-extinction risk of the population (Lande, Engen et al. 2003). Matrix models are also used to predict the potential effects of fishing pressure or recovery efforts on the population growth rates.

Growth Estimation

Ideally, the size-specific growth rate data for this study would have represented individuals from a broad size range, from the same population, and for the same time period because growth rates may vary spatially and temporally. Unfortunately, juvenile growth could not be determined for the Point Loma population because no tagged abalone smaller than 79 mm were re-encountered during the four years of this study. Juvenile growth data were supplemented from data obtained in the early 1970's with similar methods from Santa Catalina Island, California (Tutschulte 1976). In addition, temporal variation in growth rates was not considered for this population because of the high measurement errors associated with the growth increments measured during the first two years of recapture. An alternative method of *in situ* measurements that reduced measurement error was utilized during the final two years of the tag-recapture study. However, the use of only these higher quality measurements necessitated the temporal averaging of the growth data. The consideration of temporal variability in growth rates should be addressed in future studies.

The predicted growth rates for individuals in the Point Loma population were slower than those reported for populations in Baja California, México (Doi, Guzmán del Próo et al. 1977; Marín Aceves 1981; Guzmán del Próo 1992; Shepherd and Avalos-Borja 1997) but were similar to those reported for Santa Catalina Island, California, based on analyses of size-frequency distributions in 1971 and 1972 (Tutschulte and Connell 1988). Depending on the location along the Baja California coast, the time to reach 94 mm is between 3 and 5 years. The time to reach 159 mm is between 8 and 15 years. Growth rates at Santa Catalina Island, CA yielded estimates of 8 years and 20 – 23

years for the times to reach 94 mm and 159 mm, respectively (Tutschulte and Connell 1988).

Model Selection

The choice of which data to include in the growth analyses strongly influenced the relative ranks of the models fit to those data. Because the laboratory data included individuals in the slower-growing intermediate size classes (40 – 100 mm), the models fit to those data required a more rapid dampening of the growth rates than the models fit to the data excluding the laboratory-reared abalone. Although the ANCOVA results confirmed that there was no effect of treatment alone on the growth rates of the abalone, the significant interaction effect between treatment and initial size suggests that the inclusion of laboratory-reared abalone in the growth rate analysis may introduce bias. The effect of the treatment was seemingly most pronounced in intermediate-sized abalone (40 – 70 mm) based on a visual inspection of the data. Intermediate-sized abalone maintained in the laboratory and those caged in the field seem to have grown slower on average than abalone that had been released to the wild. However, the growth of the mark-recapture abalone in that size range is only represented by two abalone, making it inappropriate to test the statistical significance of this relationship.

One possible explanation for the seeming discrepancy in growth rates between individuals maintained in artificial and natural environments is that individuals maintained at higher densities may be subject to increased competition for space or food resources (Koike, Flassch et al. 1979; Clavier 1982; Chen 1984). On the other hand, the abalone in the laboratory and in cages were fed continuously which is usually thought to

increase potential growth rates. However, growth rates may be hindered if the quality of the food provided to the abalone was relatively low (Vilchis, Tegner et al. 2005).

Despite the influence of data choice on the shape of the growth curves, the mean age-at-size estimates were little changed by the choice of data inclusion. The average time between sizes-of-interest also differed by only one to two years between the most parsimonious models of the two analyses (Tables 3.8 and 3.9). Given the similarity of these results between the two sets of analyses, the choice of which model to use to describe individual growth rates may best be made by identifying the purpose to which the model will be applied.

Many previous studies of growth rates report only von Bertalanffy parameters for those populations and statistical methods have been developed to compare the growth rates across populations when 95% confidence intervals are reported (Kimura 1980; Day and Fleming 1992). If the von Bertalanffy equation is appropriate for describing the growth rates in the population, then instantaneous mortality estimates may be calculated from the parameters of this growth model (Beverton and Holt 1956; Ssentongo and Larkin 1973; Alverson and Carney 1975). Sainsbury (1982) and Rogers-Bennett et al.(2007) used multiple methods of calculating mortality rates using von Bertalanffy growth parameters for populations of *H. iris* and *H. rufescens*, respectively. They found relatively consistent results in the estimates from the different methods (maximum difference in instantaneous mortality rates, Z, for: *H. iris* – 0.07, *H. rufescens* – 0.12).

Despite the simplicity of the growth and mortality estimation techniques using the von Bertalanffy parameters, this model may overestimate the growth rates of juveniles if data for juveniles are lacking (Yamaguchi 1975). Rogers-Bennett et al. (2003; 2007)

found that the von Bertalanffy growth equation was the worst-fitting model of six candidates for red abalone (*Haliotis rufescens*) and red sea urchins (*Strongylocentrotus franciscanus*) when juvenile growth data were considered. In this study, the growth models fit to all of the available data revealed that the von Bertalanffy equation was the second worst-fit model. The Ricker equation was found to be completely inappropriate for this dataset. The four best-fit models (Logistic dose-response, Tanaka, Richards, and Gaussian) were equivalent based on the AIC and R^2 values. The model with the smallest SSR and least sensitivity to parameter permutations was the Logistic dose-response model (LDRE). The Tanaka equation was the next best-fit model based on the SSR ranks, but the extreme sensitivity of this model to parameter permutations made this model impractical to use. Of the remaining two best-fit models, the Gaussian equation had a higher SSR value but lower sensitivity than the Richards equation. Based on the low SSR and sensitivity values, I chose to calculate growth transition probabilities for the matrix model based on the LDRE model fit to all of the available data.

Rogers-Bennett et al. (2003; 2007) found that the LDRE also fit well to growth increment data of red sea urchins (*Strongylocentrotus franciscanus*) and red abalone (*H. rufescens*) in northern California. These authors rejected the LDRE fit to red abalone growth because the model assumes an unusual characteristic of constant growth prior to a transition period at intermediate size classes. They favored the Gaussian model for red abalone instead because it has well-defined biological meaning for the parameters and the time-to-fishery estimate was similar to that given for the LDRE. For the present study, the initial constant growth period is quite short, such that this feature is imperceptible in the graph of the curve (Figure 3.3).

Gender Determination and Size-at-Maturity

The non-lethal method for determining the gender by inspecting a small syringe sample of the gonad gives much less biased results than the standard non-lethal method of visually inspecting the gonad color through the dermal tissue layer. The effect of this gender determination method on the growth rates of animals was not assessed with this study, but the process is likely to stress the individual to some extent. Considering the potential influence that stress may have on the growth of the individual, this method should only be applied to individuals whose gender is in question.

The size-at-maturity estimates based on the syringe method of gender determination is a potential improvement over other non-lethal estimates because of the reduced bias in the determinations. However, the presence of eggs in the gonad does not necessarily indicate that the eggs are mature. On the other hand, immature eggs tend to locate near the outer walls of the gonad attached to the densely-packed trabeculae (connective tissue). The gonad sample in the syringe was obtained from primarily the center of the gonad where mature eggs may be more prevalent. Mature eggs are detached from the trabeculae and are located closer to the center of the gonad (Young and DeMartini 1970; Huchette, Soulard et al. 2004; Rogers-Bennett, Dondanville et al. 2004). The potential for preferential sampling of the mature eggs with this method would increase the relevance of the results to the true size-at-maturity of the population. However, until the correlation between gender determination by gonad sampling and maturity is verified, the estimates of size-at-maturity from this method should be used cautiously.

The estimate of size-at-maturity based on the non-lethal syringe-sampling method may be improved by examining the size-frequency distribution of the eggs in the samples. The average size of immature eggs is significantly smaller than mature eggs in some species of abalone (Brickey 1979; Rogers-Bennett, Dondanville et al. 2004). In addition, staining the egg samples would further improve the distinction among immature, mature, and necrotic (degenerating) eggs.

Survival Estimation

The survival of individuals larger than 79 mm in the Point Loma pink abalone population was high (0.77 yr^{-1} ± 0.05 SE) which is consistent with adult survival estimates for other pink abalone populations (Santa Catalina Island, CA: 0.82 yr^{-1} (Tutschulte 1976); Baja California, México: 0.65-0.70 yr^{-1} (Doi, Guzmán del Próo et al. 1977; Marín Aceves 1981); *reviewed in* Shepherd and Breen (1992)). Temporal variability in survival rates were not pronounced, such that none of the best-fit survival models included time as a factor. I also found no differences in survivorship between males and females in this population, the potential for which has not been examined for pink abalone in prior studies. The equality of survival between genders is important for assessing the appropriateness of a female-only matrix model to represent the dynamics of the population.

Damage to the foot of the abalone during the collection process (i.e. bar cuts) negatively impacted average survival of the most severely cut individuals relative to those individuals with no damage. Although the average survival rates of the light- to moderately-cut abalone increased, the confidence intervals around the average estimates broadened with increased damage to the foot. This increase in the variability around the

mean estimate could be explained by the smaller sample sizes of damaged individuals in this study.

Burge et al. (1975) and Tegner et al. (1989) suggested that bar cuts of sublegal individuals were responsible for sublegal mortality in the California abalone fisheries. Burge et al. (1975) found that 12.6% of the legal pink abalone landings in the early 1970s had been cut, and they estimated that smaller abalone would be cut at a higher rate. Tegner et al. (1989) examined size-frequency distributions of empty red abalone shells in 1980-1982 and concluded that a minimum of 10% of the total mortalities were due to bar cuts. Burge et al. (1975) experimentally tested the mortality of red abalone inflicted with a 13 mm cut to the foot and found that nearly 60% of the abalone died as a result. The description of the cut does not clearly define whether the measurement refers to the length along or depth through the foot. If the cut was made through the foot, toward the body, then that cut would have been characterized as severe in the present study.

An additional factor that may contribute to sub-legal mortality in fished abalone populations is extended exposure to air as the divers inspect the catch for sub-legal individuals. If those sub-legal individuals are then replaced in an inappropriate location or simply thrown back into the water from the boat, that individual will be exposed to greater predation pressure as it locates another safe place to settle. Abalone are particularly vulnerable to predation if the foot is exposed (i.e. upside down) or if the abalone is travelling because the suction of the foot is greatly reduced (*personal observation*). The results of the present study indicate that the survival of light to moderate-cut individuals is not reduced if the if individuals are properly replaced to appropriate substrate.

Burge et al. (1975) also discussed the mortality due to an interaction of bar cuts and predation following replacement of abalone to the substrate. He described a feeding frenzy of bat rays (*Myliobatis californica*), sheephead (*Semicossyphus pulcher*), and other large predatory fish during one tagging operation in the Channel Islands, California. Bat rays were apparently attracted to the stressed abalone (Tegner and Butler 1985) and took two large bags of tagged abalone before the abalone could be replaced to appropriate habitat. The rays were also seen crushing recently replaced abalone. This intense predation pressure was never encountered during the present mark-recapture study in the Point Loma kelp forest (2003-2007). Although I only encountered a bat ray twice during the five years of diving in the area, I did discover possible evidence of bat ray predation in the form of crushed shells of abalone and other large snails (Tegner and Butler 1985). The reduction in the numbers of large predators such as bat rays, and sea otters in the area may account for higher survivorship of damaged abalone in the modern Point Loma kelp forest (Dayton, Tegner et al. 1998). Commercially unimportant invertebrate predators (i.e. sea stars) may still impact the survival rates of abalone in the modern kelp forest but the abundances of these species were not investigated during this study.

CONCLUSIONS

Knowledge of vital rates for a population, and the inherent variability of those rates, is important for guiding recovery efforts in depleted populations. The results of this study indicate that the estimated growth rates, and resulting transition probabilities, are robust to choices of data inclusion and model selection processes. Likewise, the average age-at-size estimates did not differ appreciably between the two analyses, although sensitivities to parameter permutations were dependent on the model selected.

The number of years of reproduction prior to entering the fishery was estimated to be between 13 and 15 years for the top models describing the two datasets. The consistency of the results across multiple analyses and models fit to the data lends confidence to the use of the growth transition probability matrices as foundations for building matrix population models for the Point Loma pink abalone.

ACKNOWLEDGEMENTS

This work was funded by California Sea Grant, the University of California Marine Council Coastal Environmental Quality Initiative, the Edna B. Sussman Fund, the Mia J. Tegner Memorial Fund, the Halliday Field Research Fund, and the California Department of Fish and Game. Special thanks to I. Taniguchi, and P. Haaker for their tireless enthusiasm for tagging abalone and the invaluable advice they gave me early in the development of this project. This work would not have been possible without the additional help of many volunteer divers from SIO and the NOAA white abalone lab at the Southwest Fisheries Science Center. Particular thanks to M. Kasuya, R. Todd, S. Mau, K. Riser, J. Schaeffer, J. MacDonald, and B. Pister for help in the field throughout the many years of this project. The material in this chapter is in preparation to submission to the journal Marine Ecology Progress Series, and was co-authored by Laura Rogers-Bennett. The dissertation author was the primary investigator and author of this paper.

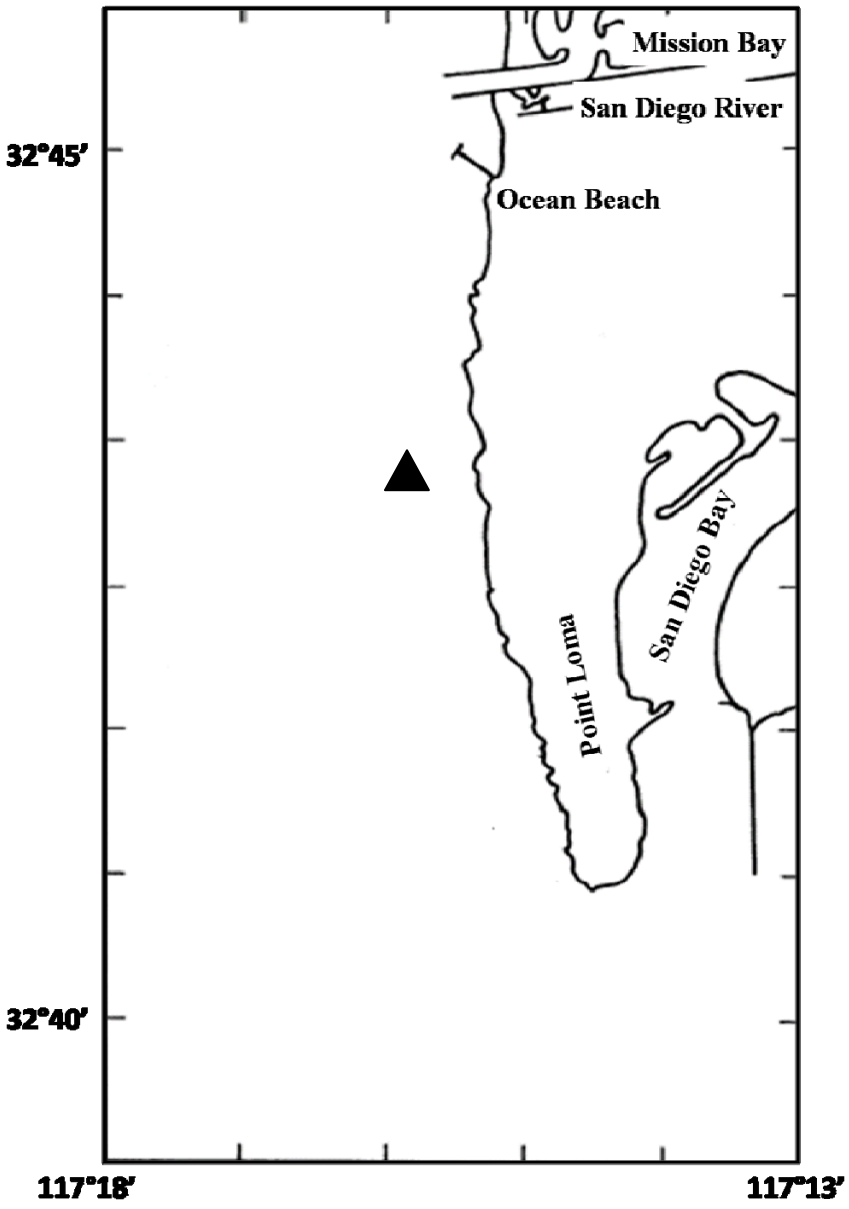

Figure 3.1 Map of Point Loma, San Diego (modified from Dayton *et al*.(1992). The ▲ indicates the approximate location of the 9-hectare study area.

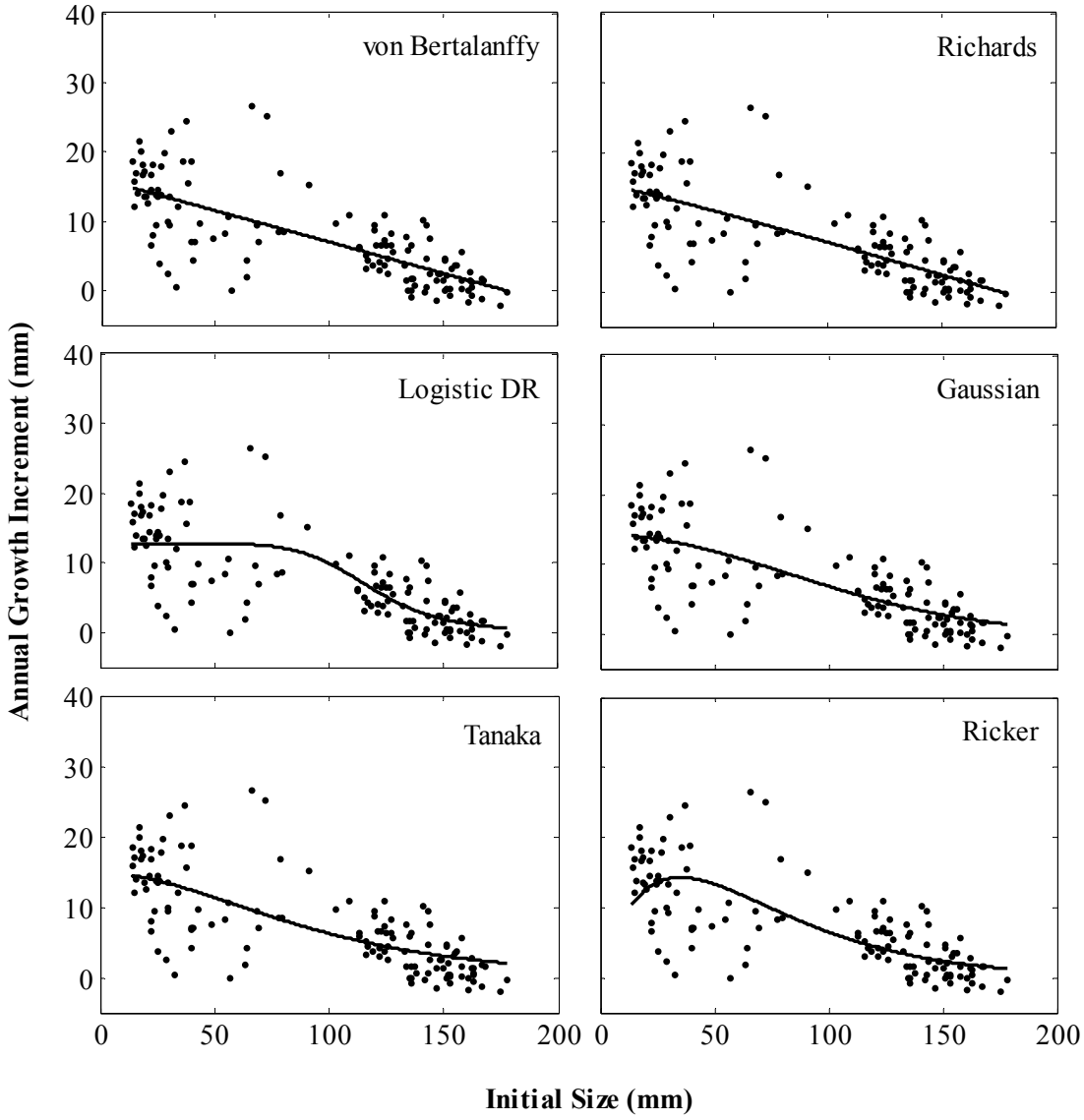

Figure 3.2 Pink Abalone growth using data on abalone grown in non-laboratory conditions. (Change in length as a function of the intial length at tagging). Six growth models are fit to the same data – von Bertalanffy, Richards, Logstic Dose-Response, Gaussian, Tanaka, and Ricker growth functions. $N = 131$ abalone.

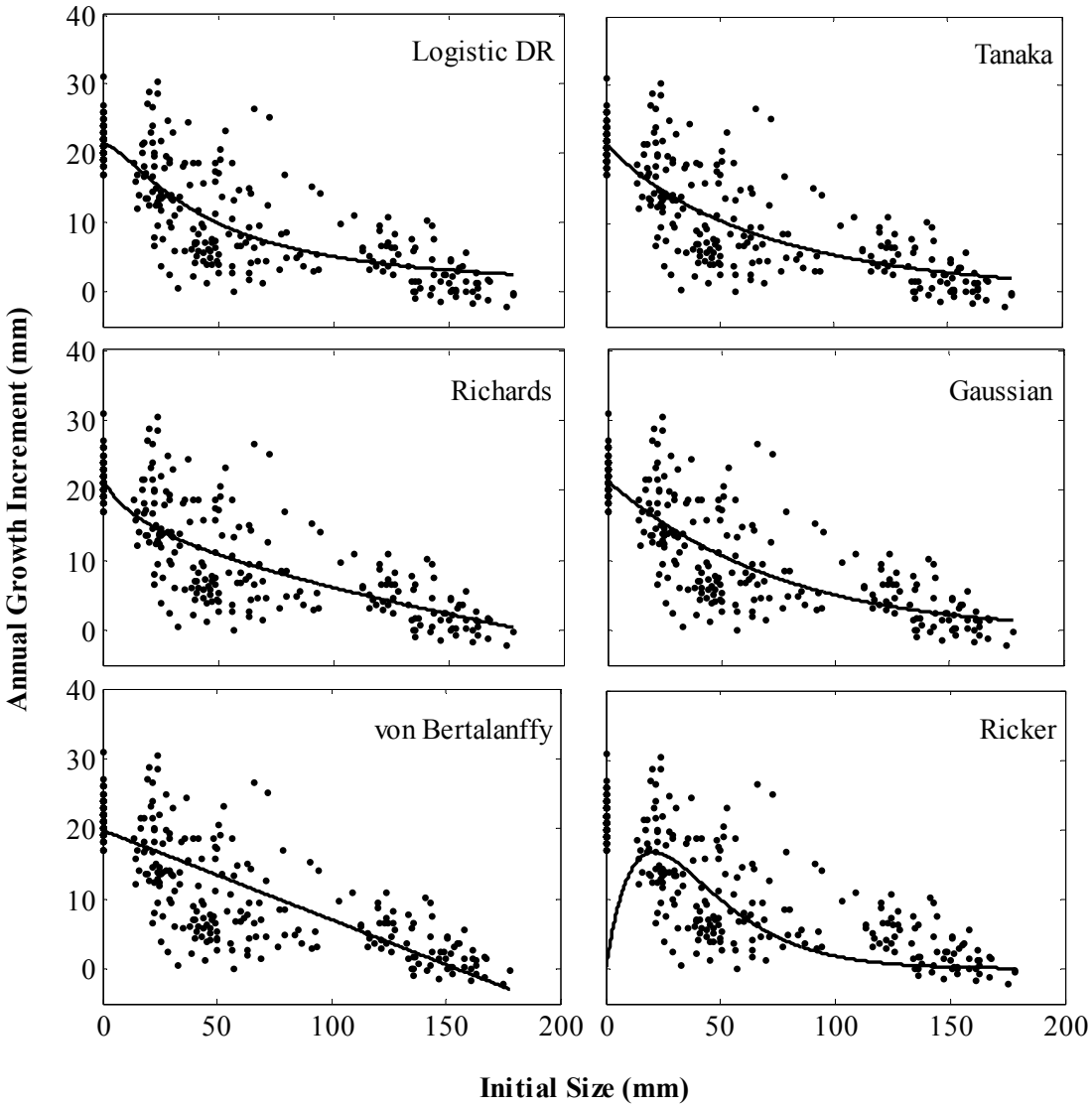

Figure 3.3. Pink Abalone growth using all available data. (Change in length as a function of the intial length at tagging). Six growth models are fit to the same data – Logistic Dose-Response, Tanaka, Richards, Gaussian, von Bertalanffy, and Ricker growth functions. $N = 336$ abalone.

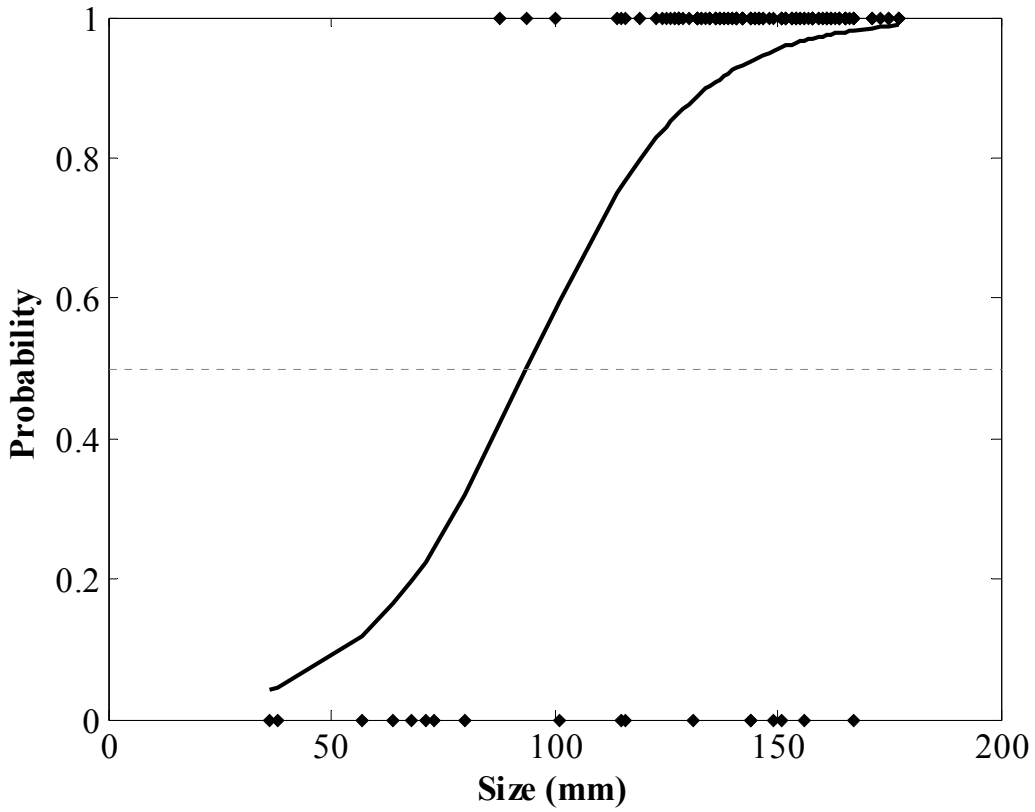

Figure 3.4 Size-at-Maturity estimated by fitting a generalized linear model with a binomial distribution to gender determination data. The black diamonds are the raw data used to generate the model. Data for males and females were similar, so they were pooled together for this analysis. Gender was determined by taking a small sample of the gonad of live animals with a 16-gauge syringe. The estimated size at 50% gender determination is 94 mm.

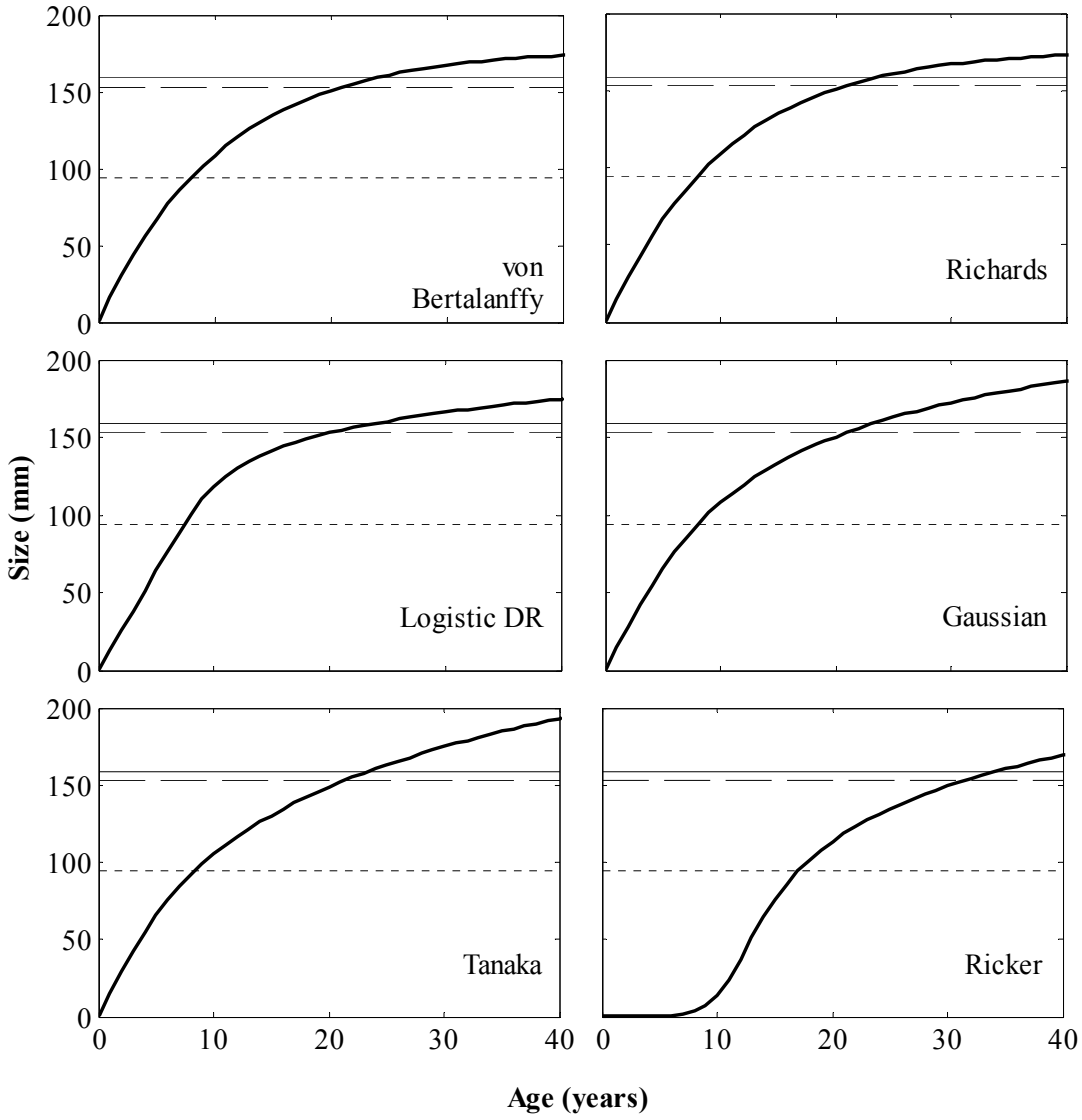

Figure 3.5 Size at age calculations based on the six growth curve models (no laboratory-reared abalone) . The solid horizontal line indicates the historic minimum legal size for the commercial fishery (159 mm). The dashed line is the historic minimum legal size for the recreational fishery (153 mm). The dotted line is the estimated average size-at-maturity for this population of pink abalone (94 mm).

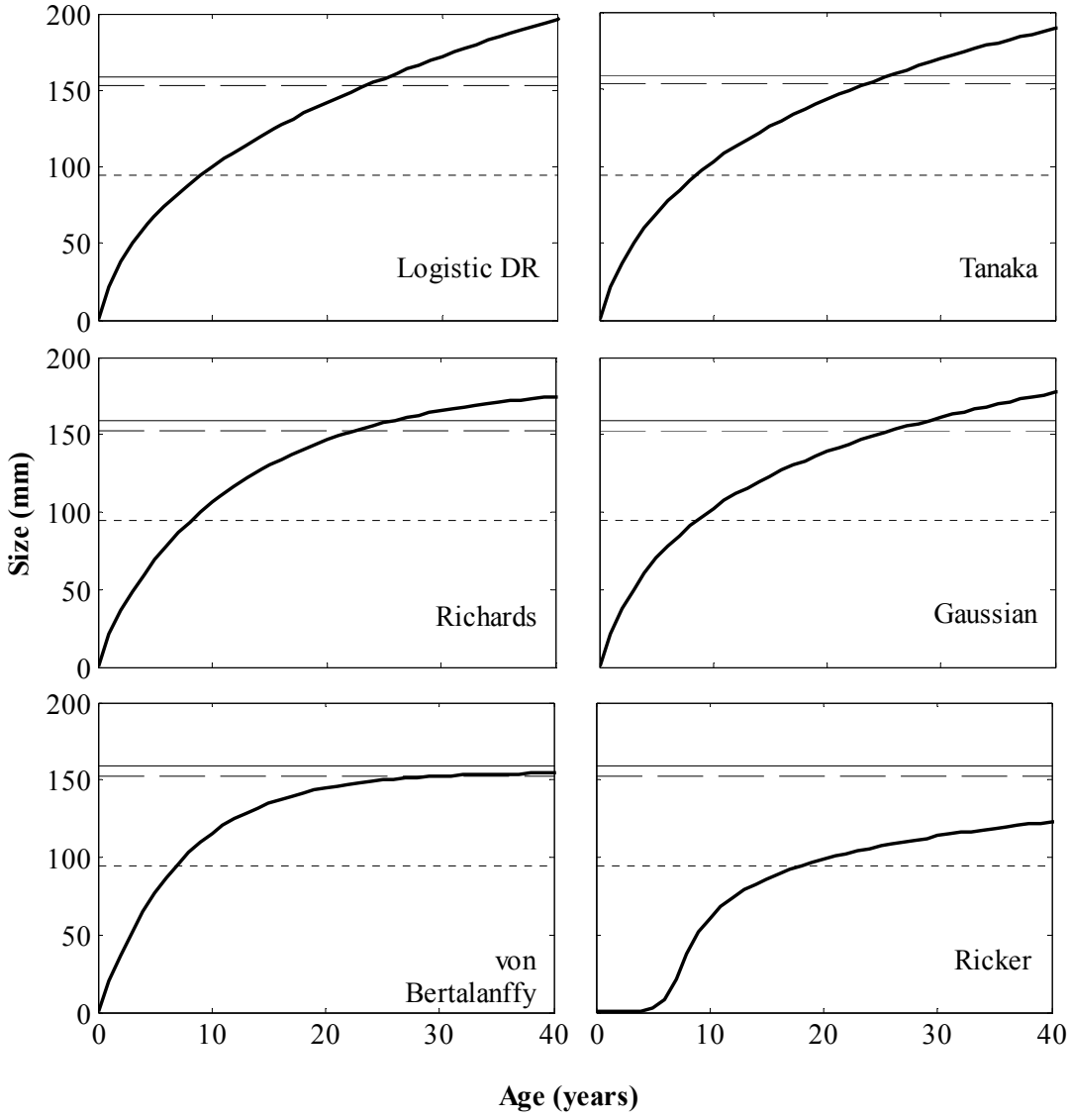

Figure 3.6 Size-at-age models based on the fitted growth models (all data). The solid horizontal line indicates the historic minimum legal size for the commercial fishery (159 mm). The dashed line is the historic minimum legal size for the recreational fishery (153 mm). The dotted line is the estimated average size-at-maturity for this population of pink abalone (94 mm).

Table 3.1 Group-specific capture-mark-recapture (CMR) summary statistics for the Point Loma pink abalone 2003-2007. Three different analyses are summarized – damage level, gender, and all individuals (minus severely cut individuals and juveniles). The census occasion (i) is the median date of the census period. The total number of days in the census period is shown in the parentheses. n_i is the number of new abalone tagged on census occasion i. m_i is the number of tagged abalone re-encountered at census occasion i. z_i is the number of abalone captured before census occasion i . R_i is the number of tagged abalone released at occasion i. r_i is the number re-encountered before or after census occasion i but not during the ith period.

			Census Occasion (i)					
		CMR	1 (1)	2 (176)	3 (9)	4 (111)	5 (178)	6 (29)
Analysis	Group	Statistic	12/17/2003	6/17/2004	2/3/2005	7/7/2005	8/26/2006	6/5/2007
Damage	No Damage	n_i	36	76	20	81	10	-
		m_i	-	23	1	38	84	32
		z_i	-	7	59	33	12	-
		R_i	36	110	21	119	100	-
		r_i	30	53	12	63	20	-
	Light Cut	n_i	6	20	15	20	4	-
		m_i	-	5	1	11	28	16
		z_i	-	0	14	13	4	-
		R_i	6	25	16	31	32	-
		r_i	5	15	10	19	12	-
	Moderate Cut	n_i	3	11	4	7	1	-
		m_i	-	2	0	8	9	8
		z_i	-	1	10	4	3	-
		R_i	3	13	4	15	10	-
		r_i	3	9	2	8	5	-
	Severe Cut	n_i	0	12	6	9	1	-
		m_i	-	0	0	3	5	2
		z_i	-	0	5	3	1	-
		R_i	0	12	6	12	6	-
		r_i	0	5	1	3	1	-

Table 3.1 continued

Analysis	Group	CMR Statistic	Census Occasion (i) 1 12/17/2003	2 6/17/2004	3 2/3/2005	4 7/7/2005	5 8/26/2006	6 6/5/2007
Gender only	Females	n_i	2	69	0	35	8	-
		m_i	-	1	2	27	41	17
		z_i	-	1	37	12	5	-
		R_i	2	70	2	62	49	-
		r_i	2	38	2	34	12	-
	Males	n_i	1	46	0	50	8	-
		m_i	-	0	0	17	39	17
		z_i	-	1	28	11	5	-
		R_i	1	4	0	67	43	-
		r_i	1	27	0	33	12	-
All individuals	No group	n_i	45	107	39	108	15	-
		m_i	-	30	2	57	121	56
		z_i	-	8	83	50	19	-
		R_i	45	148	41	165	142	-
		r_i	38	77	24	90	37	-

Table 3.2 Candidate models for estimating annual growth increments ΔL for a given initial size L_t. The six models differ in the number of parameters and the biological interpretability of those parameters. When applicable, the units of measure for each parameter are given. "--" indicates that the parameter is dimensionless.

Candidate Models	Equations	Parameter	Units
Richards	$\Delta L = \left(L_\infty^{-1/n}(1-e^{-K}) + L_t^{-1/n}e^{-K}\right)^{-n} - L_t$	L_∞	mm
		K	yr^{-1}
		n	--
von Bertalanffy	$\Delta L = L_\infty(1-e^{-K}) - L_t(1-e^{-K})$	L_∞	mm
		K	yr^{-1}
Ricker	$\Delta L = BL_te^{-KL_t}$	B	mm
		K	yr^{-1}
Gaussian	$\Delta L = Ae^{-(L_t-m)^2/2s^2}$	A	mm
		m	mm
		s	mm
Logistic Dose-Response	$\Delta L = a/(1+(L_t/b)^c)$	a	--
		b	--
		c	--
Tanaka	$\Delta L = \left(1/\sqrt{f}\right)ln\left\|2G + 2\sqrt{G^2+fa}\right\| + d - L_t$	a	--
	$G = (E/4) - (fa/E) + f$	d	--
	$E = e^{\sqrt{f}(L_t-d)}$	f	--

Table 3.3 Description of the candidate models used in the analysis of survival and recapture probabilities. The top four models were used in all three analyses whereas the bottom five models were only used when a group factor was being considered (i.e. damage level or gender).

	Description of Factors	
Candidate Model	Survival (φ)	Recapture (p)
$\varphi_t\, p_t$	Time	Time
$\varphi_.\, p_t$	Constant	Time
$\varphi_t\, p_.$	Time	Constant
$\varphi_.\, p_.$	Constant	Constant
$\varphi_G\, p_.$	Group	Constant
$\varphi_G\, p_t$	Group	Time
$\varphi_G\, p_G$	Group	Group
$\varphi_.\, p_G$	Constant	Group
$\varphi_t\, p_G$	Time	Group

Table 3.4 Goodness-of-fit results for the six growth functions used to model pink abalone size-specific growth. AIC = Akaike Information Criterion; BIC = Bayesian Information Criterion; SSR = Sum of Squared Residuals; R^2 = R-squared value. Models were ranked based on the AIC values. The fits to the abalone grown in non-laboratory conditions are shown in the left-hand columns. The right-hand columns show the goodness-of-fit results for all of the data combined.

	Non-laboratory conditions					All data				
Model	AIC	BIC	SSR	R^2	Rank	AIC	BIC	SSR	R^2	Rank
von Bertalanffy	541.1	547.9	2596	0.56	1	797.6	804.4	8513	0.67	5
Richards	543.0	553.2	2596	0.56	2	759.0	769.2	7055	0.73	3
LDRE	547.4	557.6	2649	0.55	3	758.2	768.3	7028	0.73	1
Gaussian	549.7	559.8	2677	0.54	4	760.0	770.1	7086	0.73	4
Tanaka	554.3	564.4	2734	0.53	5	758.4	768.5	7034	0.73	2
Ricker	575.8	582.5	3048	0.48	6	1257.5	1264.2	71569	-1.75	6

Table 3.5 Parameter estimates and 95% confidences intervals for the six growth functions fit to two datasets. Results of fitting to the growth data from non-laboratory conditions are given in the left-hand columns. The results of fitting to all available data are given in the right-hand column.

		Non-laboratory conditions			All Data		
Model	Parameter	μ	L95%	U95%	μ	L95%	U95%
von Bertalanffy	K	0.09	0.08	0.11	0.14	0.13	0.15
	L_∞	178	162	193	155	146	164
Richards	K	0.10	0.05	0.15	0.07	0.05	0.09
	L_∞	176	157	196	183	162	205
	n	-1.04	-1.41	-0.67	-0.79	-0.84	-0.75
Logistic DR	a	12.8	11.5	14.0	21.5	20.8	22.2
	b	119	109	129	45	40	50
	c	7.4	3.1	11.7	1.5	1.2	1.7
Gaussian	A	14	10	18	636	-5765	7038
	m	-1.2	-77.9	75.5	-513.3	-1934.0	907.3
	s	83.5	42.0	125.0	197.1	-56.9	451.0
Tanaka	a	$4.46\text{x}10^{-3}$	$1.01\text{x}10^{-3}$	$7.91\text{x}10^{-3}$	$-2.68\text{x}10^{-3}$	$-8.40\text{x}10^{-3}$	$3.04\text{x}10^{-3}$
	d	402	249	555	461	301	621
	f	$2.43\text{x}10^{-4}$	$3.47\text{x}10^{-5}$	$4.51\text{x}10^{-4}$	$1.67\text{x}10^{-4}$	$4.95\text{x}10^{-5}$	$2.84\text{x}10^{-4}$
Ricker	B	1.1	0.9	1.3	2.2	1.2	3.2
	K	0.03	1.28	0.03	0.05	3.15	0.06

Table 3.6 Growth transition probability matrices for a stage-based matrix model of pink abalone. The transition probabilities were estimated from the best-fit model describing the growth of pink abalone in non-laboratory conditions only (von Bertalanffy)(*top*) and to the best-fit model fit to all available growth data (Logistic Dose-Response)(*bottom*). The four stages are J = juvenile (25-50mm), SA = sub-adult (50-100mm), A1 = intermediate-sized adults (100-153mm), and A2 = large adults (>153mm). Probabilities are given as mean (lower 95% CI; upper 95% CI).

Stage class	Non-laboratory Conditions			
	Juvenile (J)	Sub-Adult (SA)	Adult 1 (A1)	Adult 2 (A2)
J	0.52 (0.63; 0.34)	0	0	0
SA	0.48 (0.37; 0.66)	0.85 (0.90; 0.78)	0	0
A1	0	0.15 (0.10; 0.22)	0.96 (0.99; 0.91)	0
A2	0	0	0.04 (0.01; 0.09)	1

Stage class	All Available Data			
	Juvenile (J)	Sub-Adult (SA)	Adult 1(A1)	Adult 2 (A2)
J	0.51 (0.58; 0.43)	0	0	0
SA	0.49 (0.42; 0.57)	0.89 (0.89; 0.89)	0	0
A1	0	0.11 (0.11; 0.11)	0.94 (0.93; 0.94)	0
A2	0	0	0.06 (0.07; 0.06)	1

Table 3.7 Parameter estimates and summary statistics for the fit of a generalized linear model to the binomial gender determination data. The equation fit to the data is $P(L_i) = \left(e^{\beta_0+\beta_1 L_i}\right)/\left(1+e^{\beta_0+\beta_1 L_i}\right)$ where L_i is the length of the abalone and $P(L_i)$ is the probability of successful gender determination (either male or female).

Parameter	Estimate	SE	t-statistic	p-value
β_0	-5.0914	1.4995	-3.3954	0.0007
β_1	0.0543	0.0116	4.6657	0.0000

Table 3.8 Age-at-size estimates from the growth functions fit to the abalone grown in non-laboratory conditions – age-at-maturity (94mm), time to reach the historic recreational minimum legal size (MLS_R), and the time to reach the historic commercial minimum legal size (MLS_C). MLS_R = 153 mm; MLS_C = 159 mm. Sensitivity is the age-at-size estimates with ±10% changes in the growth function parameters. The "NA" indicates that the MLSC was not attainable with a 10% reduction in the parameter estimates for the Richards growth function. The models are shown in the order of the AIC ranks for these data.

	Maturity		MLS_R		MLS_C	
Model	μ	Sensitivity	μ	Sensitivity	μ	Sensitivity
von Bertalanffy	8	7 – 11 y	21	15 – 37 y	24	17 – 61 y
Richards	8	7 – 10 y	21	16 – 37 y	24	17 y – NA
LDRE	8	7 – 9 y	21	15 – 31 y	24	17 – 38 y
Gaussian	9	7 – 10 y	21	17 – 21 y	24	19 – 33 y
Tanaka	9	8 – 18 y	22	14 – 48 y	24	15 – 53 y
Ricker	17	17 – 18 y	32	29 – 36 y	35	31 – 40 y

Table 3.9 Age-at-size estimates from the growth functions fit to all of the available data – age-at-maturity (94mm), time to reach the historic recreational minimum legal size (MLS_R), and the time to reach the historic commercial minimum legal size (MLS_C). MLS_R = 153 mm; MLS_C = 159 mm. Sensitivity is the age-at-size estimates with ±10% changes in the growth function parameters. The "NA" indicates that no estimate of age was possible under the conditions of the model. The models are shown in the order of the AIC ranks for these data.

	Maturity		MLS_R		MLS_C	
Model	μ	Sensitivity	μ	Sensitivity	μ	Sensitivity
LDRE	9	8 – 11 y	24	21 – 27 y	26	23 – 29 y
Tanaka	9	2 – 23 y	24	8 – 57 y	26	9 – 62 y
Richards	9	7 – 10 y	23	17 – 37 y	26	19 – 48 y
Gaussian	9	8 – 11 y	26	21 – 36 y	29	23 – 40 y
von Bertalanffy	7	6 – 10 y	32	16 y – NA	NA	18 y – NA

Table 3.10 Summary results of goodness-of-fit statistics for the three sets of analyses on the global model (fully time-dependent model) within the candidate model set. Test2 and Test3 are results from the program RELEASE. Test2 addresses the assumption that all abalone have equal probability of surviving from one census period to the next. Test3 addresses the assumption that all abalone have equal probability of being recaptured. A non-significant *p*-value indicates the assumptions of the Cormack-Jolly-Seber tests are met by the data. A median ĉ value of 1 indicates that the model describes the variability in the data well. A median ĉ value greater than 1 indicates that the data are overdispersed and values greater than 3 indicate that the model is not appropriate.

	Number of	Test 2			Test 3			Test 2 + Test 3			Median
Analysis	Individuals	X^2	df	*p*-value	X^2	df	*p*-value	X^2	df	*p*-value	ĉ
Damage Only	342	12.944	10	0.227	5.813	20	0.999	18.756	30	0.945	1.10
Gender Only	215	2.687	5	0.748	5.386	8	0.716	8.073	13	0.839	1.22
All Individuals	314	17.929	4	0.001	7.323	7	0.396	25.252	11	0.008	1.95

Table 3.11 Summary of the best-fit survival and detectability models for the Point Loma pink abalone 2003-2007. The models are as described in Table 3.3. A subscript of *d* means that damage was a factor in the model, *g* refers to gender, *t* refers to time, and a "." indicates that the survival or recapture probability was constant through time and / or across groups. $QAIC_c$ is the ĉ-adjusted AIC, Delta $QAIC_c$ is the difference in the $QAIC_c$ values from the most parsimonious model. $QAIC_c$ Weight is the weighting used for average survival and detectability across the best-fit models. Qdeviance is the ĉ-adjusted deviance of each model. ĉ is the "median ĉ value" estimated by logistic regression on simulation values. The ĉ is a measure of overdispersion of the data. If ĉ = 1, then the data is described well by the model.

Analysis	Number of Individuals	Models	Number of Parameters	$QAIC_c$	$\Delta QAIC_c$	$QAIC_c$ Weight	Qdeviance	Median ĉ
Damage	342	$\varphi_d p_t$	9	985.76	0.00	0.74	131.45	1.10
		$\varphi_. p_t$	6	988.44	2.68	0.20	140.30	
		$\varphi_t p_t$	9	990.75	4.98	0.06	136.43	
Gender	219	$\varphi_. p_t$	6	521.62	0.00	0.70	38.92	1.21
		$\varphi_g p_t$	7	523.69	2.07	0.25	38.90	
		$\varphi_t p_t$	9	526.68	5.06	0.05	37.69	
All Individuals	314	$\varphi_. p_t$	6	531.30	0.00	0.91	43.36	1.95
		$\varphi_t p_t$	9	535.93	4.63	0.09	41.82	

Table 3.12 Survival and recapture estimates for four levels of damage to the foot of abalone. Estimates and 95% confidence intervals are given for the best-fit model ($\varphi_d p_t$) and for the weighted average of the best three models (Table 3.11).

	Apparent Annual Survival							*Recapture Probability*					
	Best-fit Estimate			Weighted Average				Best-fit Estimate			Weighted Average		
Damage Level	μ	L95	U95	census	μ	L95	U95	μ	L95	U95	μ	L95	U95
No Damage	0.74	0.65	0.82	2	0.76	0.59	0.88	0.73	0.55	0.85	0.72	0.55	0.85
				3	0.76	0.55	0.89	0.01	0.00	0.06	0.01	0.00	0.06
				4	0.73	0.53	0.87	0.36	0.28	0.44	0.36	0.28	0.45
				5	0.75	0.64	0.83	0.60	0.48	0.71	0.60	0.48	0.72
				6	0.73	0.00	1.00	0.31	0.22	0.42	0.32	0.00	1.00
Light Cut	0.84	0.67	0.93	2	0.83	0.62	0.94	same estimates as above			same estimates as above		
				3	0.83	0.57	0.95						
				4	0.80	0.50	0.94						
				5	0.82	0.64	0.92						
				6	0.80	0.00	1.00						
Moderate Cut	0.86	0.59	0.97	2	0.85	0.56	0.96	same estimates as above			same estimates as above		
				3	0.85	0.51	0.97						
				4	0.82	0.44	0.96						
				5	0.84	0.57	0.95						
				6	0.82	0.00	1.00						
Severe Cut	0.52	0.31	0.72	2	0.59	0.27	0.85	same estimates as above			same estimates as above		
				3	0.59	0.26	0.85						
				4	0.56	0.29	0.80						
				5	0.58	0.30	0.81						
				6	0.56	0.00	1.00						

Table 3.13 Survival and recapture estimates for females and males. Estimates and 95% confidence intervals are given for the best-fit model ($\varphi_. p_t$) and for the weighted average of the best three models (Table 3.11).

	Apparent Annual Survival							*Recapture Probability*					
	Best-fit Estimate			Weighted Average				Best-fit Estimate			Weighted Average		
Gender	μ	L95	U95	census	μ	L95	U95	μ	L95	U95	μ	L95	U95
Female	0.73	0.62	0.82	2	0.75	0.56	0.87	0.33	0.03	0.88	0.33	0.03	0.88
				3	0.72	0.58	0.83	0.02	0.00	0.09	0.02	0.00	0.09
				4	0.75	0.56	0.87	0.51	0.38	0.64	0.51	0.38	0.64
				5	0.73	0.61	0.83	0.66	0.49	0.80	0.66	0.49	0.80
				6	0.73	0.00	1.00	0.33	0.21	0.48	0.33	0.00	1.00
Male	0.73	0.62	0.82	2	0.75	0.56	0.87						
				3	0.73	0.58	0.84						
				4	0.75	0.56	0.87	same estimates as above			same estimates as above		
				5	0.73	0.60	0.83						
				6	0.74	0.00	1.00						

Table 3.14 Survival and recapture estimates for four all individuals (> 79 mm), except those with severe cuts to the foot. Estimates and 95% confidence intervals are given for the best-fit model ($\varphi_{.} p_t$) and for the weighted average of the two best models (Table 3.11).

Apparent Annual Survival							*Recapture Probability*					
Best-fit Estimate			Weighted Average				Best-fit Estimate			Weighted Average		
μ	L95	U95	census	μ	L95	U95	μ	L95	U95	μ	L95	U95
0.77	0.64	0.86	2	0.79	0.58	0.91	0.73	0.49	0.88	0.72	0.48	0.88
			3	0.77	0.52	0.91	0.01	0.00	0.10	0.01	0.00	0.10
			4	0.75	0.48	0.91	0.37	0.26	0.49	0.37	0.26	0.49
			5	0.77	0.63	0.87	0.62	0.45	0.76	0.62	0.45	0.76
			6	0.75	0.00	1.00	0.32	0.20	0.47	0.33	0.00	1.00

REFERENCES

Akaike, H. (1974) A new look at the statistical model identification. *IEEE Transactions on Automatic Control*, **19**(6), 716-723.

Alverson, D.L., M.J. Carney (1975) Graphic review of growth and decay of population cohorts. *Journal Du Conseil*, **36**(2), 133-143.

Babcock, R., J. Keesing (1999) Fertilization biology of the abalone *Haliotis laevigata*: Laboratory and field studies. *Canadian Journal of Fisheries & Aquatic Sciences*, **56**(9), 1668-1678.

Beal, B.F., M.G. Kraus (2002) Interactive effects of initial size, stocking density, and type of predator deterrent netting on survival and growth of cultured juveniles of the soft-shell clam, Mya arenaria L., in eastern Maine. *Aquaculture*, **208**(1-2), 81-111.

Beverton, R.J.H., S.J. Holt (1956) A review of methods for estimating mortality rates in exploited fish populations, with special reference to sources of bias in catch sampling. *Rapports et procès-verbaux des réunions / Conseil permanent international pour l'exploration de la mer*, **140**(1), 67-83.

Breen, P.A. (1992) A review of models used for stock assessment in abalone fisheries. In: S.A. Shepherd, M.J. Tegner & S.A. Guzmán del Próo (Eds). *Abalone of the World: Biology, Fisheries, and Culture*. Fishing News Books, Cambridge, MA: 253-275.

Brickey, B.E. (1979) The histological and cytological aspects of oogenesis in the California abalonies. California State University, Long Beach: 88.

Burge, R., S. Shultz, et al. (1975) Draft report on recent abalone research in California with recommendations for management. *Department of Fish and Game*.

California Department of Fish and Game (2002). *Draft Abalone Recovery and Management Plan*. California Department of Fish and Game, Marine Region, Sacramento, CA.

Chen, H.-C. (1984) Recent innovations in cultivation of edible molluscs in Taiwan, with special reference to the small abalone *Haliotis diversicolor* and the hard clam *Meretrix lusoria*. *Aquaculture*, **39**, 11-27.

Clarke, C.B., R.G. Creese (1998) On-growing cultured abalone (*Haliotis iris*) in northern New Zealand. *Journal of Shellfish Research*, **17**(3), 607-613.

Clavier, J. (1982) (Initial data on natural ormer (*Haliotis tuberculata*) stocks in the St. Malo region.) Rapport d'étude, Association pour la Mise en Valeur du Littoral de la Côte

d'Emeraude. (Translated into English in. *Canadian Translation of Fisheries and Aquatic Sciences (1983) (4928)*.

Cooch, E., G.C. White (eds.) (2008). *Program Mark: "A gentle introduction"*: 744 pp.
Cormack, R.M. (1964) Estimates of survival from the sighting of marked individuals. *Biometrika*, **51**, 429-438.

Cox, K. (1962) California abalones, Family Haliotidae. *Fish Bulletin*, **118**, 1-135.
Day, R., P. Gilmour, et al. (2004) Effects of density and food supply on postlarval abalone: Behaviour, growth and mortality. *Journal of Shellfish Research*, **23**(4), 1009-1018.

Day, R.W., A.E. Fleming (1992) The determinants and measurement of abalone growth. *Abalone of the world. Biology, fisheries and culture. Proceedings of the 1st international symposium on abalone.*: 141-168.

Dayton, P.K., M.J. Tegner, et al. (1998) Sliding baselines, ghosts, and reduced expectations in kelp forest communities. *Ecological Applications*, **8**(2), 309-322.

Dayton, P.K., M.J. Tegner, et al. (1992) Temporal and spatial patterns of disturbance and recovery in a kelp forest community. *Ecological Monographs*, **62**(3), 421-445.

Diaz, F., A.D. Re, et al. (2006) Thermal preference and tolerance of green abalone Haliotis fulgens (Philippi, 1845) and pink abalone Haliotis corrugata (Gray, 1828). *Aquaculture Research*, **37**(9), 877-884.

Doi, T., S.A. Guzmán del Próo, et al. (1977) Análisis de la población y diagnostic de la pequería de abulón amarillo Haliotis corrugata en al area de Abreojos e Isla de Cedros B.C. *Instituto Nacional de Pesca México Serie Cientifica*, **18**, 1-17.

Dowling, N.A., S.J. Hall, et al. (2004) Assessing population sustainability and response to fishing in terms of aggregation structure for greenlip abalone (*Haliotis laevigata*) fishery management. *Canadian Journal of Fisheries and Aquatic Sciences*, **61**(2), 247-259.

Gascoigne, J., R.N. Lipcius (2004) Allee effects in marine systems. *Marine Ecology Progress Series*, **269**, 49-59.

Guzmán del Próo, S.A. (1992) A review of the biology of abalone and its fishery in México. In: S.A. Shepherd, M.J. Tegner & S.A. Guzmán del Próo (Eds). *Abalone of the World: Biology, Fisheries, and Culture*. Fishing News Books, Cambridge, MA: 341-360.

Haaker, P.L., D.O. Parker, et al. (1998) Growth of red abalone, *Haliotis rufescens* (Swainson), at Johnsons Lee, Santa Rosa Island, California. *Journal of Shellfish Research*, **17**(3), 747-753.

Huchette, S.M.H., J.P. Soulard, et al. (2004) Maternal variability in the blacklip abalone, Haliotis rubra leach (Mollusca : Gastropoda): effect of egg size on fertilisation success. *Aquaculture*, **231**(1-4), 181-195.

Jennings, S., J.D. Reynolds, et al. (1998) Life history correlates of responses to fisheries exploitation. *Proceedings of the Royal Society of London - Series B: Biological Sciences*, **265**(1393), 333-339.

Jolly, G.M. (1965) Explicit estimates from capture-recapture data with both dead and immigration-stochastic model. *Biometrika*, **52**, 225-247.

Karpov, K.A., P.L. Haaker, et al. (1998) The red abalone, *Haliotis rufescens*, in California: Importance of depth refuge to abalone management. *Journal of Shellfish Research*, **17**(3), 863-870.

Kimura, D.K. (1980) Likelihood methods for the von Bertalanffy growth curve. *Fishery Bulletin*, **77**(4), 765-776.

Koike, Y., J. Flassch, et al. (1979) Biological and ecological studies on the propogation of the ormer, *Haliotis tuberculata* (L.). II Influence of food and density on the growth of juveniles. *La Mer*, **17**, 43-52.

Krebs, C.J. (1999). *Ecological methodology*. Benjamin/Cummings, Menlo Park, Calif.: xii, 620 p. pp.

Lande, R., S. Engen, et al. (2003) Stochastic population dynamics in ecology and conservation. In: R. Lande (Ed). *Stochastic population dynamics in ecology and conservation*. Oxford University Press, New York, NY: 1-212.

Lebreton, J.D., K.P. Burnham, et al. (1992) Modeling survival and testing biological hypotheses using marked animals: a unified approach with case studies. *Ecological Monographs*, **62**(1), 67-118.

Leighton, D.L. (1974) The Influence of Temperature on Larval and Juvenile Growth in 3 Species of Southern California Abalones. *Fishery Bulletin*, **72**(4), 1137-1145.

Marín Aceves, V. (1981) Parametros poblacionales y diagnostico de la pesquería de abulón amarillo (*Haliotis corrugata*) en Bahía Tortugas, B.C.S. In: I.N.d. Pesca (Ed). *Ciencia Pesquera*. Secretaría de Pesca. México: 66-79.

McShane, P.E. (1994) Estimating the abundance of abalone (Haliotis spp.) stocks-examples from Victoria and southern New Zealand. *Fisheries Research (Amsterdam)*, **19**(3-4), 379-394.

McShane, P.E. (1995) Recruitment variation in abalone: Its importance to fisheries management. *Marine & Freshwater Research*, **46**(3), 555-570.

Morris, W.F., D. Doak (2002). *Quantitative conservation biology: Theory and practice of population viability analysis*. Sinauer Associates, Inc., Sunderland, Massachusetts: 480 pp.

Prince, J.D., T.L. Sellers, et al. (1988) Confirmation of a relationship between the localized abundance of breeding stock and recruitment for *Haliotis rubra* Leach Mollusca Gastropoda. *Journal of Experimental Marine Biology & Ecology*, **122**(2), 91-104.

Rogers-Bennett, L., R.F. Dondanville, et al. (2004) Size specific fecundity of red abalone (*Haliotis rufescens*): Evidence for reproductive senescence? *Journal of Shellfish Research*, **23**(2), 553-560.

Rogers-Bennett, L., R.T. Leaf (2006) Elasticity analyses of size-based red and white abalone matrix models: Management and conservation. *Ecological Applications*, **16**(1), 213-224.

Rogers-Bennett, L., D.W. Rogers (2006) A semi-empirical growth estimation method for matrix models of endangered species. *Ecological Modelling*, **195**(3-4), 237-246.

Rogers-Bennett, L., D.W. Rogers, et al. (2003) Modeling red sea urchin (Strongylocentrotus franciscanus) growth using six growth functions. *Fishery Bulletin (Seattle)*, **101**(3), 614-626.

Rogers-Bennett, L., D.W. Rogers, et al. (2007) Modeling growth and mortality of red abalone (Haliotis rufescens) in Northern California. *Journal of Shellfish Research*, **26**(3), 719-727.

Sadovy, Y. (2001) The threat of fishing to highly fecund fishes. *Journal of Fish Biology*, **59**(Supplement A), 90-108.

Sadovy, Y., M. Domeier (2005) Are aggregation-fisheries sustainable? Reef fish fisheries as a case study. *Coral Reefs*, **24**(2), 254-262.

Sainsbury, K.J. (1982) Population dynamics and fishery management of the paua, *Haliotis iris*. 1. Population structure, growth, reproduction, and mortality. *New Zealand Journal of Marine and Freshwater Research*, **16**(2), 147-161.

Seber, G.A.F. (1965) A note on the multiple-recapture census. *Biometrika*, **52**, 249-259.
Shepherd, S.A., M. Avalos-Borja (1997) The shell microstructure and chronology of the abalone Haliotis corrugata. *Molluscan Research*, **18**(2), 197-207.

Shepherd, S.A., P.A. Breen (1992) Mortality in abalone: Its estimation, variability, and causes. In: S.A. Shepherd, M.J. Tegner & S.A. Guzmán del Próo (Eds). *Abalone of the World: Biology, Fisheries, and Culture*. Fishing News Books, Cambridge, MA: 276-304.
Shepherd, S.A., L.D. Brown (1993) What is an abalone stock: Implications for the role of refugia in conservation. *Canadian Journal of Fisheries & Aquatic Sciences*, **50**(9), 2001-2009.

Ssentongo, G.W., P.A. Larkin (1973) Some simple methods of estimating mortality rates of exploited fish populations. *Journal of the Fisheries Research Board of Canada*, **30**(5), 695-698.

Tegner, M.J. (1989) The California abalone fishery, USA: Production ecological interactions and prospects for the future. In: J.F. Caddy (Ed). *Marine Invertebrate Fisheries: Their Assessment and Management*. John Wiley and Sons, Inc, Somerset, New Jersey, USA: 401-420.

Tegner, M.J. (2000) Abalone (Haliotis spp.) enhancement in California: What we've learned and where we go from here. *Canadian Special Publication of Fisheries & Aquatic Sciences*, **130**, 61-71.

Tegner, M.J., P.A. Breen, et al. (1989) Population biology of red abalones *Haliotis rufescens* in southern California USA and management of the red and pink *Haliotis corrugata* abalone fisheries. *Fishery Bulletin*, **87**(2), 313-340.

Tegner, M.J., R.A. Butler (1985) The Survival and Mortality of Seeded and Native Red Abalones *Haliotis rufescens* on the Palos-Verdes Peninsula California USA. *California Fish & Game*, **71**(3), 150-163.

Troynikov, V.S., H.K. Gorfine (1998) Alternative approach for establishing legal minimum lengths for abalone based on stochastic growth models for length increment data. *Journal of Shellfish Research*, **17**(3), 827-831.

Tutschulte, T.C. (1976) The comparative ecology of three sympatric abalones. *Scripps Institution of Oceanography*. University of California, San Diego.

Tutschulte, T.C., J.H. Connell (1988) Growth of Three Species of Abalones Haliotis in Southern California USA. *Veliger*, **31**(3-4), 204-213.

Uki, N., S. Kikuchi (1982) Influence of food levels on maturation and spawning of the abalone *Haliotis discus hannai* related to effective accumulative temperature. *Bulletin of Tohoku National Fisheries Research Institute*, **45**, 45-54.

Vilchis, L.I., M.J. Tegner, et al. (2005) Ocean warming effects on growth, reproduction, and survivorship of Southern California abalone. *Ecological Applications*, **15**(2), 469-480.

White, G.C., K.P. Burnham (1999) Program MARK: survival estimation from populations of marked animals. *Bird Study*, **46**(Suppl.), 120-138.

Yamaguchi, M. (1975) Estimating growth parameters from growth-rate data - Problems with marine sedentary invertebrates. *Oecologia*, **20**(4), 321-332.

Young, J.S., J.D. DeMartini (1970) The reproductive cycle, gonadal histology, and gametogenesis of the red abalone, Haliotis rufescens (Swainson). *California Fish and Game*, **56**, 298-309.

CHAPTER 4.

Using Population- and Aggregation-Level Characteristics to Assess the Recovery Status of a Pink Abalone Population (*Haliotis corrugata*) near San Diego, California

ABSTRACT

The current status (2004-2007) of the Point Loma pink abalone population is described in terms of population- and aggregation-level characteristics. Population-level characteristics include population density, size-frequency, sex ratio, and spatial dispersion. Aggregation-level characteristics include distances between nearest neighbors, the average number of neighbors per abalone, aggregation sizes, and the size-frequency and sex ratio within an aggregation. I estimate the per capita egg production rate for the population based on aggregation sex ratios and size-frequencies. I also introduce a method for incorporating aggregation-level characteristics into a formal population matrix model so that a critical threshold may be defined as additional data become available.

The density of the population (~100 abalone / ha) is an order of magnitude lower than the estimated minimum spawning density (2,000 abalone / ha) for populations to persist. Yet, the broad size distribution of individuals suggests that the population is still producing new recruits. The average nearest-neighbor distance was greater than 5 meters between 2005 and 2007, corresponding to an estimated fertilization success rate of ~20%. Close to half of the "aggregations" consisted of solitary individuals, although the number of neighbors averaged across individuals ranged from nearly 4 in 2006 to almost 1 in 2007. Indices of aggregation also showed relative reductions in the degree of aggregation

between 2006 and 2007. The sex ratio of the population was consistent with a 1:1 ratio of sexes distributed randomly among aggregations. The per capita egg production estimate dropped from 2006 (426,809 eggs) to 2007 (119,064 eggs). The estimated population growth rates ranged from 0.823 – 1.302 yr^{-1} for high fertilization success conditions, and from 0.717 – 1.059 yr^{-1} for low fertilization success conditions.

The results of this work will be used to better review the potential recovery of pink abalone stocks in the San Diego area, to assess the effectiveness of future management and recovery schemes by providing important baseline data, and to provide a method for incorporating aggregation-level characteristics into a population viability analysis.

INTRODUCTION

Modern fishing pressure prior to the 1990s dramatically reduced abalone populations in southern California until a fishing moratorium was adopted in 1997 for all abalone species. The pink abalone (*Haliotis corrugata*) was the second-most fished species in California after the southern California fishery was opened to increase food production during World War II (Figure 4.1). The fishery reached a peak in the annual commercial landings of over 3.5 million pounds in the mid-1950s. Because the pink abalone is a warmer-water species, all of the landings were from southern California. Area-specific catch data after 1950 show that the commercial abalone fishing effort focused initially at sites on or near the mainland in southern California, but expanded to the more distant Channel Islands as the fishery matured (California Department of Fish and Game 2002). The largest total pink abalone catch from a mainland source between 1950 and 1995 came from Point Loma and southern La Jolla (Block 860). The catch

from this area peaked at over 250,000 pounds in the mid-1950s, soon after the fishery opened in southern California (Figure 4.2). The catch had declined to less than 50% of the peak within a few years.

The management of the abalone fishery failed by overlooking the influence of life-history traits on the susceptibility of abalone populations to overfishing (Karpov, Haaker et al. 2000). The slow-growing sedentary adult abalone rely on dense aggregations for successful fertilization of gametes (Babcock and Keesing 1999). The duration of the planktonic larval phase is fairly short (5 – 8 days (Leighton 1974)), such that populations may be largely self-recruiting (Prince, Sellers et al. 1988; Tegner 2000). Below the estimated minimum spawning density (MSD) of 2000 abalone per hectare, the population may sustain a depensation, or Allee, effect due to decreased recruitment (Allee 1931; Shepherd and Brown 1993; Karpov, Haaker et al. 1998). Most of the abalone populations in southern California are currently at densities that are orders of magnitude lower than the estimated MSD (California Department of Fish and Game 2002).

Scientists at the California Department of Fish and Game (CDFG) are monitoring the potential recovery of the southern California abalone populations under the direction of the Abalone Recovery and Management Plan (ARMP)(California Department of Fish and Game 2002). This document outlines the need to identify the extinction risk of a population based on the population abundance, size structure, and small-scale spatial structure of the stock (e.g. aggregation characteristics). The San Diego area has been designated in the ARMP as an area of interest for population recovery assessment studies

based on its historical significance in the fishery, however most recent pink abalone survey efforts have focused on sites in the Channel Islands.

According to the ARMP, a population must meet two criteria in order to be considered recovered from overfishing pressures. The population must have a broad adult size distribution (Criterion 1) and an overall density greater than 2,000 abalone per hectare (Criterion 2). Re-opening the fishery will not be considered until all populations at key locations meet these criteria and at least three-quarters of the populations reach a density of 6,600 abalone per hectare. Critical levels of aggregation characteristics are not currently defined in the ARMP for determining the recovery status of the population due to a lack of data. However, the importance of understanding the effect of low densities on aggregation behavior and reproduction is recognized.

The primary purpose of the present research is to describe the current status of the pink abalone population near Point Loma in terms that satisfy the requirements of the ARMP by quantifying both population- and aggregation-level characteristics. Population-level characteristics include population density, size-frequency, sex ratio, and spatial dispersion. Aggregation-level characteristics include distances between nearest neighbors, the average number of neighbors per abalone, aggregation sizes, and the size-frequency and sex ratio within an aggregation. The population-level characteristics may be used to compare the current status of the population with past and future levels whereas the aggregation-level characteristics provide perspectives on the reproductive potential of the population. From the aggregation-level characteristics, I calculate an average egg production value for aggregations of different sizes within the population. I also show how the egg production value may be incorporated into a formal population

matrix model for estimating the future population growth rates. The results of this work will be used to better review the potential recovery of pink abalone stocks in the San Diego area, to assess the effectiveness of future management and recovery schemes by providing important baseline data, and to provide a method for incorporating aggregation-level characteristics into a population viability analysis.

METHODS

Study Area

The Pt. Loma kelp forest is one of the largest kelp forests in the world extending ~10 km along the coast of San Diego, CA (Dayton, Tegner et al. 1992). Within the central part of the kelp forest, I demarcated a 9-hectare area (300 m x 300m) which ranges in depth between 12 and 15 meters and contains substantial pink abalone habitat (Figure 4.3). Pink abalone are more likely to be found along ledges and under boulders than on the flat rock shelf (Parnell, Dayton et al. 2006). The study area is characterized by a low-relief sandstone and mudstone substrate with scattered boulders and extensive ledge systems, and is dominated by Giant Kelp (*Macrocystis pyrifera)* with holdfasts often measuring over a meter in diameter. Clearings in the Giant Kelp are dominated by understory kelp species (*Laminaria*, *Pterygophora,* and *Eisenia*). In all cases, the survey sites within the 9-hectare area were chosen randomly using computer-generated random waypoints.

Size-Frequency Data

The first criterion of population recovery as defined in the ARMP requires a broad size distribution of emergent adults within two size categories: intermediate (100-152mm) and large (153-200mm). The division of the two categories is based on the

historical recreational minimum legal size for pink abalone. Each of the two categories is subdivided into 5mm bins. To meet the ARMP definition of recovery in the size-frequency distribution, the emergent adult sizes must occupy at least 90% of the intermediate size bins and 25% of the large size bins. I calculated the percentage of these bins that contained non-zero values for each year with sample sizes greater than 200 emergent adults. The sizes of the emergent adults were compared across all four years using a Kruskal-Wallis analysis of variance by ranks and a multiple comparison test of the median ranks with a Bonferroni correction for a 0.05 alpha value (0.05 / 3 = 0.0167). The distributions were not normally distributed so that an ANOVA was not appropriate for comparing these data. I also compared the distributions of the emergent adult sizes between survey years with six pair-wise Kolmogorov-Smirnov tests. The critical alpha value used to assess the significance of any differences was determined by applying a Bonferroni correction of a 0.05 initial alpha value (0.05 / 3 = 0.0167).

The ARMP does not include evaluation of cryptic size classes because of the lowered detectability of these individuals in the field. However, evidence of recruitment to the population (individuals smaller than 30mm) is used to qualitatively assess the health of the population (California Department of Fish and Game 2002). Juveniles are often hidden under boulders, in small rock crevices, or under sea urchin spines (Tegner and Dayton 1981). Because they utilize such cryptic habitat, quantification of recruitment to the population is difficult with a non-destructive search protocol. For all surveys, search methods included turning over small boulders when that habitat was present within the area so that juvenile abalone may be encountered. However, much of the habitat consisted of fixed ledges that were inaccessible to searching for juveniles.

Individual size-frequency data were collected for three consecutive years from 2004 to 2006. Abalone size was measured to the nearest millimeter along the longest axis of shell. The measurements of individuals in all surveys were pooled with additional size-frequency data from a tag-recapture study conducted within the same study area (*see Chapter 3*).

T-Square Nearest-Neighbor Distance Methods

The most difficult characteristic to estimate for a low-density patchily-distributed population such as abalone is the population abundance. Because the pink abalone were in low abundance and extremely patchily distributed, standard transect or quadrat methods of estimating abundance may insufficiently sample the population (Krebs 1999). I chose instead to use the T-square nearest-neighbor (TS) method which offers a relatively robust population density estimate for low-density populations (*see Chapter 2*). In addition, this method allows characterization of the population in terms of the average distance between nearest neighbors, the average size of aggregations, and the overall spatial dispersion in the population. In order to obtain nearest-neighbor distances relevant to fertilization potential, all T-square sampling was conducted during the summer and early fall at the peak of the local spawning season for pink abalone. These data are available for three consecutive years from 2005 to 2007. In addition to the distance measurements, I also recorded the size of each abalone involved in the survey. In 2006 and 2007, I also counted the number of abalone within a 2.5 m radius of the first abalone in order to quantify aggregation sizes in the population (method: NN-AS). The 2.5m radius was chosen based on an *in situ* study of fertilization success with increasing distance (Babcock and Keesing, 1999; *see Chapter 2*).

The method for estimating density and spatial dispersion from t-square nearest-neighbor distance data is clearly described by Krebs (1999) (*see also Chapter 2*). Because these data exhibit a negative binomial distribution, I used a Kruskall-Wallis test to determine if there were any significant differences in the median nearest-neighbor distances or aggregation sizes across years. I also performed multiple Kolmogorov-Smirnov tests to compare the distributions of the samples across years. The critical value used to determine significance of the multiple comparison tests was a Bonferroni-corrected alpha-value of 0.05 (Table 4.5).

Transect Mapping

In 2006 and 2007, I mapped the locations, sizes, and genders of all individuals along 30m x 5m band transects. These data provide additional estimates of the population density, spatial dispersion, and aggregation sizes. The index of spatial dispersion is based on the variance-to-mean ratio (VMR) of the transect densities. If the variance is equal to the mean, then the spatial dispersion may be described by a Poisson process. To test the equality of the variance and the mean, the VMR is multiplied by the degrees of freedom ($n - 1$), the product of which has a X^2 distribution.

I also used transect mapping data to quantify aggregation-level characteristics. After creating a map of the locations of every abalone along the band transect, six contiguous circular plots (radius = 2.5 m) were superimposed on the map and the number of individuals in each circle was recorded as the aggregation size (method: Map-AS). Three summary statistics originally described by Lloyd (1967) to measure characteristics of crowding are "mean density," "mean crowding," and "patchiness." Mean density ($\bar{x}$) is defined as the number of abalone found in the circular plots (N) divided by the number

of circular plots (Q). Mean Crowding ($\dot{x}$) is the average number of neighbors *per individual* per circular plot. Patchiness ($\dot{x}/\bar{x}$) describes the relative degree of aggregation. If the patchiness is equal to one, then an individual is as crowded as it would be in a randomly distributed population.

In addition to recording the number of abalone, I also recorded the sex and size of the individuals in each circle to obtain aggregation-specific size frequencies and sex ratios. The standard method for gender determination in abalone involves visually inspecting gonad color through the skin (dark green = female; creamy white = male); however this technique biases the results in favor of females. Underdeveloped or spawned-out males appear to have darker gonads, similar to a female gonad. I found that analyzing a small sample of gonad taken with a 16-gauge syringe results in much more accurate sexing of individuals and does not cause mortality in either pink or red abalone (*see Chapter 3*).

By comparing the observed distribution of sex ratios with the expected distribution for a specific aggregation size, I tested the hypothesis that abalone sex ratios were determined by random processes. A Pearson's Chi-Square statistic was calculated for the observed data and compared to a distribution of bootstrap Pearson's Chi-Square statistics in order to estimate the *p*-value of the test. This method is preferred to the standard Chi-Square test when sample sizes are small (Sokal and Rolf 1995). The null hypothesis is that the observed distribution of sex ratios is the same as the expected distribution.

Estimating Reproductive Potential

The ultimate goal of the transect mapping survey was to estimate the reproductive potential of spawning aggregations of different sizes based on the demographic characteristics of real aggregations. I estimated the reproductive potential of the aggregations as the number of eggs produced by a mixed-gender aggregation, dependent on the sizes of the females. If an aggregation contained individuals of only one sex, then the reproductive potential was zero. The number of potential eggs produced by a female of a given size was estimated by:

$$F = ae^{3.324ln(L)-10.4595}$$

where, F is the average female fertility, L is the length of the abalone in millimeters, a = 3,848 eggs / g wet body weight (σ = 1,359) and the exponential portion of the equation converts the shell length to wet body weight (Tutschulte 1976). The reproductive potentials of each female in an aggregation were summed to give the total reproductive potential (TRP) for that aggregation. I ran a regression analysis to determine the relationship between aggregation sizes and the average TRP. In order to maximize the number of aggregations included in the analysis, I averaged the TRPs across both survey years.

In addition to the aggregation-specific reproductive potentials, I calculated stage-specific potential egg production by summing the reproductive potentials of each female within a particular size range that was located in a mixed-gender aggregation and dividing by the total number of females in that size range. Rogers-Bennett and Leaf (2006) estimated first year survival probability (P_0) for a red abalone population in a no-take reserve in northern California to be 2.13 x 10^{-5} yr^{-1} for individuals smaller than

25mm. This estimate is a combined fertilization success and survival rate estimate which is multiplied by the female fertility estimate to calculate the expected fecundity. Because the model red abalone population is at a much higher density, with larger aggregations and closer nearest-neighbor distances, the fertilization rate is likely higher in this population. Nearby red abalone populations at Ocean Cove had average aggregation sizes of 14 abalone and nearest-neighbor distances of 1.2 meters (*see Chapters 2 and 5*). This distance corresponds to a ~70% fertilization success using Babcock and Keesing's (1999) fertilization curve. If the fertilization success rate is decreased to 20% (corresponding to distances > 5m) so that it might better relate to the pink abalone fertilization rates, then the P_0 estimate is 6.09×10^{-6} yr^{-1}. Multiplying this modified P_0 estimate by the stage-specific female reproductive potential gives a stage-specific approximation of the potential recruitment to the population in the following year per female. Dividing this value by two estimates the stage-specific production of female offspring, assuming a 1:1 sex ratio.

Estimates of stage-specific recruitment potential based on the measured aggregation characteristics were put into a matrix population model in order to determine the expected net reproductive rate of the population (R_0) and the population growth rate (λ_1). R_0 is related to the annual λ_1 because it is an estimate of the average number of successful female offspring produced during the lifetime of each female. Success is measured by the offspring surviving to sexual maturity. If R_0 equals one, each individual on average produces one successful offspring over the lifetime and the population neither grows nor shrinks. The value of R_0 with respect to 1 is directly related to the value of λ with respect to 1 for that year (Caswell 2001).

I created a four-stage matrix model of the pink abalone with the growth transition probabilities and adult survival rates described in Chapter 3. The four stage classes included in the matrix were cryptic juveniles (25-50mm), cryptic subadults (50-100mm), intermediate-sized emergent adults (100-153mm), and large-sized emergent adults (>153mm). The cutoff between the two adult stage classes was defined by the historic minimum legal size for the recreational fishery in California. The growth transition matrix (**G**) was calculated based on a model fit to growth increment data (Rogers-Bennett and Rogers 2006) for pink abalone obtained from Tutschulte (1976) and from the tag-recapture study discussed in Chapter 3. Tutschulte's data included both laboratory-reared individuals and those recaptured from the wild. I approximated a size-at-maturity probability curve based on the probability of gender determination using the gonad-sampling method (*see Chapter 3*).

I estimated an upper and lower bound on the results using the upper and lower 95% confidence intervals of the estimated growth and survival parameters (*see Chapter 3*). I used the survival estimates of 0.51 yr^{-1} (0.41-0.61) for the two cryptic size classes and 0.77 yr^{-1} (0.64-0.86) for the two emergent size classes. The growth transition probabilities in **G** were multiplied by the survival rates for the corresponding stage class to obtain a 4x4 transition matrix (**T**). The transition probability matrix (**T**) shows the probability that an individual starting in one size class will survive, and either remain in that size class or grow to another size class in the following year (Table 4.8). Six 4x4 fecundity matrices (**F**) consisted of zeros in all but the 3 rightmost cells of the top row (Table 4.9). The average stage-specific fecundities and 95% confidence intervals were calculated for the two levels of fertilization success – high (70%) and low (20%).

The fundamental matrix (**N**) used to calculate R_0 was created by taking the inverse of the transition matrix (**T**) subtracted from a 4x4 identity matrix (**I**):

$$\mathbf{N} = \text{inv}(\mathbf{I} - \mathbf{T})$$

and

$$\mathbf{R} = \mathbf{FN}$$

where, R_0 is the r_{11} (upper left corner) entry in the matrix **R** (Caswell 2001)**.** The population growth rate was estimated from the matrix **A** = **T** + **F** by calculating the dominant eigenvalue (λ_1) of the matrix. In its simplest interpretation, if λ_1 equals one, then the population is neither growing nor shrinking.

RESULTS

Population-Level Characteristics

Population Density

The population density estimate from the T-square nearest-neighbor distance data remained steady, near 100 abalone per hectare, for all three years of the study. These estimates are based on 14 (2005), 28 (2006), and 11 (2007) pairs of distance measurements. The population density estimates from the transect mapping data were similarly low, 230 and 77 abalone per hectare average densities in 2006 and 2007, respectively (Figure 4.4). The average density, combining the transect data from 2006 and 2007, was 170 abalone per hectare. Total areas of 3,000 m^2 in 2006 and 1,950 m^2 in 2007 were surveyed during the transect mapping study.

Size-Frequency Distributions

The sizes of individuals measured in 2004-2006 ranged from 22 mm to 193 mm. The majority of individuals detected were emergent adults greater than 100 mm in length

(Figure 4.5). The size-frequency recovery criterion defined by the ARMP was met during all three years (Table 4.1). The size distribution in 2004 was significantly different from the distributions in 2005 and 2006 (Table 4.2). The average adult size was significantly smaller in 2004 than in the later years of the study (Kruskal-Wallis $X^2_{2,703}$ = 26.69; p-value = 0.0000). This size increase was due in part to a reduction in the relative number of individuals in the smaller adult size-classes, which is suggestive of variable annual recruitment in the population.

Despite the difficulties in detecting juveniles in complex habitats, annual recruitment was confirmed for 2003-2005 by the presence of individuals between 20 and 40 mm (~1 year old) encountered during the 2004-2006 survey years. The broad size distribution of juveniles encountered in 2006 further supports the hypothesis that recent recruitment occurred for several years in a row. However, the magnitude of the recruitment events cannot be determined.

Population Sex Ratio

In 2006, the gonads of 94 abalone were sampled in order to determine their genders. The genders of 17 abalone were not determinable because of insufficient sperm or eggs for detection with the syringe method. With the exception of one individual (156mm length), these abalone were all less than 100mm in length. The larger abalone may have already spawned the majority of its gonad by the time I had sampled it. Of the remaining 77 abalone, 37 were male (48% male). The sex ratio within the population was not significantly different from a one-to-one ratio (two-tailed binomial exact goodness-of-fit: p-value = 0.8199).

Spatial Dispersion

The spatial dispersion of individuals within the population in both 2005 and 2006 was highly aggregated according to the T-square index of dispersion, but was randomly distributed in 2007 (Table 4.3). The variance-to-mean ratios of the transect data in 2006 and 2007 also suggest a decrease in the degree of aggregation in 2007 although the value still shows significant aggregation in the population (Table 4.4). Lloyd's Patchiness statistic shows that the abalone were 7.8 (2006) and 5.7 (2007) times more aggregated than a randomly distributed population.

Aggregation-Level Characteristics

Nearest-Neighbor Distances

Figure 4.6 shows the distribution of nearest-neighbor distances in the summers of 2005-2007. Each bar in the histogram is equivalent to 2.5 m in order to put the data into the context of fertilization distance (Babcock and Keesing 1999)(*also, see Chapter 2*). The proportion of abalone with neighbors less than 2.5m away was consistently less than 50% each year. The average distance between nearest neighbors was greater than 5 meters in all three years of this study (Table 4.3). There were no significant differences in the median nearest-neighbor distances among the three years (Kruskal-Wallis $X^2_{2,52}$ = 2.23; p-value = 0.3284). The distributions of the distances were also not significantly different (Table 4.5).

Aggregation Sizes

Aggregation sizes ranged from 1 to 9 abalone, with a plurality of aggregations consisting of solitary individuals (Figure 4.7 and 4.8). The average aggregation size measured with the nearest-neighbor method (NN-AS) was 1.6 and 2.0 abalone in 2006

and 2007, respectively (Table 4.3). The average aggregation size estimated from the transect mapping method (Map-AS) was 2.6 and 1.4 abalone in 2006 and 2007, respectively (Table 4.4). The results of the two methods for determining aggregation sizes were not significantly different in either 2006 (Kruskal-Wallis $X^2_{1,47} = 1.07$; p-value = 0.3004) or in 2007 (Kruskal-Wallis $X^2_{1,18} = 0.10$; p-value = 0.7486). Comparisons of the median aggregation sizes showed no significant differences between 2006 and 2007 for either the NN-AS method (Kruskal-Wallis $X^2_{1,36} = 0.27$; p-value = 0.6053) or the Map-AS method (Kruskal-Wallis $X^2_{1,29} = 2.21$; p-value = 0.1375). Likewise, Kolmogrov-Smirnov tests comparing the distributions of aggregation sizes showed no significant differences between years or methods (Table 4.5).

Although a large proportion of the aggregations in both years consisted of only one individual, the proportion of sampled abalone in aggregations greater than one was high. In 2006, 69% (NN-AS) and 81% (Map-AS) of the abalone sampled were in aggregations greater than one. In 2007, 45% (NN-AS) to 56% (Map-AS) of the abalone were in aggregations greater than one. The Map-AS summary statistics for 2006 show that although the average number of abalone per circular plot was only 0.5 (mean density), the average number of neighbors *per abalone* was 3.8 (mean crowding). The 2007 results show a reduction in these statistics (Table 4.6).

Aggregation-Specific Sex Ratios

Because of the extremely small sample sizes obtained in 2007, only the data from 2006 were used to analyze the distribution of sex ratios within aggregations. In 2006, 22 out of the 120 circular plots from the transect mapping surveys contained pink abalone. In 2007, only 8 out of 78 circular plots contained pink abalone. Only one of those 8 plots

contained more than one adult. The observed distributions of sex ratios within aggregations of 1, 2, and 3 were not significantly different from the expected values based on probabilities assuming a 1:1 overall population sex ratio (Table 4.7).

Aggregation-Specific Reproductive Potential

The reproductive potentials of 14 aggregations were calculated from the combined 2006 and 2007 transect mapping data. The sizes of the aggregations were $2^{(6)}$, $3^{(4)}$, $4^{(1)}$, $6^{(2)}$, and $8^{(1)}$ abalone per aggregation. Superscripts indicate the number of aggregations in each category. All aggregations of three or more abalone contained both sexes, whereas 2/3 of the aggregations with 2 abalone contained both sexes. Non-zero reproductive potentials ranged from 568,919 to 4,844,350 eggs. The average reproductive potential increased linearly with aggregation size (Figure 4.9).

The overall reproductive potential of the sampled aggregations in 2006 was 22,620,863 eggs for 53 abalone, which gives a per capita potential egg production of 426,809 eggs per abalone. The total reproductive potential in 2007 was 1,309,706 eggs for 11 abalone, giving a per capita potential egg production in 2007 of 119,064 eggs per abalone. The estimated per capita next-year recruitment potential was 2.60 recruits per abalone in 2006 and 0.72 recruits per abalone in 2007.

*Stage-specific Recruitment Potential (**F**)*

Because so few abalone were encountered during the aggregation mapping study in 2007 (11 abalone), estimates of the stage-specific recruitment potentials were based on the combine 2006 and 2007 survey results (70 abalone). This analysis resulted in six fecundity matrices (**F**) describing the mean and 95% confidence intervals of the stage-specific recruitment potentials for the two levels of fertilization success considered in this

study (Table 4.9). The large adult stage (A2) fecundity was nearly twice that of the intermediate adult stage (A1), and approximately 16 times the fecundity of the subadult stage (SA). None of the genders of individuals in the juvenile stage surveyed in 2006 were determinable, so the fecundity of the juvenile stage was set to zero. A 71% reduction in the fecundity estimates resulted from the reduction in fertilization success from high to low.

Net Reproductive Rate (R_0) and Population Growth (λ_1)

I used the six fecundity estimates from the combined 2006 and 2007 data (**F**) and three transition matrices (**T**) in order to calculate 18 estimates (mean and 95% C.I.) of R_0 and λ_1 considering two levels of fertilization success for the population (Table 4.10). Estimated population growth rates ranged from 0.823 – 1.302 yr^{-1} for high fertilization success conditions, and from 0.717 – 1.059 yr^{-1} for low fertilization success conditions. Estimated net reproductive rates ranged from 0.350 – 5.873 successful female offspring per lifetime for high fertilization success conditions, and from 0.010 – 1.678 for low fertilization success conditions. This result translates into a 13 – 19% reduction in λ_1 and a 71 – 72% reduction in R_0 for a 72% reduction in fertilization success. For the high fertilization success conditions, the mean and upper 95% confidence interval transition matrices both yielded estimates of positive population growth and R_0 values greater than one (Figures 4.10 and 4.11). For the low fertilization success conditions, only the upper 95% confidence interval transition matrix yielded estimates of positive population growth and R_0 greater than one. The mean population growth rates were 1.070yr^{-1} (R_0 = 1.512) for high fertilization success and 0.902 yr^{-1} (R_0 = 0.430) for low fertilization success conditions.

DISCUSSION

The results of this study indicate that the pink abalone population in Point Loma is partially recovered as defined by the ARMP. The first recovery criterion, requiring a broad size-frequency distribution of emergent adults, is more than satisfied in this population with 90-100% of intermediate size classes and 60-70% of large size classes represented. New recruits to the population were discovered during three consecutive years between 2004 and 2006, suggesting that reproductive failure is not occurring in this population. In addition, the even sex ratio in this population is consistent with previous abalone records (California Department of Fish and Game 2002), indicating that demographic stochasticity is not strongly influencing the dynamics. This is an important feature because demographic stochasticity most strongly influences the dynamics of populations near extinction (Lande, Engen et al. 2003).

However, the population density (~100 abalone / ha) is an order of magnitude lower than the estimated minimum spawning density (2,000 abalone / ha) required to satisfy the second ARMP recovery criterion. Such a low-density abalone population is considered at high risk for recruitment failure and local extinction in the absence of artificial recovery efforts (Shepherd and Brown 1993; Shepherd and Partington 1995; California Department of Fish and Game 2002). This possibility is particularly troublesome because the Point Loma population is considered one of the highest-density pink abalone populations in southern California (Peter Haaker (CDFG), *personal communication*). Additionally, the average nearest-neighbor distances were greater than 5 meters during all three years of the study, which is suggestive of low fertilization rates (~20%) of spawned eggs. The mean predicted population growth rate under low

fertilization conditions is only 0.91 yr^{-1}, indicating that this population may be declining by 9% each year.

Population Viability – λ_1 and R_0

Population viability analysis (PVA) provides a formal method for estimating the risk of quasi-extinction, or the risk of reaching such a low population size that extinction is extremely likely. PVAs often use estimates of population growth rate (λ_1) and net reproductive rate (R_0) from demographic models to predict the future trajectory of the population. The International Union for the Conservation of Nature (IUCN) has adopted rules that partially define the threat levels to species of concern corresponding to specific R_0 and λ_1 values – vulnerable ($R_0 \leq 0.928$; $\lambda_1 \leq 0.978$), endangered ($R_0 \leq 0.794$; $\lambda_1 \leq 0.933$), and critically endangered ($R_0 \leq 0.585$; $\lambda_1 \leq 0.851$) (Caswell 2001; IUCN 2001). Considering the mean predicted values of λ_1 and R_0 for the Point Loma pink abalone population within the context of the IUCN classification scheme, this population should be classified as endangered if the fertilization success in the population is as low as is suggested by the average nearest-neighbor distances. If the probability of fertilization success were high, then the population would not qualify for any of the IUCN classifications.

Abalone are known to exhibit high levels of spatial and temporal variability in vital rates (Vilchis, Tegner et al. 2005; Leaf, Rogers-Bennett et al. 2007), and that variability through time may negatively impact the long-run growth rate of the population (Lande, Engen et al. 2003). Time-variant models are useful for predicting both the long-run growth rate of the population and the probability of reaching quasi-extinction over a specified number of years or generations (Caswell 2001; Morris and Doak 2002; Lande,

Engen et al. 2003). The estimates used in the current study represent the variability in the predictions based on aggregation-influenced fecundity estimates for just one year. A time-variant model for this population should incorporate aggregation-influenced fecundity estimates from multiple years of surveys, or from simulated sets of aggregations where the average aggregation size is dependent on the density of the population. The probability of fertilization success within the population will also be dependent on the population density and the degree of aggregation in the population and may be calculated based on simulated spawning events (Claereboudt 1999). The effects on the long-run growth rate by varying fecundity and fertilization rate over time with population density should be investigated in the future.

An Historical Perspective

Any conclusions about the extinction risk of the pink abalone population based solely on the current population density may be misleading, especially if the current levels are not considered within the context of historical abundances. Estimating the historic abundances of the abalone populations in San Diego is difficult due to the sweeping and long-term anthropogenic impacts to the local kelp forest ecosystem (Dayton, Tegner et al. 1998). The greatest threat to the pink abalone populations prior to the 1800s was probably from the local sea otter population. Sea otters are voracious predators on benthic invertebrates, with particular preferences for abalone and sea urchins (Wild and Ames 1974; Costa 1978). In central California, abalone are restricted to deep crevices that are inaccessible to the resident sea otter population (Hines and Pearse 1982; Micheli, Shelton et al. 2008). Within the depth range of the pink abalone in the Point Loma kelp forest, much of the crevice habitat is too small to offer protection from otter

predation (*personal observation*). By 1911, the southern sea otter population near San Diego had been completely extirpated. There are no records quantifying pink abalone abundances prior to the extirpation of the otter population.

No quantitative surveys of pink abalone populations were conducted in Point Loma prior to the 1970s, during the peak harvesting period of the modern fishery. In the years following the close of the fishery, three surveys of the Pt. Loma kelp forest reported densities of pink abalone. A 1998 survey of 200m^2 at a depth of 34 feet yielded 2 pink abalone, giving an approximate adult density of 100 / ha (Coastal Resources Management 1999). In 1999, another survey found an average adult density of 84 / ha for depths between 33 and 39 feet (total area: 835m^2) (L.A. de Wit - Consultant and Coastal Resources Management 2000). The same authors reported an average adult density of 13 / ha for depths between 44 and 50 feet in 2000 (total area: 790m^2). They also found juveniles by intensively sampling a subset of the study area. In 1999, the average density of juvenile pink abalone was 240 / ha (total area: 164m^2). No juveniles were found in 2000 at the deeper locations (total area: 159m^2). The similarity of the most recent density estimates to the results of the present study suggests that the population abundance in Point Loma has not declined since the close of the fishery in 1997, and may have actually increased a small amount. The presence of a large number of juveniles in 1999, and the continued recruitment discovered during 2004-2006, further suggests that the population remains reproductive.

Recruitment

Although abalone populations are thought to be largely self-recruiting (Prince, Sellers et al. 1988; McShane 1996; Dowling, Hall et al. 2004), the source of the

recruitment to the Point Loma pink abalone population is unknown. One of the assumptions of the matrix population model is that the population acts as a closed system, such that all of the individuals produced by the population remain within the population, and no larval supply from other nearby populations enter. Considering the high density of the Point Loma population relative to known nearby pink abalone populations, the number of incoming larvae from other populations may be negligible. However, there may be higher density areas within the Point Loma kelp forest or the surrounding areas that have not yet been discovered. The area surveyed for this study (9 ha) represents a small portion of the potential habitat for pink abalone within the Point Loma kelp forest (~225 ha (Ed Parnell, *unpublished data*)). Additionally, the habitat in Imperial Beach, the Coronado Islands, and the Mexican mainland to the south is not as well documented as Point Loma. The habitat in nearby La Jolla to the north is complex with extremely deep crevices such that large numbers of abalone may not be detected. Given the strength of the local currents (2 – 5 cm/s) and the temporally shifting direction (north or south) of these currents (Ed Parnell, *personal communication*), any of these locations could act as either larval sources or sinks for the Point Loma population.

Aggregation Characteristics

Despite the extremely low density, the Point Loma pink abalone population maintained a highly-aggregated spatial dispersion as demonstrated by all three indices of aggregation (T-square index of dispersion: Table 4.3, Transect variance-to-mean ratio: Table 4.4, and Lloyd's patchiness: Table 4.6). The strong habitat affinity of the abalone to patchy, higher-relief areas may facilitate this aggregated spatial distribution at low densities (Parnell, Dayton et al. 2006). However, the average aggregation size measured

by both the NN-AS and Map-AS methods was only ~2 abalone (Table 4.3, Table 4.4), with close to half of the aggregations consisting of only one individual (Figure 4.7 and 4.8). Another way to view these data is to average the aggregation sizes across individuals as described by Lloyd (1967). The average number of neighbors *per individual* within a series of circular plots estimated by Lloyd's mean crowding method was 3.8 (±2.9) in 2006 but only 0.8 (±1.2) in 2007 (Table 4.6). That translates to an average aggregation size *per individual* of nearly 5 (2006) to less than 2 abalone (2007).

Although the majority of the aggregations surveyed during this study with more than one abalone contained both genders, the frequency of sex ratios within the aggregations was consistent with the hypothesis that individuals aggregate irrespective of gender. This conclusion is based on very small sample sizes and should be investigated further. If abalone do not actively aggregate toward individuals of the opposite sex, the probability of generating mixed-gender aggregations is reduced. However, the maintenance of an even sex ratio in the population maximizes the probability of creating mixed-gender aggregations when sexes are randomly-distributed (Figure 4.12). Within the range of average aggregation sizes *per individual*, the probability of generating mixed-gender aggregations is 50% (2 abalone) to 94% (5 abalone), assuming that all individuals in the aggregation are mature.

Fertilization Success

Quantifying the number of abalone in an aggregation is important in order to determine the probability of a mixed-gender aggregation as well as the relative number of potential gametes in the water column, both of which influence fertilization success (Pennington 1985; Levitan, Sewell et al. 1992; Claereboudt 1999). However, the

distances between the individuals within the aggregations also greatly influences the fertilization success (Pennington 1985; Levitan 1991; Babcock and Keesing 1999). The average distance between nearest-neighbors measured in this study was greater than 5 meters during all three years. This distance is associated with less than 20% fertilization success due to a decrease in the relative sperm:egg concentration as the distance from the source of sperm increases (Babcock and Keesing 1999). This estimate of fertilization is based on an *in situ* experiment with gametes of *Haliotis laevigata*, a South Australian abalone species. Many other abalone species, including the pink abalone, require similar relative gamete concentrations in order to optimize fertilization success (Kikuchi and Uki 1974; Leighton and Lewis 1982; Clavier 1989; Babcock and Keesing 1999; Riffell 2005).

The critical distance between spawning individuals will change as a function of environmental factors such as the speed, directionality, and turbulence of the current flow (Levitan, Sewell et al. 1992; Denny, Nelson et al. 2002; Crimaldi and Browning 2004). These environmental factors are, in turn, influenced by the complexity of the habitat structure. The flow velocity and turbulence characteristics in crevice and ledge habitats where pink abalone are most abundant are significantly reduced relative to open areas (Riffell and Zimmer 2007). The average current velocity measured by Babcock and Keesing (1999) during the *in situ* fertilization experiment (0.055 m/s) was very similar to the average current velocity measured by Riffell and Zimmer (2007) for the crevice and ledge habitat in the Point Loma kelp forest (0.052 m/s). Babcock and Keesing (1999) did not report turbulence characteristics in their study area, but the lack of canopy-forming kelps in South Australia may subject those populations to greater effects from ocean swell (i.e. surge) that could create a higher turbulent environment (Jackson and Winant

1983; Jackson 1984; Jackson 1998). From descriptions of the unidirectional and non-directional current flow during the *in situ* study, the effects of ocean swell may have been slight on the days of the experiment. In addition, *H. laevigata* most occupies habitat that is less than 1 meter high which is similar in height to the habitat structure in Point Loma (Shepherd and Partington 1995). Due to the potential similarities in gamete concentration requirements for fertilization and to similarities in the environmental characteristics of *H. laevigata* during the *in situ* study period, the pink abalone fertilization success may follow a similar trend to that reported for *H. laevigata.* This tentative conclusion regarding fertilization success and distance between individuals is only reasonable if the abalone spawn at times when these environmental conditions are met.

CONCLUSIONS

Population- and aggregation-level characteristics help to inform different aspects of abalone population biology. Population-level characteristics provide a broad overview of the status of a population which can be easily compared with past levels for management purposes. Changes in population density over time are particularly useful for predicting the trajectory of a population. The size distribution of the population may indicate potential recruitment or mortality problems in the population. Aggregation-level characteristics provide insight into potential Allee effects that may be influencing the population trajectory at low densities. The nearest-neighbor distances may be useful as a metric for the relative probability of fertilization success in the population and aggregation sizes dictate the probability of mixed-gender aggregations in the population. The effect of these aggregation-level characteristics on the individual fecundities is

important to consider, especially for low density populations that may be most impacted by the reductions in mating and fertilization success (*see Chapter 5*). The density-dependence of these aggregation characteristics should also be considered.

The matrix model described for the pink abalone population provides an option for incorporating density-dependent aggregation data into the fecundity parameters in order to consider the potential Allee effect of reduced fertilization success on population growth rates at low population densities. An intensive tag-recapture study emphasizing juvenile tagging is required in order to improve the survival and growth estimates for the smaller size classes of pink abalone. In addition, a thorough investigation of fertility and size-at-maturity is also needed to improve the fecundity estimates for the Point Loma population and to optimize the structure of the stage-based matrix model. The utility of matrix models in population viability analyses should help to motivate the collection of these required data. As the parameter estimates for this matrix model improves, we may use the model to assess the critical aggregation-level characteristics required to ensure population growth.

ACKNOWLEDGEMENTS

This work was funded by California Sea Grant, the University of California Marine Council Coastal Environmental Quality Initiative, the Edna B. Sussman Fund, the Mia J. Tegner Memorial Fund, a Halliday Field Research grant, the Hicks Foundation, and the Wyer Foundation. Special thanks to P. Haaker and I. Taniguchi who were instrumental in helping me start the tag-recapture study. This work would not have been possible without the additional help of many volunteer divers from the Scripps Institution of Oceanography. In particular, I would like to thank K. Riser, M. Kasuya, J. Shaeffer, S.

Mau, R. Todd, J. MacDonald, B. Pister, C. Gonzalez, C. Lennert-Cody, D. Cie, and M. Goldstein for their enthusiastic help in the field. Thanks also to J. Leichter, and P. Dayton for giving valuable feedback on earlier drafts of this chapter. The material in this chapter is in preparation to submission to the journal Ecological Applications, and was co-authored by Laura Rogers-Bennett. The dissertation author was the primary investigator and author of this paper.

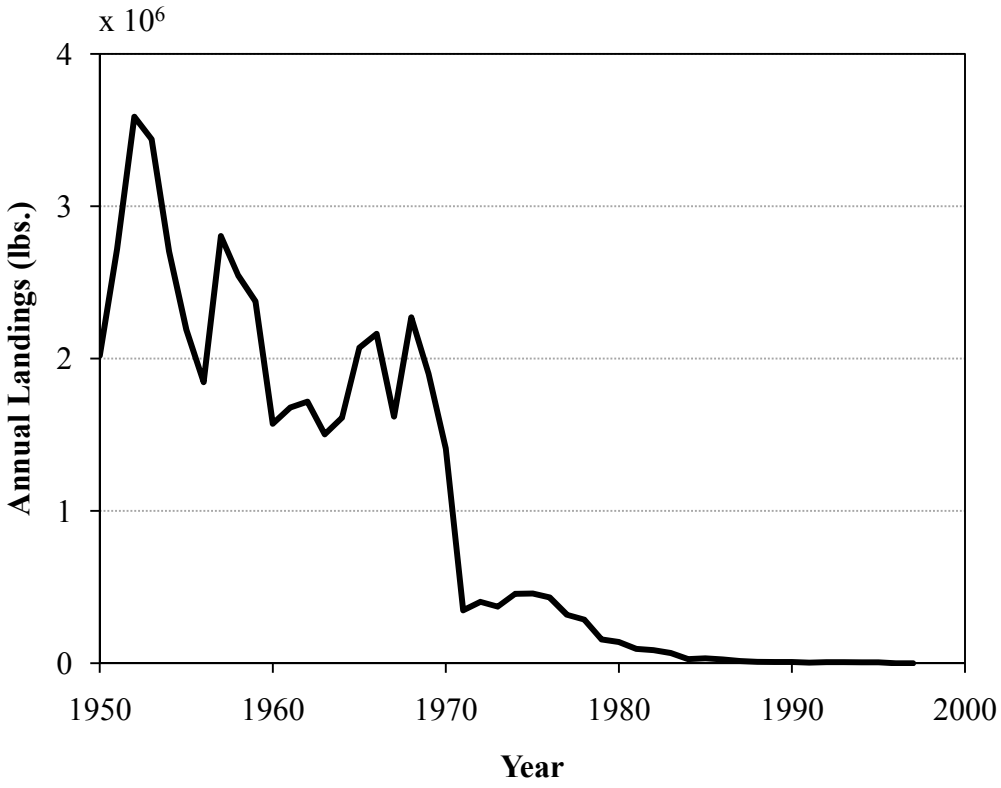

Figure 4.1 Annual commercial landings in pounds for the pink abalone fishery in California. Species-specific landings data is currently unavailable prior to 1950.

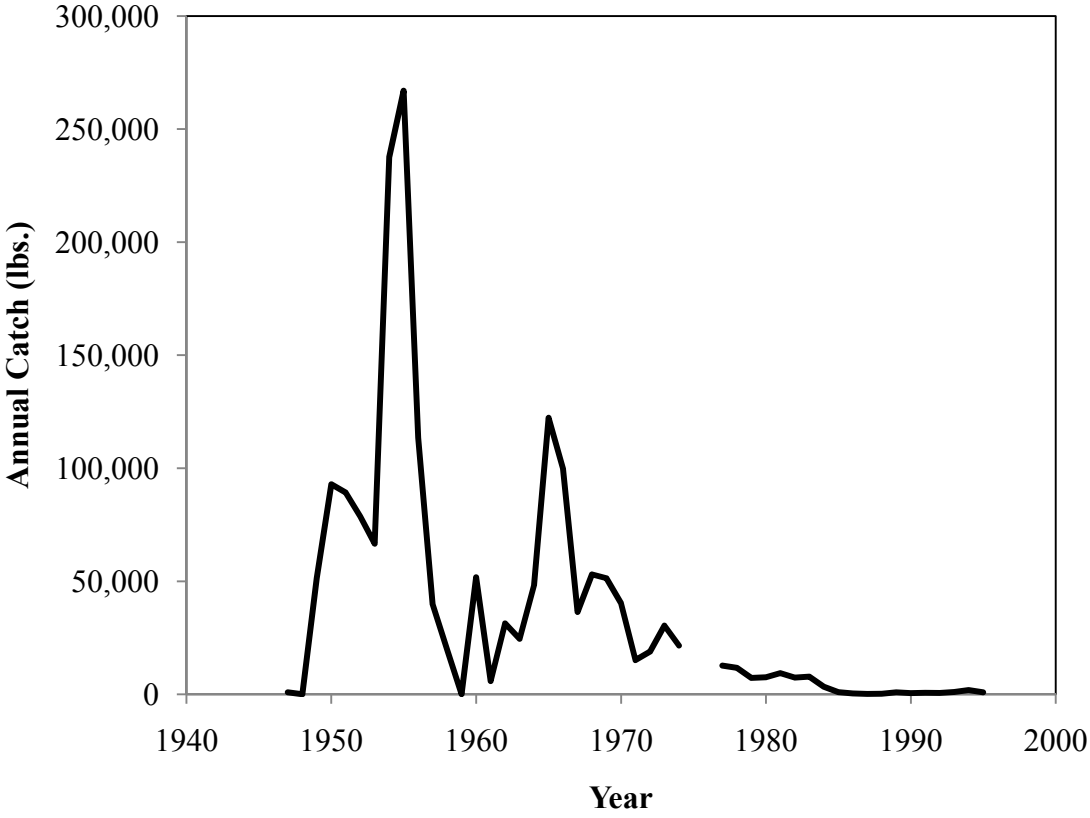

Figure 4.2 Annual commercial catch from Block 860 (Point Loma and southern La Jolla) in pounds for pink abalone in California 1948-1997. Data from 1976 and 1977 was not available.

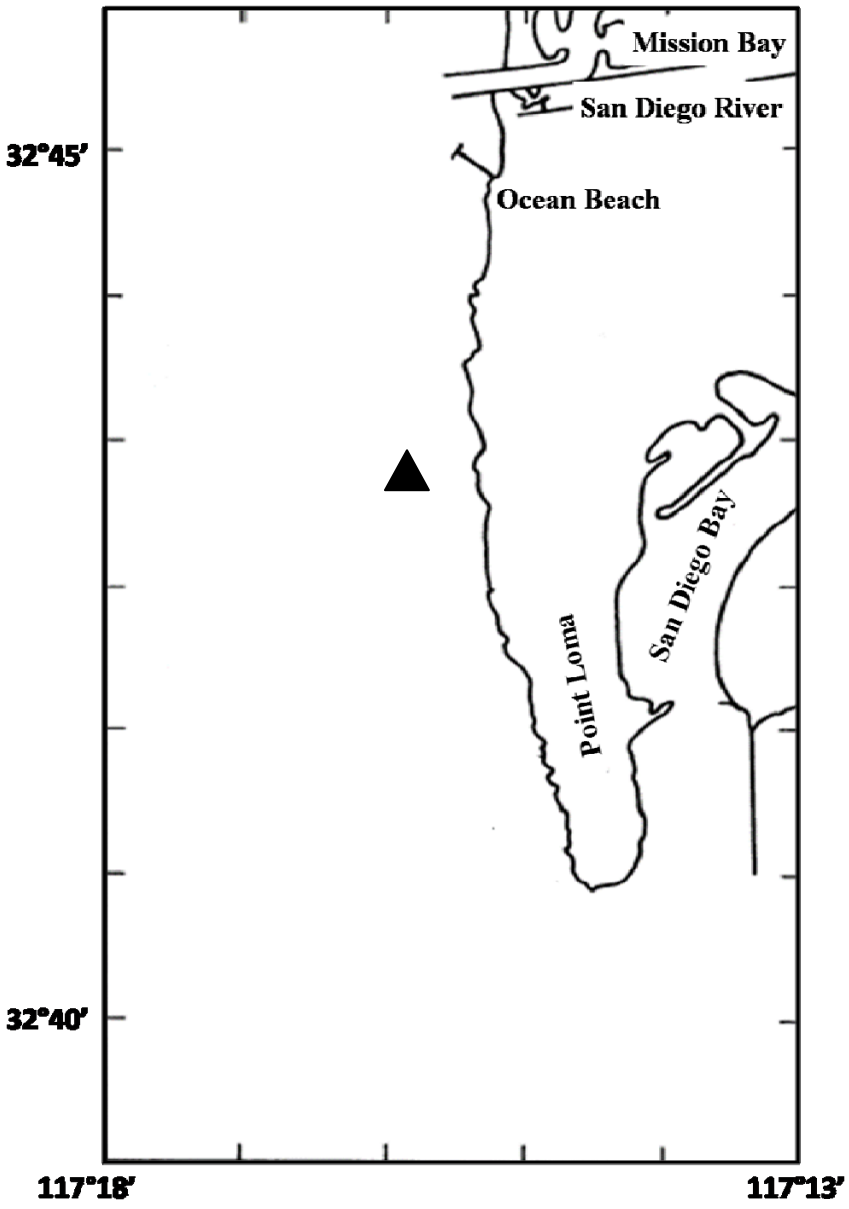

Figure 4.3 Map of the Pt. Loma kelp forest (modified from Dayton *et al*., 1992). The ▲ indicates the approximate location of the 9-hectare study area.

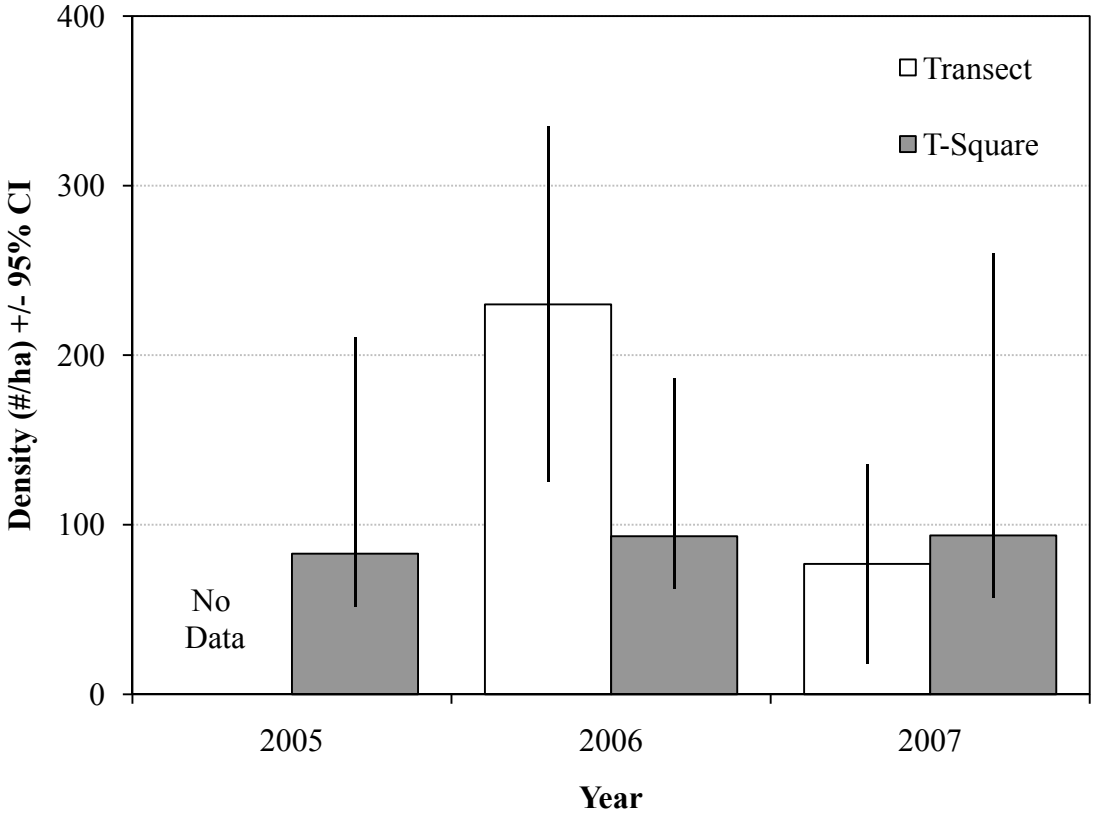

Figure 4.4 Pink Abalone population density estimates (# abalone / hectare) from transect mapping (white) and t-square nearest-neighbor distance (gray) sampling methods 2005-2007. Error bars are standard errors. No transect data are available for 2005.

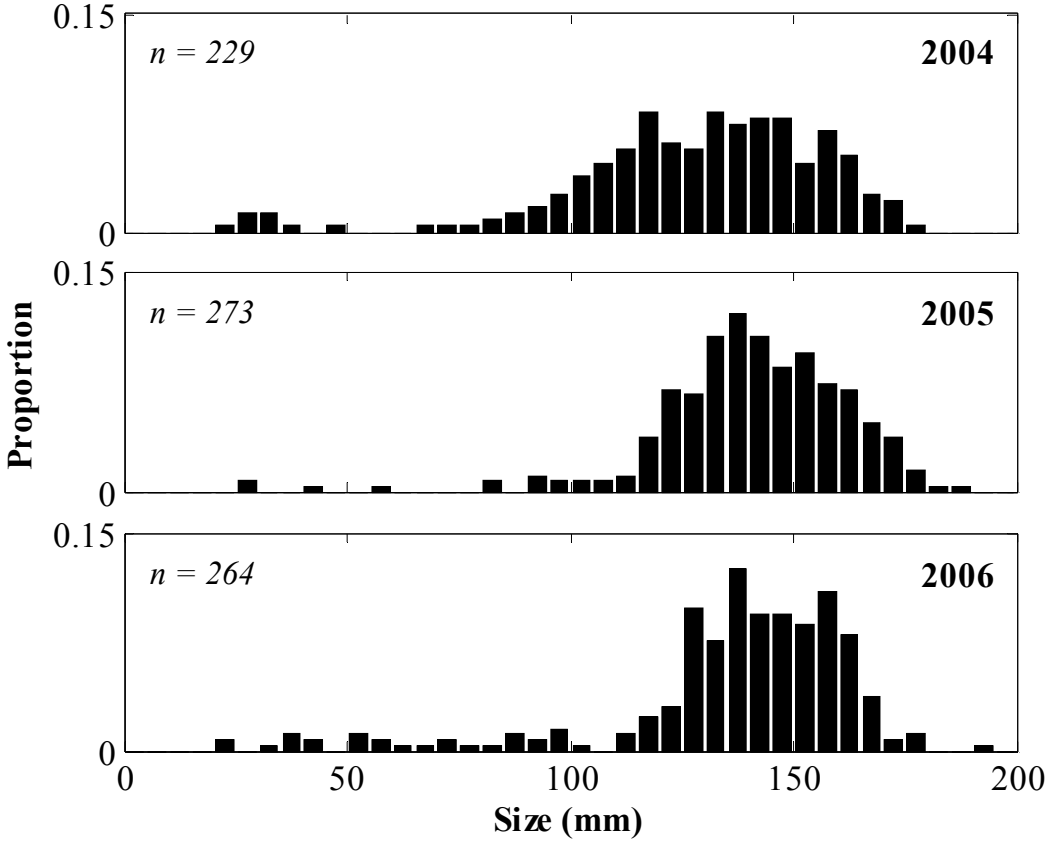

Figure 4.5 Pink Abalone size-frequency distributions 2004-2007. Individuals <100 mm have reduced detectability in the field. *n* is the number of abalone included in the analysis each year. Table 4.1 gives summary statistics of the emergent size classes. Table 4.2 gives the results comparing the distributions of emergent adults between years.

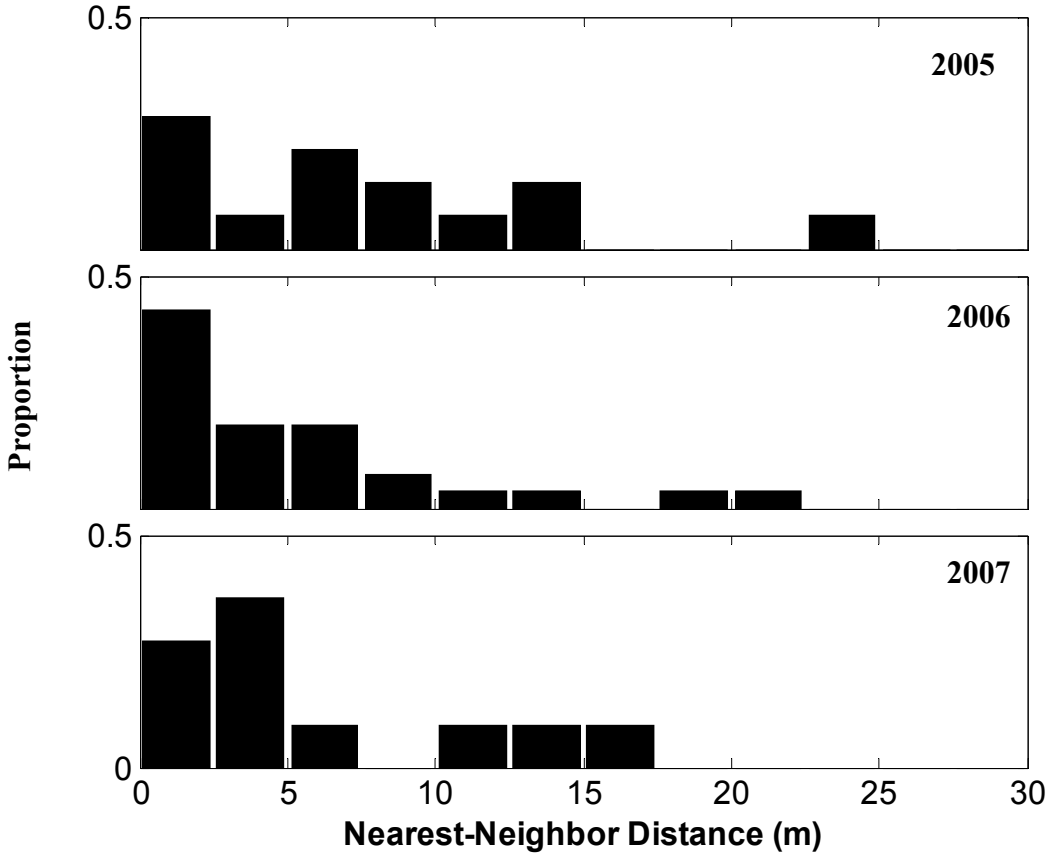

Figure 4.6 Pink Abalone nearest-neighbor distances 2005-2007. Each bar corresponds to bins of 2.5m distances to put the results into the context of the fertilization radius. Fewer than 50% of the individuals have a neighbor within the fertilization radius used for this study. Table 4.3 gives summary statistics for the distributions of nearest-neighbor distances.

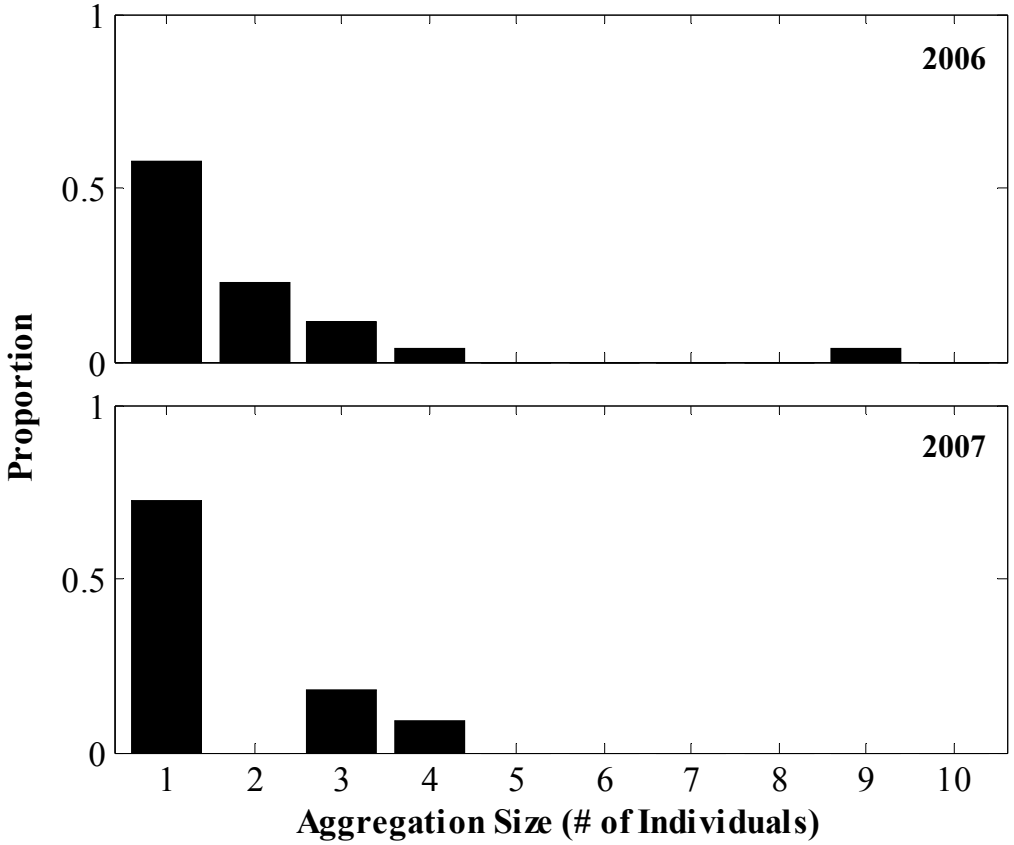

Figure 4.7 Aggregation sizes determined from the nearest-neighbor distance method in 2006 and 2007. Table 4.3 gives summary statistics for these data. More than 50% of the aggregations consisted of solitary individuals in both survey years.

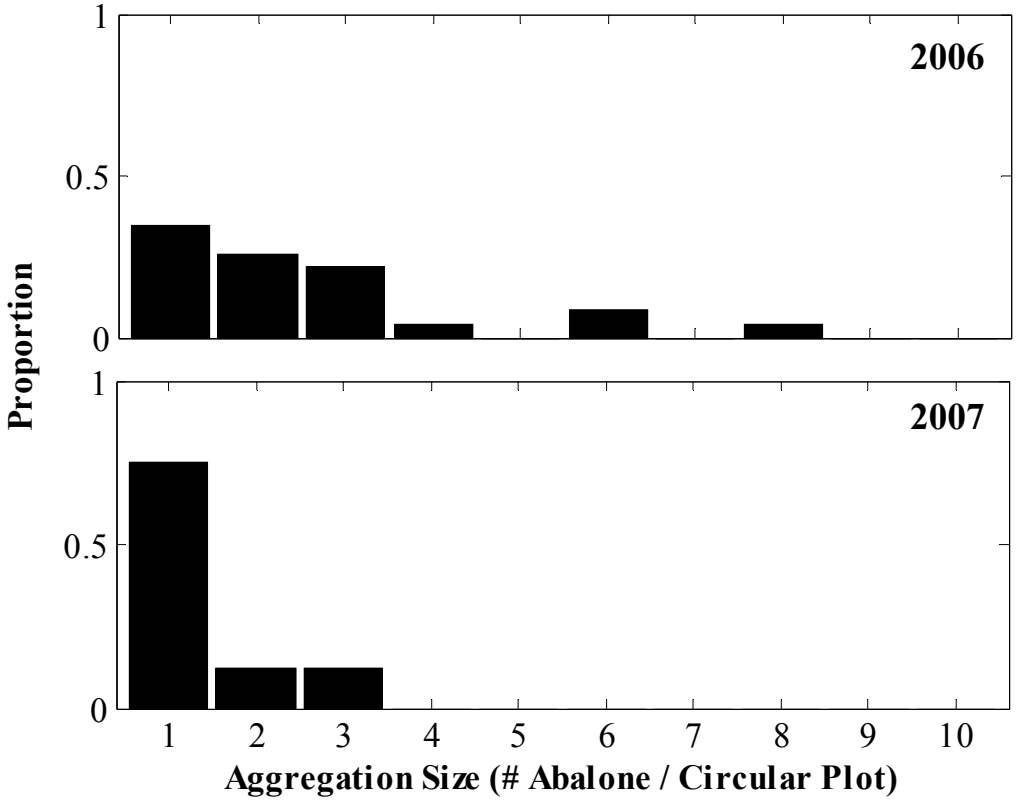

Figure 4.8 Aggregation sizes determined from the transect mapping data (Map-AS) for 2006 and 2007. Table 4.4 gives summary statistics for these data. A plurality of the aggregations consisted of solitary individuals.

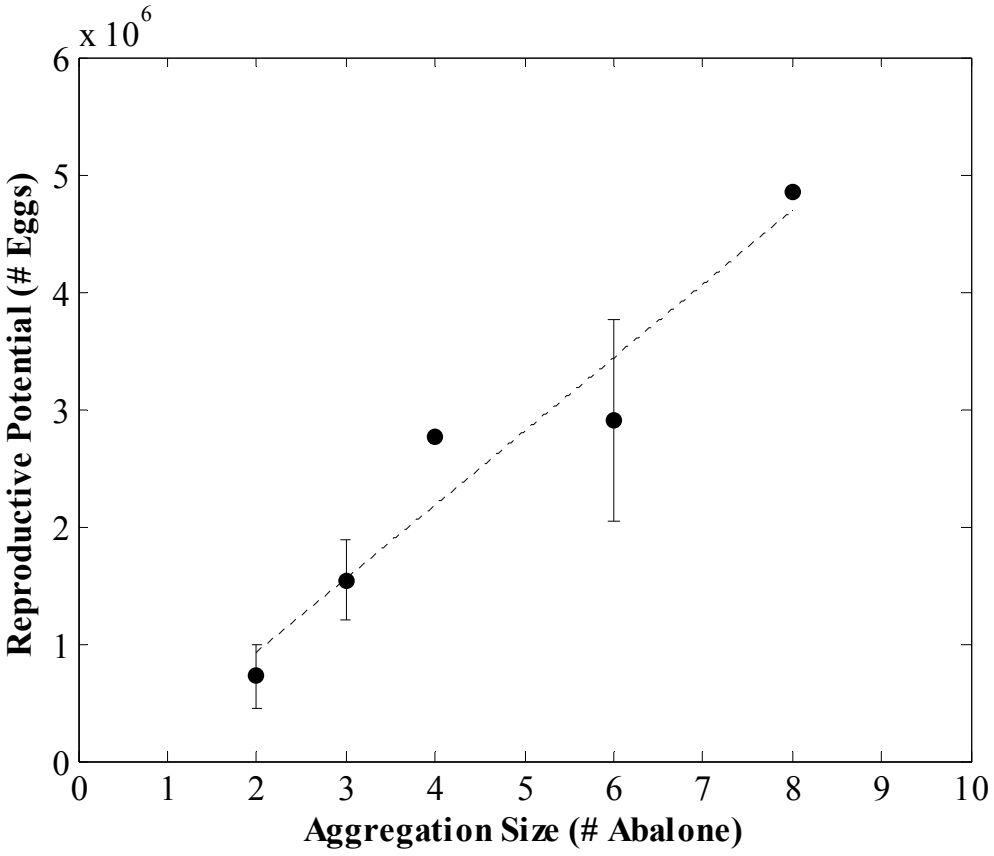

Figure 4.9 Average reproductive potential from the 2006 and 2007 transect mapping data combined. Error bars are standard errors. No errors were calculated for aggregations sizes 4 and 8 because only one sample was available for each. The dashed line indicates the linear fit to the average values: $y = 6.26 \times 10^5 x - 3.27 \times 10^5$; $R^2 = 0.9309$; p-value = 0.0005.

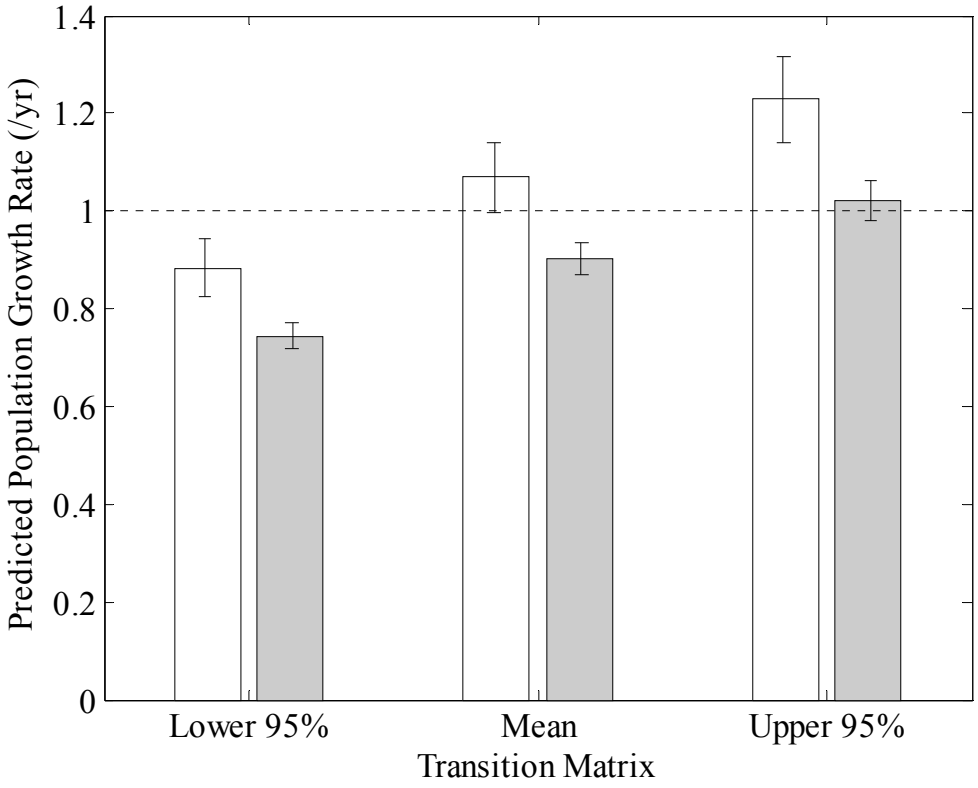

Figure 4.10 Predicted λ for three different transition matrices based on the mean and 95% confidence intervals of the vital rates (growth and survival), and for two levels of fertilization – high fertilization (white bars) and low fertilization (gray bars). High fertilization success assumes that the 1st year survival rate for a high-density red abalone ((Rogers-Bennett and Leaf 2006) included 70% fertilization success. Low fertilization success decreased the 1st year survival rate to include a 20% fertilization success (*see methods*). The error bars represent the predicted λ value for the three transition matrices incorporating the mean and 95% confidence intervals of the size-specific fecundity relationship for shallow water pink abalone reported by Tutschulte (1976). The dashed line at λ=1 represents neutral population growth.

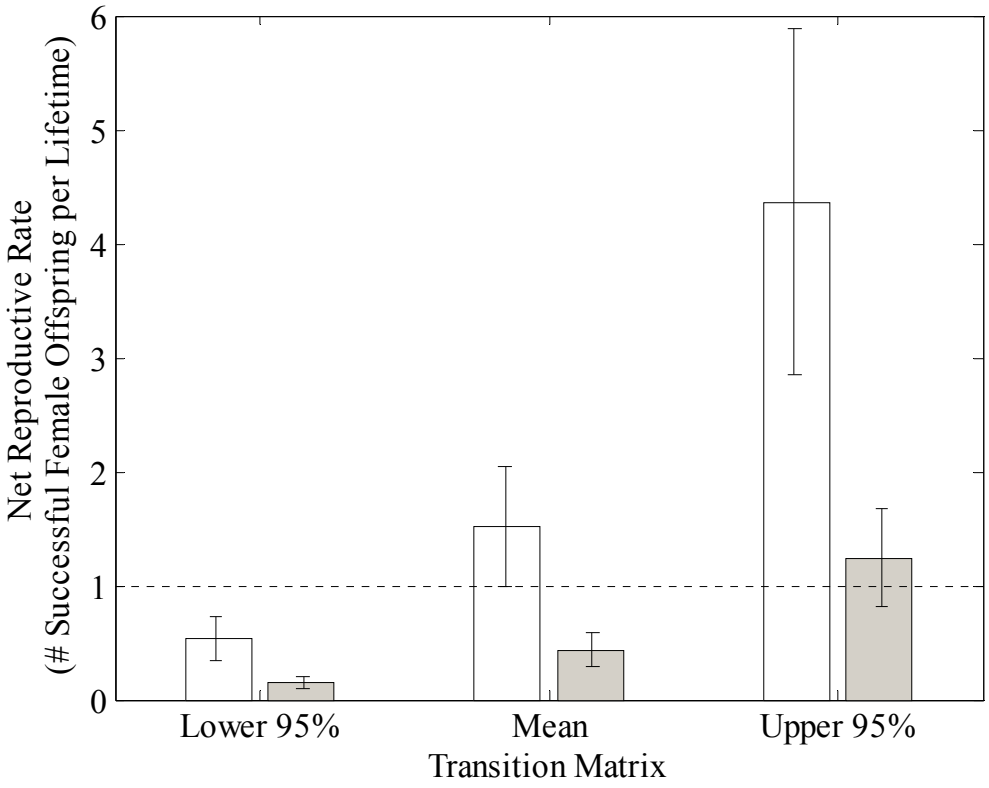

Figure 4.11 Predicted R_0 (net reproductive rate) for three different transition matrices based on the mean and 95% confidence intervals of the vital rates (growth and survival), and for two levels of fertilization – high fertilization (white bars) and low fertilization (gray bars). High fertilization success assumes that the 1st year survival rate for a high-density red abalone ((Rogers-Bennett and Leaf 2006) included 70% fertilization success. Low fertilization success decreased the 1st year survival rate to include a 20% fertilization success (*see methods*). The error bars represent the predicted λ value for the three transition matrices incorporating the mean and 95% confidence intervals of the size-specific fecundity relationship for shallow water pink abalone reported by Tutschulte (1976). The dashed line at R_0 =1 represents the number of lifetime successful offspring equals the number of adults.

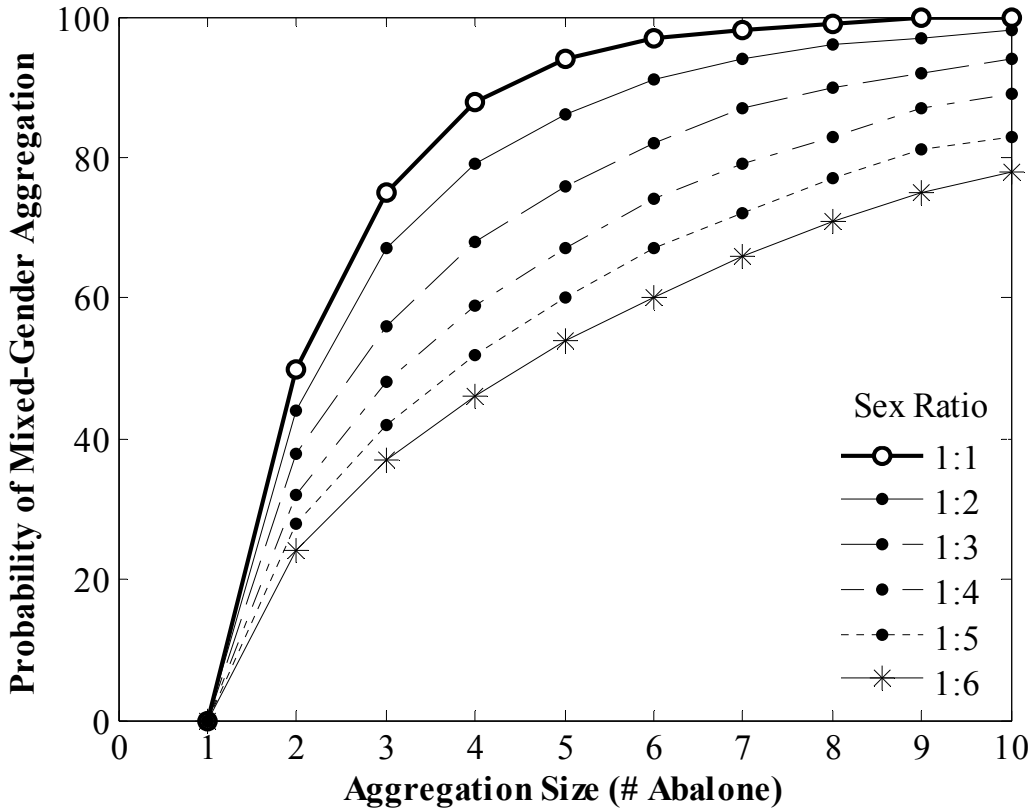

Figure 4.12 Probability of mixed-gender aggregations for aggregations of 1 to 10 abalone. The probabilities are calculated for six different sex ratios (male:female or female:male) – 1:1, 1:2, 1:3, 1:4, 1:5, and 1:6. The probability is maximized with an overall population sex ratio of 1:1 when the abalone aggregate irrespective of gender.

Table 4.1 Statistics describing the size distribution of emergent adults (>100 mm) for each year of the study (2004-2006). n_E is the total number of emergent adults; μ_E is the average size; σ_E is the standard deviation. Intermediate-sized individuals are 100-152mm in length. Large individuals are those greater than the historic recreational minimum size limit of 152mm. *n* is the number of abalone in each size category. "% bins" is the percentage of 5mm bins within each size category with non-zero values. NA means that the analysis was not performed for that year due to the small sample size. "% Large" is the percentage of emergent adults that are greater than 152mm.

				Intermediate		Large		
Year	n_E	μ_E	σ_E	*n*	% bins	*n*	% bins	% Large
2004	203	136	19	159	100	44	60	22
2005	264	144	17	182	100	82	70	31
2006	237	145	15	155	90	82	60	35

Table 4.2 Kolmogorov-Smirnov test results comparing the distributions of emergent adult sizes between two years (X_1 and X_2). The null hypothesis for this test is that the two data vectors have the same continuous distribution. The Bonferroni-corrected critical value for multiple comparisons is 0.05 / 3 = 0.0167. The emergent adult size distribution in 2004 was significantly different from the distributions in 2005 and 2006.

X_1	X_2	p-value
2004	2005	**0.0001**
2004	2006	**0.0000**
2005	2006	0.6762

Table 4.3 Spatial statistics from the nearest-neighbor methods (nearest-neighbor distance, aggregation size, and spatial distribution of the population) for 2005-2007. The spatial distribution is described by the Hines test statistic for randomness of T-square nearest-neighbor distance data. NA = Not Applicable / No data collected during this year. *n* = sample size; μ = average; σ = standard deviation.

	Distance (m)			Aggregation Size			Spatial Dispersion	
Year	*n*	μ	σ	*n*	μ	σ	Description	*p*-value
2005	14	7.4	6.4	NA	NA	NA	Aggregated	**< 0.010**
2006	28	5.1	5.7	26	2.0	1.8	Aggregated	**< 0.005**
2007	11	6.0	5.3	11	1.6	1.1	Random	> 0.050

Table 4.4 Spatial statistics from the transect mapping data (average aggregation size and spatial distribution of the population) for 2006 and 2007. The sample size (*n*) is the number of circles containing abalone; μ is the average number of abalone per circle including only those circles with abalone. VMR is the variance-to-mean-ratio of the transect densities (# / ha). *df* is the degrees of freedom of the transect densities.

	Aggregation Size			Spatial Dispersion			
Year	*n*	μ	σ	Description	VMR	df	p-value
2006	23	2.6	1.9	Aggregated	249	19	**0.000**
2007	8	1.4	0.7	Aggregated	152	12	**0.000**

Table 4.5 Kolmogorov-Smirnov test results comparing the distributions of two data vectors (X_1 and X_2). "Distance" refers to the nearest-neighbor distances; NN-AS is the nearest-neighbor distance method of determining aggregation sizes; Map-AS is the transect mapping method of determining aggregation sizes. Critical α is the Bonferroni-corrected critical alpha value for multiple comparisons of the same data ($0.05 / n$). n is the number of comparison tests performed. The results indicate no significant distances in the distribution of nearest-neighbor distances among the three survey years. Additionally, the distributions of the aggregation sizes were not significantly different between years or methods.

X_1		X_2			
Method	Year	Method	Year	*p*-value	Critical α
Distance	2005	Distance	2006	0.1260	0.0167
Distance	2006	Distance	2007	0.7245	
Distance	2005	Distance	2007	0.5231	
NN-AS	2006	NN-AS	2007	0.9342	0.0125
Map-AS	2006	Map-AS	2007	0.6029	
NN-AS	2006	Map-AS	2006	0.9997	
NN-AS	2007	Map-AS	2007	0.9997	

Table 4.6 Aggregation statistics as described by Lloyd (1967). *N* is the total number of abalone found in the circular plots from the transect mapping data. *Q* is the number of circular plots. "Mean Density" ($\bar{x}$) is the average number of abalone per circular plot (*N* / *Q*). "Mean Crowding" ($\dot{x}$) is the average number of neighbors per individual per circular plot. "Patchiness" ($\dot{x}/\bar{x}$) describes the relative degree of aggregation. If the patchiness were equal to one, then an individual is as crowded as it would be in randomly distributed population.

			Mean Density		Mean Crowding		Patchiness	
Year	*N*	*Q*	$\bar{x}$	SE ($\bar{x}$)	$\dot{x}$	SE ($\dot{x}$)	$\dot{x}/\bar{x}$	SE ($\dot{x}/\bar{x}$)
2006	59	120	0.5	0.13	3.8	1.49	7.8	2.18
2007	11	78	0.1	0.05	0.8	0.63	5.7	3.89

Table 4.7 Comparisons of observed versus expected sex ratio distributions for aggregations of 1, 2, and 3 adult abalone (data from 2006 only). Sex ratios refer only to the relative number of males and females, not to the order in which they appear. *n* is the number of circular plots from the transect mapping data that contained 1, 2, or 3 adults. The observed sex ratio distributions are the raw data describing the number of aggregations that contained the sex ratio illustrated to the left. The expected distribution is the number of aggregations predicted to contain the sex ratio (Probability x *n*). The results suggest that abalone aggregate irrespective of gender, although this conclusion is based on small sample sizes and should be investigated further.

Aggregation Size	Sex Ratios	Probability	*n*	Distributions		Pearson's X^2	*p*-value
				Observed	Expected		
1	♂	0.500	10	5	5	0.0	1.0000
	♀	0.500		5	5		
2	♂♂	0.250	5	0	1.25	2.2	0.5961
	♂♀	0.500		4	2.50		
	♀♀	0.250		1	1.25		
3	♂♂♂	0.125	3	0	0.375	1.4	0.9999
	♂♂♀	0.375		1	1.125		
	♀♀♂	0.375		2	1.125		
	♀♀♀	0.125		0	0.375		

Table 4.8 Transition probability matrix (**T**), not including fecundity estimates, for four stage classes of pink abalone. Juvenile (J) = 25 – 50mm; Subadult (SA) = 50 – 100mm; Adult 1 (A1) = 100 – 153mm; Adult 2 (A2) = 153+mm. The growth transition probabilities were calculated from a logistic dose-response growth equation fit to pink abalone growth data (*see Chapter 3*). Stage-specific survival rates for the adult stages was estimated from mark-recapture data for Point Loma pink abalone (*see Chapter 3*). Juvenile and subadult survival rates were obtained from Tutschulte (1976) for pink abalone near Santa Catalina Island, California. 95% confidence intervals of the transition probabilities are shown in parentheses.

Stage Class	Juvenile (J)	Subadult (SA)	Adult 1 (A1)	Adult 2 (A2)
J	0.26 (0.24 – 0.26)	0	0	0
SA	0.25 (0.17 – 0.35)	0.45 (0.36 – 0.54)	0	0
A1	0	0.06 (0.05 – 0.07)	0.72 (0.60 – 0.81)	0
A2	0	0	0.05 (0.04 – 0.05)	0.77 (0.64 – 0.86)

Table 4.9 Estimates of stage-specific female fecundities with two different levels of fertilization success. High fertilization success assumes that the 1st year survival rate for a high-density red abalone (Rogers-Bennett and Leaf 2006) included 70% fertilization success. Low fertilization success decreased the 1st year survival rate to include a 20% fertilization success (*see methods*). 95% confidence intervals are shown in parentheses.

Fertilization	Stage Class			
Success	Juvenile	Subadult	Adult 1	Adult 2
High	0	0.71 (0.46 - 0.95)	5.87 (3.84 - 7.90)	11.39 (7.45 - 15.33)
Low	0	0.20 (0.13 - 0.27)	1.68 (1.10 - 2.26)	3.25 (2.13 - 4.38)

Table 4.10 Population growth rate (λ_1) and net reproductive value (R_0) based on the average stage-specific fecundities (Table 4.9) calculated from the measured aggregation-level characteristics in 2006 and 2007 (combined data). Three transition matrices based on the mean and 95% confidence intervals of the vital rates (growth and survival) were analyzed for two levels of fertilization (Table 4.8). The 95% confidence intervals (in parentheses) represent the predicted λ and R_0 values for the three transition matrices incorporating the mean and 95% confidence intervals of the size-specific fecundity relationship for shallow water pink abalone reported by Tutschulte (1976).

Transition Matrix	High Fertilization Success		Low Fertilization Success	
	λ	R_0	λ	R_0
Lower 95%	0.883 (0.823 – 0.933)	0.538 (0.350 – 0.722)	0.744 (0.717 – 0.768)	0.153 (0.010 – 0.206)
Mean	1.070 (0.998 – 1.130)	1.512 (0.986 – 2.031)	0.902 (0.868 – 0.931)	0.430 (0.281 – 0.580)
Upper 95%	1.228 (1.141 – 1.302)	4.368 (2.853 – 5.873)	1.023 (0.982 – 1.059)	1.246 (0.815 – 1.678)

REFERENCES

Allee, W.C. (1931). *Animal Aggregations*. The University of Chicago Press, Chicago: 431 pp.

Babcock, R., J. Keesing (1999) Fertilization biology of the abalone *Haliotis laevigata*: Laboratory and field studies. *Canadian Journal of Fisheries & Aquatic Sciences*, **56**(9), 1668-1678.

California Department of Fish and Game (2002). *Draft Abalone Recovery and Management Plan*. California Department of Fish and Game, Marine Region, Sacramento, CA.

Caswell, H. (2001). *Matrix population models: Construction, analysis, and interpretation*. Sinauer Associates, Inc. Publishers, Sunderland, MA: 722 pp.

Claereboudt, M. (1999) Fertilization success in spatially distributed populations of benthic free-spawners: A simulation model. *Ecological Modelling* **121**(2-3), 221-233.

Clavier, J. (1989) Fecundity and optimal sperm density for fertilization in the ormer (*Haliotis tuberculata* L.). In: S.A. Shepherd, M.J. Tegner & S.A. Guzman Del Proo (Eds). *Abalone of the world: biology, fisheries and culture*. Blackwell, Oxford, United Kingdom.

Coastal Resources Management (1999) U.S. Navy Southwest Division P-706 and San Diego Bay Channel Dredge Project, First and second-year monitoring report. Tierra Data Systems, Inc., Escondido, CA: 34.

Costa, D.P. (1978) The ecological energetics, water and electrolyte balance of California sea otter, *Enhydra lutris*. *Biology*. University of California, Santa Cruz, Santa Cruz: 75.
Crimaldi, J.P., H.S. Browning (2004) A proposed mechanism for turbulent enhancement of broadcast spawning efficiency. *Journal of Marine Systems*, **49**(1-4), 3-18.

Dayton, P.K., M.J. Tegner, et al. (1998) Sliding baselines, ghosts, and reduced expectations in kelp forest communities. *Ecological Applications*, **8**(2), 309-322.

Dayton, P.K., M.J. Tegner, et al. (1992) Temporal and spatial patterns of disturbance and recovery in a kelp forest community. *Ecological Monographs*, **62**(3), 421-445.

Denny, M.W., E.K. Nelson, et al. (2002) Revised estimates of the effects of turbulence on fertilization in the purple sea urchin, *Strongylocentrotus purpuratus*. *Biological Bulletin*, **203**(3), 275-277.

Dowling, N.A., S.J. Hall, et al. (2004) Assessing population sustainability and response to fishing in terms of aggregation structure for greenlip abalone (*Haliotis laevigata*)

fishery management. *Canadian Journal of Fisheries and Aquatic Sciences*, **61**(2), 247-259.

Hines, A.H., J.S. Pearse (1982) Abalones shells and sea otters: Dynamics of prey populations in central California USA. *Ecology*, **63**(5), 1547-1560.

IUCN (2001). *IUCN Red List Categories and Criteria: Version 3.1*. IUCN Species Survival Commission, Cambridge, UK: 35 pp.

Jackson, G.A. (1984) Internal wave attenuation by coastal kelp stands. *Journal of Physical Oceanography*, **14**(8), 1300-1306.

Jackson, G.A. (1998) Currents in the high drag environment of a coastal kelp stand off California. *Continental Shelf Research*, **17**(15), 1913-1928.

Jackson, G.A., C.D. Winant (1983) Effect of a kelp forest on coastal currents. *Continental Shelf Research*, **2**(1), 75-80.

Karpov, K.A., P.L. Haaker, et al. (1998) The red abalone, *Haliotis rufescens*, in California: Importance of depth refuge to abalone management. *Journal of Shellfish Research*, **17**(3), 863-870.

Karpov, K.A., P.L. Haaker, et al. (2000) Serial depletion and the collapse of the California abalone (*Haliotis* spp.) fishery. *Canadian Special Publication of Fisheries & Aquatic Sciences*, **130**, 11-24.

Kikuchi, S., N. Uki (1974) Technical study on artificial spawning of abalone, genus *Haliotis* III. Reasonable sperm density for fertilization. *Bulletin of Tohoku Regional Fisheries Research Laboratory*, **34**, 67-71.

Krebs, C.J. (1999). *Ecological methodology*. Benjamin/Cummings, Menlo Park, Calif.: xii, 620 p. pp.

L.A. de Wit - Consultant, Coastal Resources Management (2000) Biological resources and habitat suitability study for a proposed abalone mariculture operation. Maritech Ocean Ranching, Inc., San Diego, CA: 23.

Lande, R., S. Engen, et al. (2003) Stochastic population dynamics in ecology and conservation. In: R. Lande (Ed). *Stochastic population dynamics in ecology and conservation*. Oxford University Press, New York, NY: 1-212.

Leaf, R.T., L. Rogers-Bennett, et al. (2007) Spatial, temporal, and size-specific variation in mortality estimates of red abalone, *Haliotis rufescens*, from mark-recapture data in California. *Fisheries Research (Amsterdam)*, **83**(2-3), 341-350.

Leighton, D.L. (1974) The Influence of Temperature on Larval and Juvenile Growth in 3 Species of Southern California Abalones. *Fishery Bulletin*, **72**(4), 1137-1145.

Leighton, D.L., C.A. Lewis (1982) Experimental Hybridization in Abalones. *International Journal of Invertebrate Reproduction*, **5**(5), 273-282.

Levitan, D.R. (1991) Influence of body size and population density on fertilization success and reproductive output in a free-spawning invertebrate. *Biological Bulletin (Woods Hole)*, **181**(2), 261-268.

Levitan, D.R., M.A. Sewell, et al. (1992) How distribution and abundance influence fertilization success in the sea urchin *Strongylocentrotus franciscanus*. *Ecology*, **73**(1), 248-254.

Lloyd, M. (1967) Mean crowding. *The Journal of Animal Ecology*, **36**(1), 1-30.
McShane, P.E. (1996) Patch dynamics and effects of exploitation on abalone (*Haliotis iris*) populations. *Fisheries Research (Amsterdam)*, **25**(2), 191-199.

Micheli, F., A.O. Shelton, et al. (2008) Persistence of depleted abalones in marine reserves of central California. *Biological Conservation*, **141**(4), 1078-1090.

Morris, W.F., D. Doak (2002). *Quantitative conservation biology: Theory and practice of population viability analysis*. Sinauer Associates, Inc., Sunderland, Massachusetts: 480 pp.

Parnell, P.E., P.K. Dayton, et al. (2006) Marine reserve design: optimal size, habitats, species affinities, diversity, and ocean microclimate. *Ecological Applications*, **16**(3), 945-962.

Pennington, J.T. (1985) The ecology of fertilization of echinoid eggs: The consequences of sperm dilution, adult aggregation, and synchronous spawning. *Biological Bulletin (Woods Hole)*, **169**(2), 417-430.

Prince, J.D., T.L. Sellers, et al. (1988) Confirmation of a relationship between the localized abundance of breeding stock and recruitment for *Haliotis rubra* Leach Mollusca Gastropoda. *Journal of Experimental Marine Biology & Ecology*, **122**(2), 91-104.

Riffell, J.A. (2005) Establishing the biological and chemical processes regulating fertilization success in the red abalone, *Haliotis rufescens*. *Biology*. University of California, Los Angeles: 130.

Riffell, J.A., R.K. Zimmer (2007) Sex and flow: the consequences of fluid shear for sperm-egg interactions. *Journal of Experimental Biology*, **210**, 3644-3660.

Rogers-Bennett, L., R.T. Leaf (2006) Elasticity analyses of size-based red and white abalone matrix models: Management and conservation. *Ecological Applications*, **16**(1), 213-224.

Rogers-Bennett, L., D.W. Rogers (2006) A semi-empirical growth estimation method for matrix models of endangered species. *Ecological Modelling*, **195**(3-4), 237-246.

Shepherd, S.A., L.D. Brown (1993) What is an abalone stock: Implications for the role of refugia in conservation. *Canadian Journal of Fisheries & Aquatic Sciences*, **50**(9), 2001-2009.

Shepherd, S.A., D. Partington (1995) Studies on southern Australian abalone (Genus *Haliotis*). XVI. Recruitment, habitat and stock relations. *Marine & Freshwater Research*, **46**(3), 669-680.

Sokal, R.R., F.J. Rolf (1995). *Biometry*. W.H. Freeman and Company, New York, NY: 887 pp.

Tegner, M.J. (2000) Abalone (Haliotis spp.) enhancement in California: What we've learned and where we go from here. *Canadian Special Publication of Fisheries & Aquatic Sciences*, **130**, 61-71.

Tegner, M.J., P.K. Dayton (1981) Population structure recruitment and mortality of two sea urchins *Strongylocentrotus franciscanus* and *Strongylocentrotus purpuratus* in a kelp forest. *Marine Ecology Progress Series*, **5**(3), 255-268.

Tutschulte, T.C. (1976) The comparative ecology of three sympatric abalones. *Scripps Institution of Oceanography*. University of California, San Diego.

Vilchis, L.I., M.J. Tegner, et al. (2005) Ocean warming effects on growth, reproduction, and survivorship of Southern California abalone. *Ecological Applications*, **15**(2), 469-480.

Wild, P.W., J.A. Ames (1974) A report on the sea otter, *Enhydra lutris* L., in California. *Marine Resources Technical Report*, **20**, 1-93.

CHAPTER 5.

Density-Dependent Egg Production and Population Growth Rate Analysis of Red Abalone (*Haliotis rufescens*) Populations in California

ABSTRACT

An analytical approach to investigating the potential relationship between density-dependent aggregation characteristics and population growth is demonstrated. The per capita fecundity estimates for a size-based matrix model of an unfished red abalone population were varied according to changes in the aggregation and individual size structure of the population. The results indicate that the probability of mixed-gender aggregation occurrences strongly influences the relationship between aggregation size and per capita fecundity in populations with small aggregations. The relationship is nonlinear and is well-described by a four-parameter, two-part exponential curve:

$$Y = ae^{b\bar{x}} + ce^{d\bar{x}}$$

The effect of aggregation size on fecundity translates into a rapid decline in population growth rates below a threshold average aggregation size. The critical aggregation size describing the threshold behavior of population growth rates (AS_c- λ) decreased with decreasing sizes-at-maturity, and increased with decreasing average individual sizes in the populations.

Average aggregation sizes were strongly correlated with population density, such that lower-density populations contained smaller aggregations. The reduction in population growth rates associated with small aggregation sizes may, therefore, be considered a depensatory process, or an Allee effect. The magnitude of the depensation

may be amplified when additional factors influencing fertilization success, such as nearest-neighbor distances, are considered. The relationship between nearest-neighbor distances and population density was also nonlinear, such that distances increased rapidly as the population density decreased below a threshold level.

INTRODUCTION

The red abalone (*Haliotis rufescens*) is the largest abalone species in the world and has been the primary target of the California abalone fishery since the early 1900's. In northern California, red abalone are more accessible to human exploitation because they inhabit the rocky intertidal and shallow subtidal regions (< ~15 m). In the warmer waters of southern California, the depth range of the red abalone is deeper (12 – 30 m) where cooler waters are more prevalent (Cox 1962). Fisheries for the southern California red abalone populations closed in 1997 due to severe population declines, but a recreational skin-diving only fishery still exists in northern California (Karpov, Haaker et al. 1998; Karpov, Haaker et al. 2000; California Department of Fish and Game 2002).

Red abalone are long-lived (30+ years), slow-growing, late-maturing (3-6+ years), but highly-fecund herbivores (Rogers-Bennett, Dondanville et al. 2004; Rogers-Bennett and Leaf 2006; Rogers-Bennett, Rogers et al. 2007). They are relatively sedentary as adults, and rely on dense aggregations of spawning individuals for successful fertilization of gametes (Shepherd and Brown 1993; Babcock and Keesing 1999). Fertilization occurs externally to the animal, within the water column. Physical flow characteristics, such as current velocity and turbulent mixing, manipulate the relative concentrations of gametes as they are spawned (Denny and Shibata 1989; Denny, Dairiki et al. 1992). Factors such as body-size, aggregation sizes, and distances between

nearest-neighbors can influence fertilization success in broadcast-spawning benthic invertebrates (Pennington 1985; Levitan 1991; Levitan, Sewell et al. 1992; Levitan and Young 1995; Coma and Lasker 1997).

This density-dependence in the fertilization success rates of broadcast-spawners has led to concern that the reduced abalone populations in southern California may be declining further due to an Allee effect related to reduced mating success (Shepherd 1986; Tegner 1993; Karpov, Haaker et al. 1998). A theoretical minimum spawning density of 2,000 abalone per hectare is currently used as a resource management guideline for assessing the relative health of populations and the potential need to initiate recovery efforts. Many of the proposed recovery efforts are designed to increase local densities of spawning aggregations in order to bolster future recruitment to the population (California Department of Fish and Game 2002). Although the importance of maintaining large aggregations in abalone populations is now generally accepted (Prince, Sellers et al. 1988; McShane 1996; Hobday, Tegner et al. 2001; Dowling, Hall et al. 2004), the relationship between changes in these small spatial-scale characteristics and the population growth rates have not been explored for California red abalone populations.

The purpose of this study is to describe an analytical approach to investigating the relationship between density-dependent aggregation characteristics and population growth rates as they relate to changes in fecundity. I use the size-based matrix population model reported for an unfished red abalone population in northern California (Rogers-Bennett and Leaf 2006) as a basis for calculating changes in population growth rates under different conditions of aggregation and individual size structure. The aggregation

and individual size-frequency data were measured for six red abalone populations in both northern and southern California. These populations characterize the impacts of three different fishing or predation pressures – currently fished, historically fished but now protected, and currently protected but impacted by sea otter predation. In addition to aggregation and individual sizes, I measured nearest-neighbor distances and estimated population densities in order to characterize the relationship between aggregation-level characteristics and population density for red abalone.

METHODS

Populations

Six red abalone populations were surveyed from May-October of 2007. The populations occur over a broad geographic range within California (Figure 5.1). Three of the populations are located north of San Francisco within the range of a recreational skin-diving-only fishery – Van Damme State Park (VDSP), Ocean Cove (OC), and Fort Ross (FR). These are high-density populations that are closely monitored and actively managed by the California Department of Fish and Game (CDFG). The population located near the Hopkins Marine Laboratory (HML) in Monterey Bay is protected from human-induced fishing mortality, but is subject to intense sea otter predation. The two San Miguel Island (SMI) populations are located in the southwest and southeast regions, as designated by CDFG, and have been protected from fishing since 1997 when all abalone fisheries south of San Francisco were closed due to marked declines in population abundances.

Population Surveys

The locations of the transect surveys within each study site were determined either randomly (SMI, HML) or haphazardly (VDSP, OC, FR). Likewise, the size and number of transects surveyed at each location differed by study site. The total transect area searched for each site is given in Table 5.1. For each transect, the number of individuals was recorded and divided by the total transect area for that survey location in order to calculate the density. The density estimate for each population was calculated by averaging the transect densities by the number of survey locations. Sizes of abalone were measured *in situ*, without removing the abalone from the substrate. Measurements were made with calipers to the nearest millimeter except when abalone were located in crevices or other environmental conditions (i.e. surge) precluded precise measurements. In those events, abalone were measured to the nearest centimeter. For the purpose of standardizing the precision of sizes across population surveys, I rounded all of the size distributions to the nearest centimeter and subdivided the distributions into 1-centimeter bins with the centimeter mark as the midpoint of each bin.

In order to quantify aggregation characteristics, I measured nearest-neighbor distances and aggregation sizes in each population. The protocol for the distance-based surveys is discussed in more detail in Chapter 2. I measured two distances at each survey site – the distance from a random waypoint to the nearest individual (x), and the distance from that individual to its nearest neighbor (z). Aggregations were defined as the number of abalone within a 2.5 m radius around the individual closest to the random waypoint. The minimum aggregation size was therefore equal to one. I chose the 2.5 m radius

based on *in situ* results of fertilization success with increasing distance from a conspecific described by Babcock and Keesing (1999).

Data Analyses and Simulations

Estimating Per Capita Fecundity

Per capita fecundity for each population was estimated by bootstrap analysis (Manly 1997). For all analyses, a set of 10,000 bootstrapped populations was created for each of the surveyed populations by randomly selecting from the sampled distribution of aggregation sizes. The number of aggregations simulated for each population was equal to the number of aggregations in the sampled distribution. The total number of individuals, *N*, in each simulated population was the sum of all aggregation sizes within the population. Thus, *N* was not constant across all 10,000 simulated populations.

Each individual within the aggregations was randomly assigned a length (to the nearest centimeter) from the sampled size distribution. Genders were also randomly assigned to individuals, assuming a 1:1 sex ratio within the population. The probability that an individual had reached maturity was dependent on the size and gender of the individual, according to sex-specific data reported for northern California red abalone by Rogers-Bennett et al. (2004). A generalized linear model using the logit link function for a binomial distribution was fit to the data for each gender so that the probability of maturity could be described as a continuous function of size (Myers, Montgomery et al. 2002). The function requires two parameters to be estimated, β_0 and β_1, such that

$$P(L_i) = \frac{e^{(\beta_0+\beta_1 L_i)}}{1 + e^{(\beta_0+\beta_1 L_i)}} \tag{5.1}$$

where, L_i is the size of the abalone in millimeters and $P(L_i)$ is the probability of maturity. The parameter estimates for both genders is provided in Table 5.2.

The size-specific fecundity of the mature females in each aggregation was estimated with a Gaussian function:

$$F = Ae^{-(\mu - L_i)^2/2\sigma^2} \quad (5.2)$$

where, F is the fecundity in number of mature eggs produced, A = 2,850,000 eggs yr^{-1} is the maximum productivity, μ = 215 mm is the size at maximum productivity, and σ = 38 mm describes the distribution of productivity around the maximum (Rogers-Bennett, Dondanville et al. 2004). This function indicates that the number of mature eggs declines in the largest individuals due to senescence of the eggs.

The aggregation-specific fecundities were calculated by first determining the presence of mature individuals of both sexes in the aggregation. Because a function describing the size-specific sperm production of males is unavailable, I assumed that one male was sufficient to fertilize all eggs in an aggregation. Sperm are orders of magnitude smaller than eggs, so males may hold significantly more gametes than females of comparable sizes. For aggregations that contained mature individuals of each sex (mixed-gender aggregations), the total number of eggs produced by each aggregation was calculated by summing the individual female fecundities.

The per capita fecundity, F_N, of each of the 10,000 simulated populations was calculated by summing the aggregation-specific fecundities and dividing by the total number of individuals in each population. These values were averaged over the entire set of simulated populations as a metric for comparing relative differences in the sampled red abalone populations. I also converted the average per capita fecundity estimate to an

estimate of the number of eggs produced per hectare, F_{ha}, for each of the six sampled populations. I multiplied the average transect density (# abalone / ha) by the per capita fecundity to obtain the number of eggs produced per hectare in the population.

Population-specific Fecundity Analyses

For each of the six sampled populations, I estimated F_N and F_{ha} using the bootstrapping methods described above. The distributions of aggregation and individual sizes used in each of the initial fecundity analyses were those specific to the population being investigated. The estimated values of F_N and F_{ha} were compared across sites and related to the average transect densities, aggregation sizes, and individual sizes from each site. For each population, I estimated a measure of the recruitment potential to the population (# 25mm juveniles / m^2), assuming that the first year survival (*fertilization probability* x *larval survival probability* x *post-settlement survival to 25mm length* = 2.13 x 10^{-5} (Rogers-Bennett and Leaf 2006)) was consistent across the six populations. This assumption is unrealistic, but the resulting value allows comparison among the populations within a more comprehensible framework than the very large F_{ha} values.

Comparative Analyses

In order to investigate the relative influence of aggregation sizes and individual sizes on the reproductive potential of a population, I performed multiple bootstrap analyses with different combinations of aggregation and individual sizes. In all cases, the functions relating size to fecundity and maturity remained constant. In order to understand the influence of aggregation sizes alone on the estimates of per capita fecundity and fecundity per hectare, I performed six sets of 10,000 bootstrap analyses, using a consistent size distribution, and varying the aggregation size distributions

according to those sampled in the six red abalone populations. I calculated the mean aggregation size and the F_N for each of the 60,000 simulated populations. The relationship is well-described by a two-part exponential curve:

$$\bar{F}_N = ae^{b\bar{x}} + ce^{d\bar{x}} \quad (5.3)$$

where, $\bar{F}_N$ is the average per capita fecundity for a given aggregation size, $\bar{x}$ is the average aggregation size, and a, b, c, and d are the model parameters to be fit to the data. This type of empirical model also be used to describe the relationship between aggregation size and the probability of mixed-gender aggregations in the population, assuming a 1:1 sex ratio and 100% maturity of individuals (Figure 5.8). The theoretical model for this probability relationship is $P(\bar{x}) = 1 - 0.5^{(\bar{x}-1)}$.

I performed comparative analyses of the change in F_N with different aggregation sizes for unfished populations (combined San Miguel Island size distributions), fished populations (Ocean Cove size distribution), and populations with sea otter predation (Hopkins Marine Laboratory size distribution) to determine the interaction effect of aggregation sizes and size-frequency distributions. A third analysis examined the influence of size-at-maturity probabilities on fecundities. I compared the effect of the individual size distribution on the magnitude of the F_N value and the corresponding average aggregation sizes at the critical point of the curve, where slope of the tangent line becomes very steep. I defined the critical aggregation size for the per capita fecundity AS_c-F_N by first, standardizing the values of both variables so that they ranged between 0 and 1, and then calculating the aggregation size where the derivative of the curve equaled one. At aggregation sizes lower than the critical point, the F_N values decreased rapidly.

Matrix Population Model

Per capita fecundity is used in matrix population modeling to inform the birth pulse to the population in the following year. Rogers-Bennett and Leaf (2006) provide a red abalone matrix population model for an unfished location in northern California (North Point Cabrillo marine reserve). The growth transition and survival probabilities were estimated based on mark-recapture data for the area. The size-specific fecundity estimates were based on the Gaussian function reported for northern California populations which are also used in the current study (Rogers-Bennett, Dondanville et al. 2004).

In order to determine the effect of changes in aggregation sizes on population growth rates, I modified the size-specific fecundity estimates in the North Point Cabrillo matrix model. I calculated the per capita fecundity of each size class ($F_{N,i}$) in the population and averaged those fecundities across the 10,000 simulated populations. I estimated six sets of size-based per capita fecundities based on analyses using the size distribution from an unfished population (combined San Miguel Island), a fished population (Ocean Cove) and a population subject to sea otter predation (Hopkins Marine Laboratory) and aggregations sizes from each of the six sampled populations. For each set, I incorporated the modified fecundity estimates into the matrix population model and I calculated the deterministic population growth rate (λ – dominant eigenvalue). The relationship between aggregation size and λ was described by fitting a two-part exponential curve to the averaged λ values. The critical aggregation size for the population growth rates (AS_c-λ) was determined by first, standardizing the values of both variables so that they ranged between 0 and 1, and then calculating the aggregation size

where the derivative of the curve equaled one. I also calculated a second critical aggregation size (AS_c-λ=1) where the population growth rate is predicted to be stable (λ=1).

RESULTS

Population Surveys

The highest-density sites were in northern California (Table 5.1), with densities greater than 6,600 abalone per hectare. According to the California abalone fishery management guidelines, populations with densities smaller than 6,600 abalone per hectare should be managed more conservatively so that the population densities will rebound (California Department of Fish and Game 2002). The population near the Hopkins Marine Laboratory and the two populations at San Miguel Island all have densities lower than 2,000 per hectare, the estimated minimum spawning density for abalone populations (Shepherd and Brown 1993; California Department of Fish and Game 2002).

The average population densities are strongly correlated with the average aggregation characteristics – nearest-neighbor distance and aggregation size (Figures 5.2 and 5.3) (*see Chapter 2 for a full description of these relationships*). Nearest-neighbor distances are described by a negative power function of the average transect density such that, as the population density decreases, the distance between nearest neighbors increases rapidly below a certain threshold density (~3,000 abalone / ha for the six red abalone populations; *also see Chapter 2*). The variance in the distance measures increases in lower density populations. The aggregation size is positively linearly related to population density, so that the average number of abalone in an aggregation increases

as the average density increases. The variance of the aggregation sizes also increases as the population density increases.

A Kruskal-Wallis test of the median individual sizes indicates significant differences among the six populations ($X^2_{5,2280}$= 418.02; p = 0.000). A multiple comparison test of the Kruskal-Wallis results (Bonferroni-corrected with initial $\alpha = 0.05$) indicates that the two populations at San Miguel Island are significantly different from the Hopkins Marine Laboratory population, and from the three northern California populations (Figure 5.4). The average size of individuals was not dependent on the population density, but on the history of the population. The two populations at San Miguel Island had the largest average sizes and were the only surveyed populations without either sea otter predation or fishing pressures (Table 5.1). The population near the Hopkins Marine Laboratory had the smallest average size primarily due to the intensive sea otter predation in the area. The only abalone in the area were those that could fit into deep or narrow crevices, successfully avoiding sea otter predation. Thus, crevices were thoroughly searched during the surveys of this population which may have biased the size-frequency distribution of this population in favor of smaller individuals that also typically inhabit the more cryptic crevice habitat. The average sizes of the three northern California populations were approximately equivalent to each other (172 – 175 mm) (Figure 5.4 and Table 5.1). The minimum legal size for the recreational fishery in northern California is 178 mm. The fact that the average sizes in these fished populations are just below this minimum legal size suggests that the fishing pressure in the area is impacting the upper limit of the size distributions for these populations.

Population-Specific Fecundity

The highest average per capita fecundity was estimated for the southwest region of San Miguel Island (μ = 852,660 eggs / abalone; σ = 141,440) (Table 5.2). The lowest average per capita fecundity was estimated for the population near Hopkins Marine Laboratory (μ = 63,945 eggs / abalone; σ = 40,593) although both of these populations had the same average aggregation size (3.9 abalone per aggregation (Table 5.1)). This 93% reduction in the estimated per capita fecundity is due in part to the large difference in the sizes of individuals between the two populations ($\Delta\mu$ = 89 mm). The size at which 50% of the females are mature is ~ 121 mm. The size-at-50%-maturity is smaller for males (~ 83 mm). Because the average size of individuals in the Hopkins Marine Laboratory population was smaller than the size-at-50%-maturity for females, the average percentage of aggregations that contained mature individuals of both sexes was only 30%. The percentage of mixed genders was 48 – 49% in the two San Miguel Island populations.

Of the three northern California populations, the highest per capita fecundity was estimated for the Van Damme State Park population which had the second-largest (and least variable) average aggregation size, and the largest average individual size. The Ocean Cove population had the largest average aggregation size (and most variable), but the smallest average individual size. The per capita fecundity estimate for the Ocean Cove population (μ = 784,320 eggs / abalone; σ = 71,730) was 6% lower than the Van Damme State Park value (μ = 836,530 eggs / abalone; σ = 68,122). Ninety-six percent of the aggregations at Van Damme State Park were mixed-gender, whereas 87% and 71% of

aggregations were mixed-gender in the Ocean Cove and Fort Ross simulated populations, respectively.

Despite the relatively high F_N estimate for the southwestern San Miguel Island population, the overall population density was too low to ensure a correspondingly high F_{ha} value (Table 5.3, Figure 5.5). The ranking of the populations by F_{ha} estimates, and the resulting recruitment potentials, was dominated by the influence of population density (Table 5.3, Figure 5.6). The recruitment potential calculated for the three northern California populations was an order of magnitude higher than the San Miguel Island populations. The stimated population growth rates for the six surveyed populations show a similar relationship to density as the F_{ha} value (Figure 5.5 and 5.7). This relationship is complicated by the differing aggregation and individual size-frequency distributions characterizing the six surveyed populations.

Comparative Analyses

Aggregation sizes, individual sizes, and size-at-maturity all influenced the per capita fecundity estimates in the simulated populations. The relationship between average aggregation size in the population and the per capita fecundity estimate is well described by a two-part exponential curve, with the shape of the curve dependent on the individual size-frequency distribution of the population and the size-at-maturity used in the analysis. The basis of the relationship described empirically by the two-part exponential curve comes from the probability of obtaining a mixed-gender aggregation given a 1:1 sex ratio in the population. The critical aggregation sizes calculated from the bootstrap analyses of per capita fecundity (AS_c-F_N) were ~4.7 abalone (Tables 5.4 and

5.5; Figure 5.9). The average F_N value for the critical aggregation sizes increased as the average individual size increased and as the size-at-maturity decreased.

Population Growth Rates

The strong influences of aggregation sizes, individual sizes, and size-at-maturity translate into similar patterns of influence on population growth rates (λ) although λ is less sensitive to small permutations of these population characteristics than the F_N values (Table 5.3). The relationship between average aggregation size and λ is well-described by a two-part exponential function, with a critical threshold aggregation size (AS_c- λ) close to 2.5 abalone for all three size distributions examined. The value of λ at the AS_c-λ was consistently less than one and decreased with decreasing average individual sizes in the population although a large change in the average individual size was needed in order to detect the difference (Table 5.6 and Figure 5.10). The aggregation size required to obtain a population growth rate of one (AS_c-λ=1) was 13 – 14 abalone in the simulations with the larger average sizes of individuals (San Miguel Island and Ocean Cove), but 48 abalone for the population with smaller individual sizes (Hopkins Marine Laboratory).

DISCUSSION

The results of this study indicate that the probability of creating a mixed-gender aggregation strongly influences the relationship between aggregation size and per capita fecundity in populations with small aggregations (Figure 5.8). The relationship is nonlinear and is well-described empirically by a two-part exponential curve. This effect of aggregation size on fecundity translates into a rapid decline in population growth rates below a threshold average aggregation size (Table 5.6). Because the average aggregation size is strongly correlated with the average population density in red abalone (Figure 5.3),

this reduction in population growth rates associated with small aggregation sizes may be considered a depensatory process, or an Allee effect (Allee 1931). The magnitude of the depensation may be amplified when additional factors influencing fertilization success are considered.

The probability of fertilization success depends on the relative concentrations of the gametes in the water (Lillie 1915; Benzie and Dixon 1994; Riffell 2005) which decreases approximately exponentially with increased distance from a spawning individual (Pennington 1985; Babcock and Keesing 1999; Metaxas, Scheibling et al. 2002). The results of the present study show that the distances between nearest neighbors increases rapidly as the population density decreases below a threshold level (Figure 5.2; *see also Chapter 2*). The fertilization probability related to the distance between spawning individuals may differ depending on the species of abalone and the physical characteristics of the flow during spawning (Denny and Shibata 1989; Denny, Dairiki et al. 1992), but the underlying trend of decreasing fertilization success with increased distance between individuals will likely be consistent (Babcock, Mundy et al. 1994; Levitan and Young 1995; Claereboudt 1999). Reducing the fertilization success in lower-density populations due to increased distances between spawning individuals would result in an even larger difference in the number of larvae produced by a population below the threshold density.

Relative gamete concentrations are also determined by the number of gametes released by individuals within the aggregation (Denny, Dairiki et al. 1992; Claereboudt 1999). In the present study, I assumed that the sperm from one male was sufficient to fertilize all of the eggs produced by the females in the aggregation. Estimates of size-

specific male fecundity are unavailable for red abalone, although mid-sized males (120mm length) have been recorded to spawn 20 – 60 x 10^9 sperm under artificial conditions (Riffell 2005). Presumably, larger males would release even more sperm during a spawning event. Gamete ratios less than 10,000 to 1 (sperm : eggs) have resulted in reduced fertilization success in laboratory conditions for red abalone (Riffell, Krug et al. 2004). The number of sperm and eggs produced by an aggregation depends on the sizes and number of mature individuals in that aggregation. The assumption used for the simulations in this study was that individuals were aggregated irrespective of size or gender. There is currently insufficient evidence for gender-biased aggregative behavior of abalone (*see Chapter 4*), but the average size of some marine benthic gastropods may be smaller in higher-density locations (Alfaro and Carpenter 1999; Tomascik and Holmes 2003). The potential influence of a correlation between size and local aggregation density on per capita fecundity and gamete ratios should be explored in the future (Levitan 1991). The limitation of fertilization success based on the gamete ratios produced by an aggregation would further reduce the per capita fecundity of a population and influence the estimated critical aggregation sizes for population growth rates (AS_c- λ and AS_c- λ=1).

The estimated AS_c- λ was consistently smaller than the estimated AS_c-F_N in this study for all of the analyses (Table 5.4 and 5.5). This reduction in AS_c may be due to the low elasticity of λ to small changes in fecundity for long-lived species (Crouse, Crowder et al. 1987; Gotelli 1991; Riffell, Krug et al. 2004; Rogers-Bennett and Leaf 2006). Because red abalone are slow growing, individuals may reproduce for several years before reaching the minimum legal size for the fishery in northern California, and the

largest individuals may be reproductive for more than ten years (Rogers-Bennett, Dondanville et al. 2004; Rogers-Bennett, Rogers et al. 2007). This lengthy reproductive period compensates for potential temporal variability in reproductive success throughout the lifetime of the individual (Hobday and Tegner 2002).

Consequently, some authors have suggested that conservation concerns over Allee effects based on reductions in reproductive success are not as relevant for long-lived species. They advise that management plans would be more effective if the focus were on increasing survivorship of the intermediate-sized individuals (Crouse, Crowder et al. 1987; Ebert 1998; Heppell, Caswell et al. 2000; Rogers-Bennett and Leaf 2006). These findings are important for prioritizing management efforts for populations that are currently at densities above the threshold level. However, the potential for populations to reach the lower density threshold associated with an Allee effect should be assessed. Allee effects, by definition, will be most influential to the dynamics of the population at densities below which the benefits of aggregative behavior are no longer maintained. The potential for Allee effects to influence the population dynamics may not be revealed by analyses utilizing small perturbations in vital rates.

Elasticity analyses, commonly used to assess the relative contribution of matrix elements to λ, assume that the changes in the vital rates affect the population growth rate linearly (Morris and Doak 2002). In the case of aggregation-influenced fecundities and distance-based changes in fertilization success, the change in fecundity is nonlinear (Figure 5.5). Thus, the density-dependent effect on population growth rates is also nonlinear. Resource managers should consider not just the influence of small changes in the vital rates on population growth rates, but also the magnitude of the change that

would be required in order to influence the population growth rate. The likelihood that management decisions might lead to those large changes in the vital rates (either positively or negatively) should be examined.

The predicted critical aggregation size for maintaining a population growth rate equal to one (ASc- λ=1) for the model red abalone populations with large individuals was 13 – 14 abalone, which corresponds to an average population density of 9,377 – 10,236 abalone per hectare. This AS_c- λ=1 value would decrease as the size-at-maturity decreased, and would increase as the average individual size in the population decreased. Changes in the vital rates of the population, such as increased adult mortality resulting in smaller average sizes, would likely lead to increased AS_c- λ=1 values. However, any conclusions based on the absolute value of the predicted AS_c- λ=1 of the model population for this study should be approached with caution.

The AS_c- λ=1 prediction for a population will depend on the individual size distribution in the population and on the vital rates (i.e. growth, survival, and size-at-maturity) specific to that population. The significant differences in the size-frequency distributions among the six populations are suggestive of differences in the survival rates of larger individuals. Because the matrix model used in this study was created based on the vital rates of an unfished population in northern California, the high adult survival rates incorporated into that model is not appropriate to apply to fished populations. Likewise, the survival rates of even smaller size classes in the Hopkins Marine Laboratory population will be much lower than those estimated for the model population due to the intense sea otter predation.

In addition to influencing the adult survival rates of a population, long-term fishing or other intense predation pressures may artificially select for individuals that mature at smaller sizes (Tegner and Dayton 1999; Stokes and Law 2000; Fenberg and Roy 2008). The truncated size-frequency distribution observed in the Hopkins Marine Laboratory population led to drastically reduced population growth rates when compared to the other populations with larger individuals. Because the estimated size-at-50%-maturity used in the analysis was larger than the average individual size in the Hopkins Marine Laboratory population, simulated aggregations demonstrated low probabilities of containing mature individuals of both sexes (0.30). A decrease in the size-at-maturity for the Hopkins Marine Laboratory population would increase the probability of creating mixed-gender aggregations, and would therefore decrease the critical aggregation size for the population (Table 5.4). A recent report has shown that the population levels at Hopkins Marine Laboratory have neither grown nor shrunk since the early 1970's despite intense predation by sea otters (Cooper, Wieland et al. 1977; Hines and Pearse 1982; Micheli, Shelton et al. 2008) which suggests that either the population is being supplemented by external larval sources or that the vital rates of individuals in this population are very different from those estimated for the North Point Cabrillo population. Of course, a combination of vital rate differences and larval supply may be influencing the dynamics of this population.

Vital rates of abalone are known to vary both spatially and temporally as environmental conditions vary (Vilchis, Tegner et al. 2005; Leaf, Rogers-Bennett et al. 2007; Rogers-Bennett, Rogers et al. 2007). The highly variable environmental conditions at San Miguel Island would likely result in very different growth and fecundity rates than

those estimated for the northern California populations. Red abalone thrive in colder water conditions, sustaining faster growth rates and higher fecundity in colder environments (<18°C) (Haaker, Parker et al. 1998; Vilchis, Tegner et al. 2005). The physical oceanography of the California Channel Islands is complex due to the turbulent interaction of the flow around the islands with the large-scale eddy formation in the southern California Bight south of Point Conception, a prominent headland where cold water from the north and warm water from the south meet and mix. San Miguel Island is the northwestern-most of the Channel Islands and experiences the coldest water conditions, but with pulses of warmer water that are not experienced at the three northern California sites (Hobday and Tegner 2002).

CONCLUSIONS

Density-dependent fecundity estimates are important to incorporate into a matrix population model for species that rely on aggregative spawning behavior to ensure high rates of fertilization. By exploring the effect of a broad range of aggregation-influenced fecundities on the population growth rate, an estimate of the critical aggregation size may be obtained. Threshold aggregation sizes should be determined for each population using population-specific estimates of vital rates and by exploring the variability in the bootstrapped λ predictions. The interaction between vital rates, such as growth and survival, with the density-dependent fecundity estimates was only indirectly explored in the present study by comparing the results from different individual size distributions. The sensitivity of the critical aggregation size to changes in fertilization success mediated be nearest-neighbor distances should also be explored by varying the first year survival parameter in the model (*see Chapter 4*).

ACKNOWLEDGEMENTS

This work was funded by the University of California Marine Council Coastal Environmental Quality Initiative, the Hicks Foundation, the Wyer Foundation, a Halliday Field Research grant, and the California Department of Fish and Game. I am grateful for permission to complete part of this work within the Hopkins Marine Reserve. Special thanks to L. Rogers-Bennett, I. Taniguchi, and D. Stein for supporting the inclusion of the nearest-neighbor surveys on CDFG cruises. I am also grateful to H. Fastenau and the 2007 UC Davis scientific diving class for their careful data collection at Fort Ross and Hopkins despite the long surface swims. This work would not have been possible without the additional help of many volunteer divers from SIO, CDFG, and the San Miguel Island Abalone Advisory Group. Thanks to J. Leichter for giving valuable feedback on earlier drafts of this chapter. The material in this chapter is in preparation to submission to the journal Ecological Modeling, and was co-authored by Laura Rogers-Bennett. The dissertation author was the primary investigator and author of this paper.

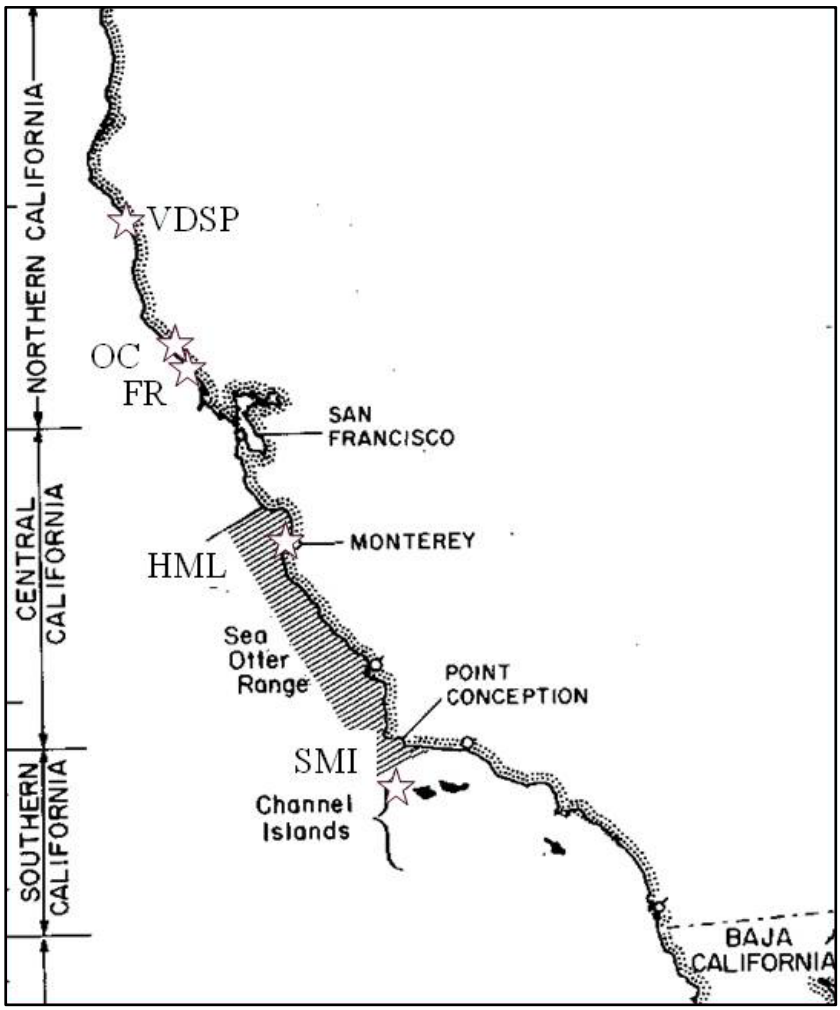

Figure 5.1 Locations of population surveys conducted. From north to south: VDSP - Van Damme State Park; OC - Ocean Cove; FR- Fort Ross; HML - Hopkins Marine Laboratory; SMI - San Miguel Island (southwest and southeast regions of San Miguel Island).

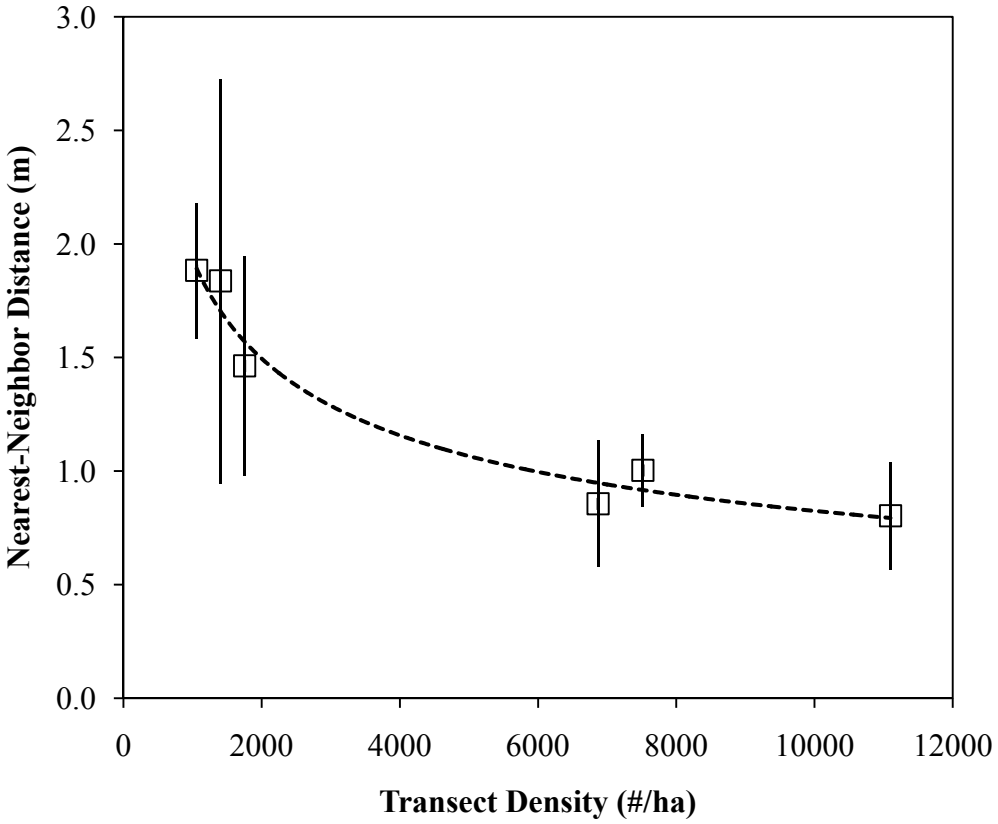

Figure 5.2 Average transect density (#/ha) versus nearest-neighbor distances (m) (±SE) for the six red abalone populations. The relationship is described by a negative power function. The population near Hopkins Marine Laboratory had the highest variance in the distance measurements.

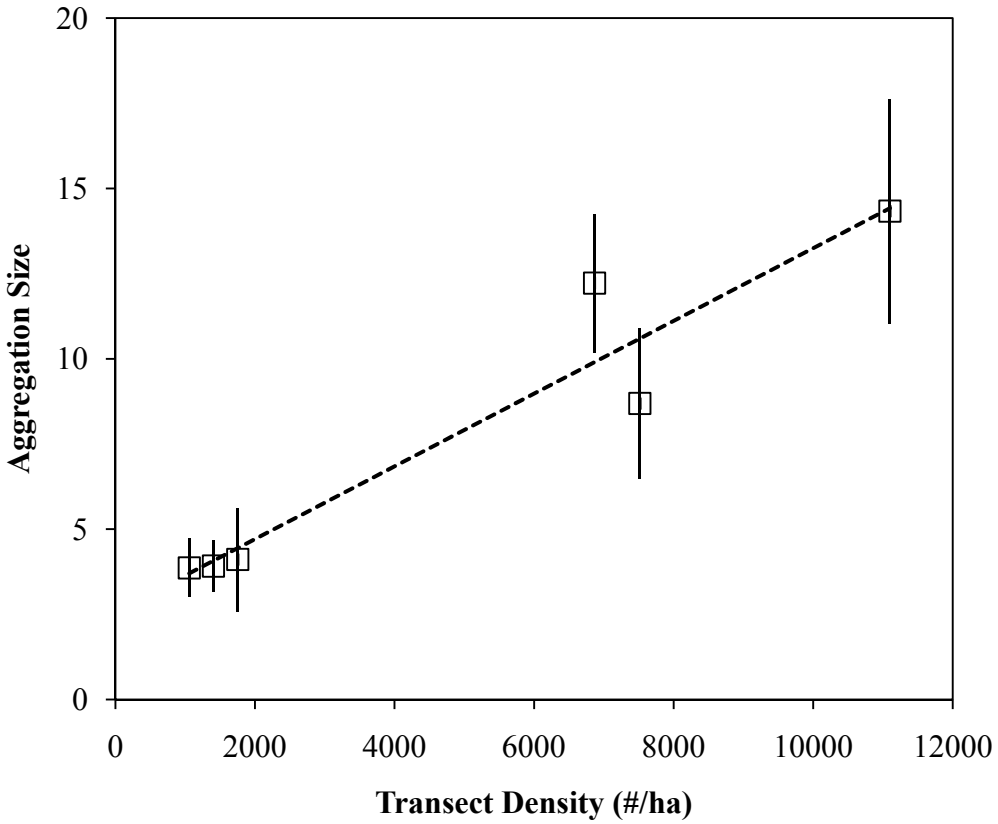

Figure 5.3 Average transect density (# / ha) versus average aggregation size (±SE). The relationship is described by a positive linear function. The variance of the aggregation sizes increases with increased population density.

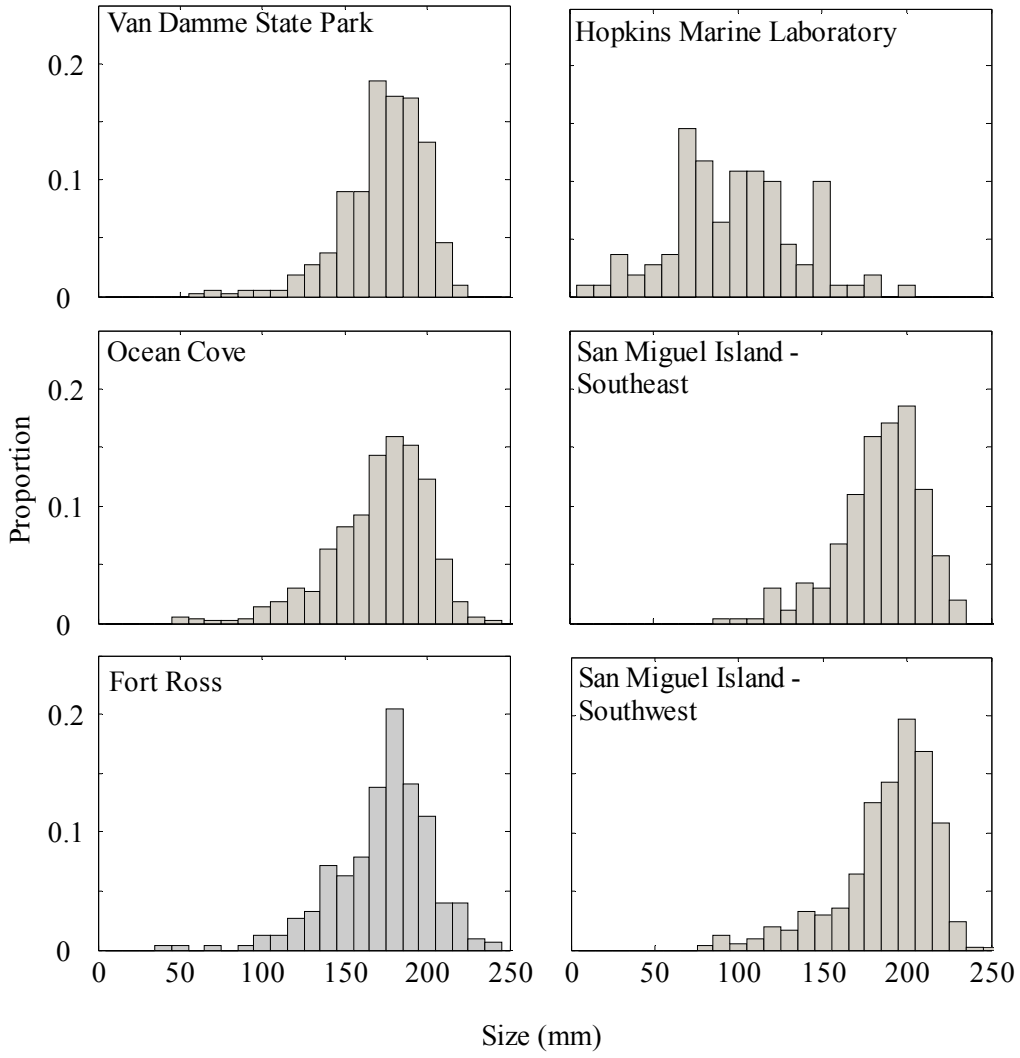

Figure 5.4 Size-frequency distributions of six red abalone populations in California (2007).

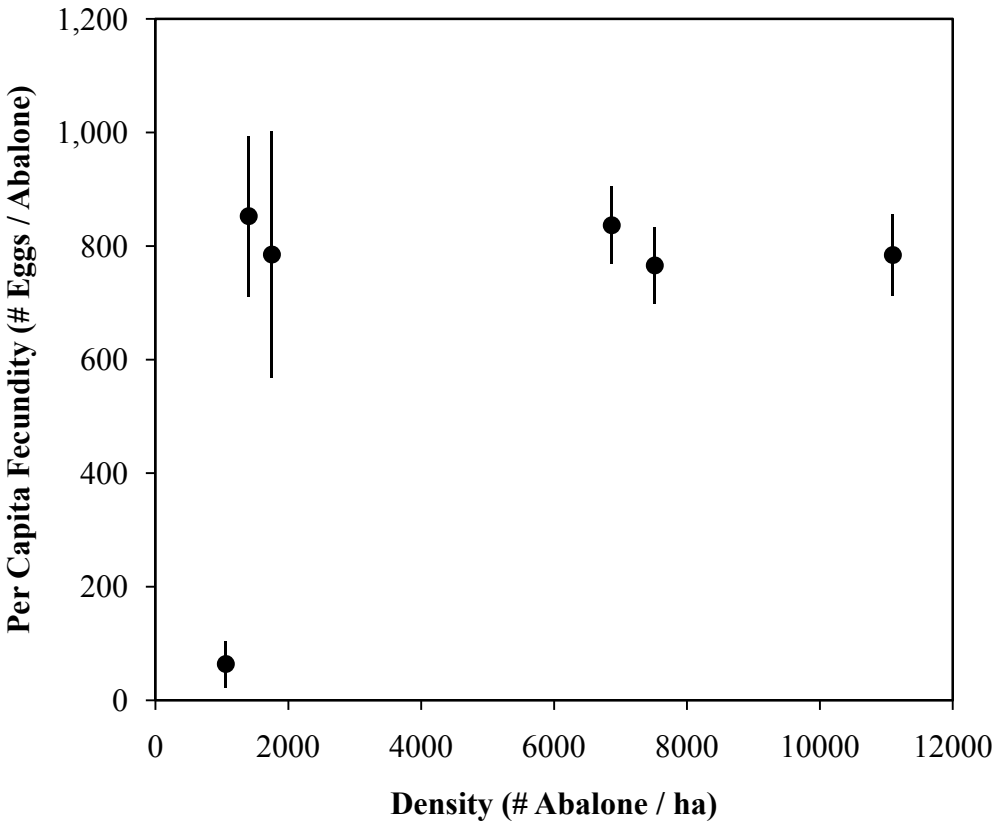

Figure 5.5 Population density versus estimated per capita fecundity (F_N) for the six surveyed red abalone populations. Errorbars are standard deviations.

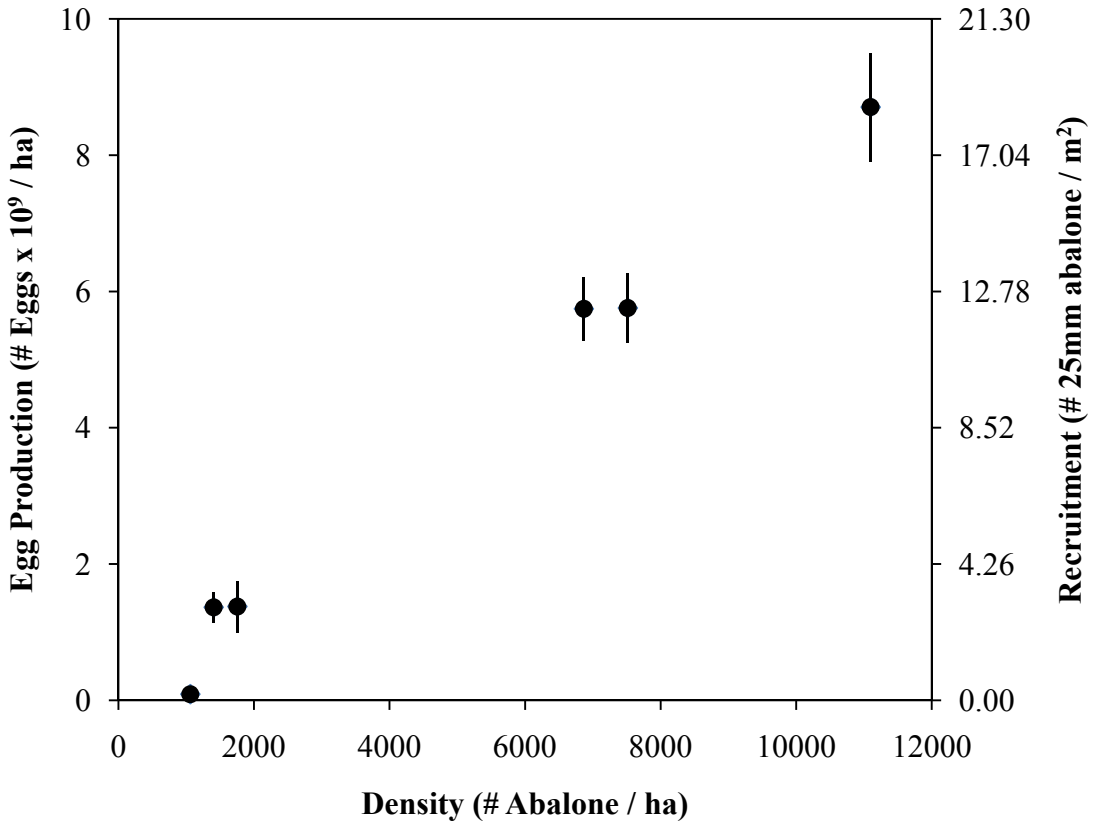

Figure 5.6 Population density versus the estimated egg production per hectare (F_{ha}) and recruitment potential / m^2 for the six surveyed red abalone populations. Errorbars are standard deviations.

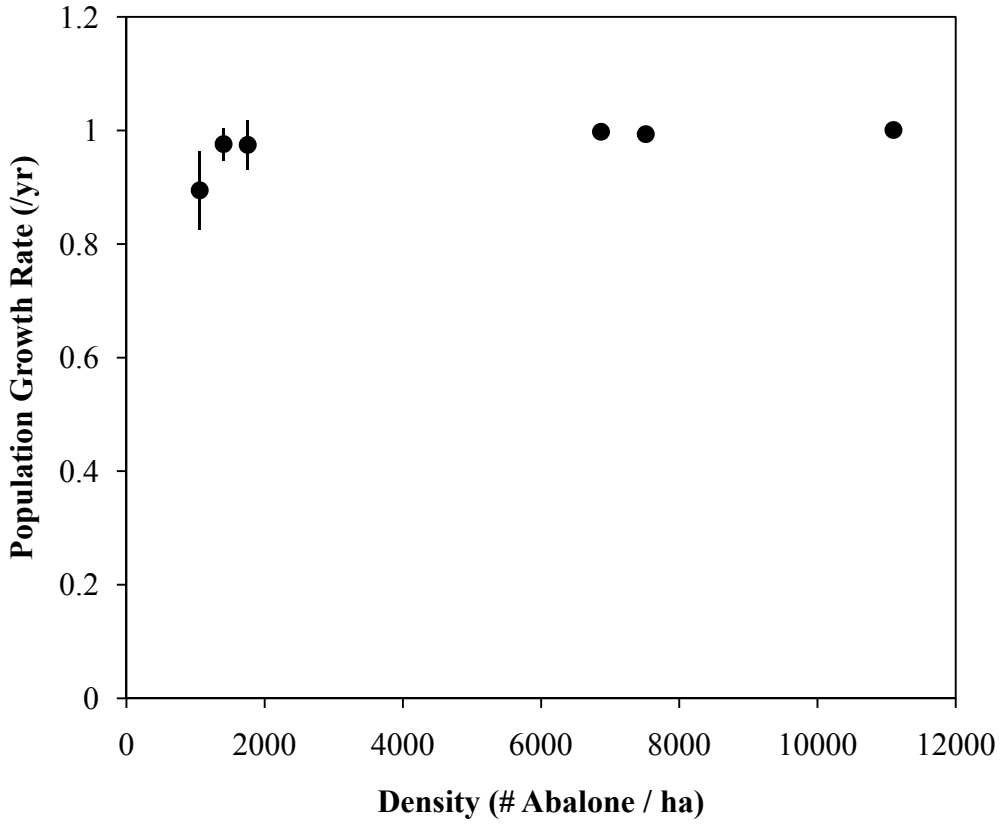

Figure 5.7 Population density versus the predicted population growth rate (λ) for each of the six surveyed populations. Errorbars are standard deviations.

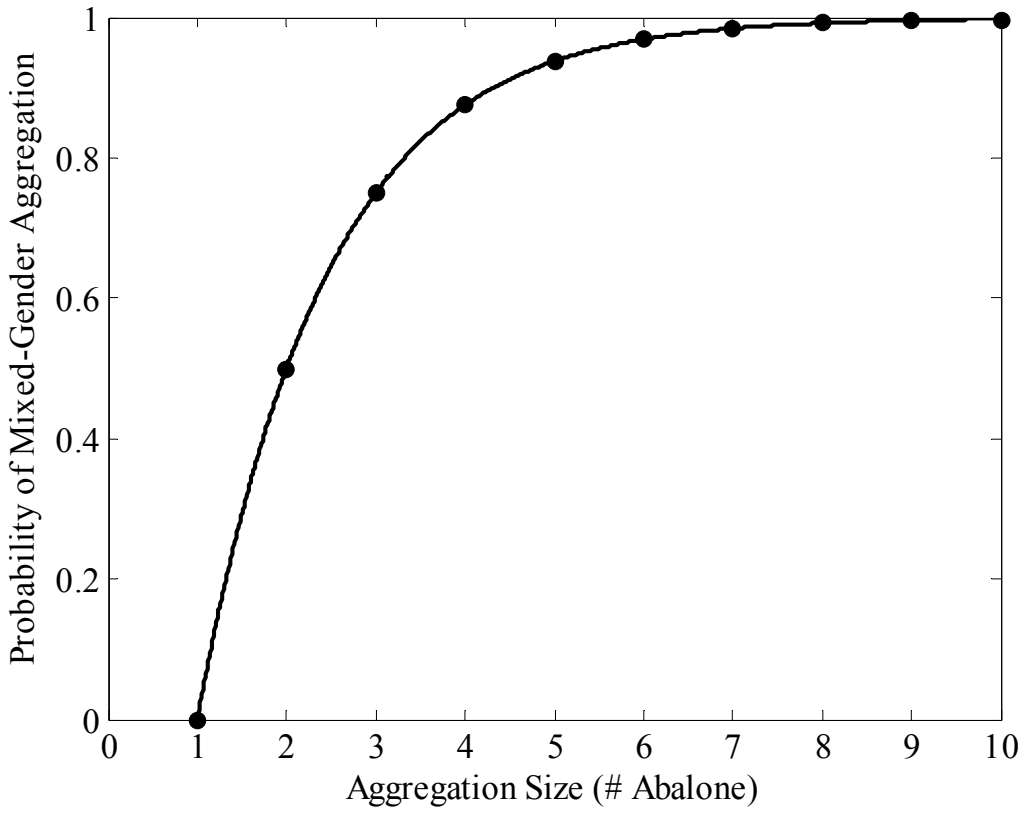

Figure 5.8 Probability of mixed-gender aggregations, assuming a 1:1 sex ratio in the population. The equation describing the theoretical probability is $P(x) = 1 - 0.5^{(x-1)}$. This relationship is also well described by the empirical model: $y = 1 - 2e^{-0.6931x}$; $R^2 = 1$.

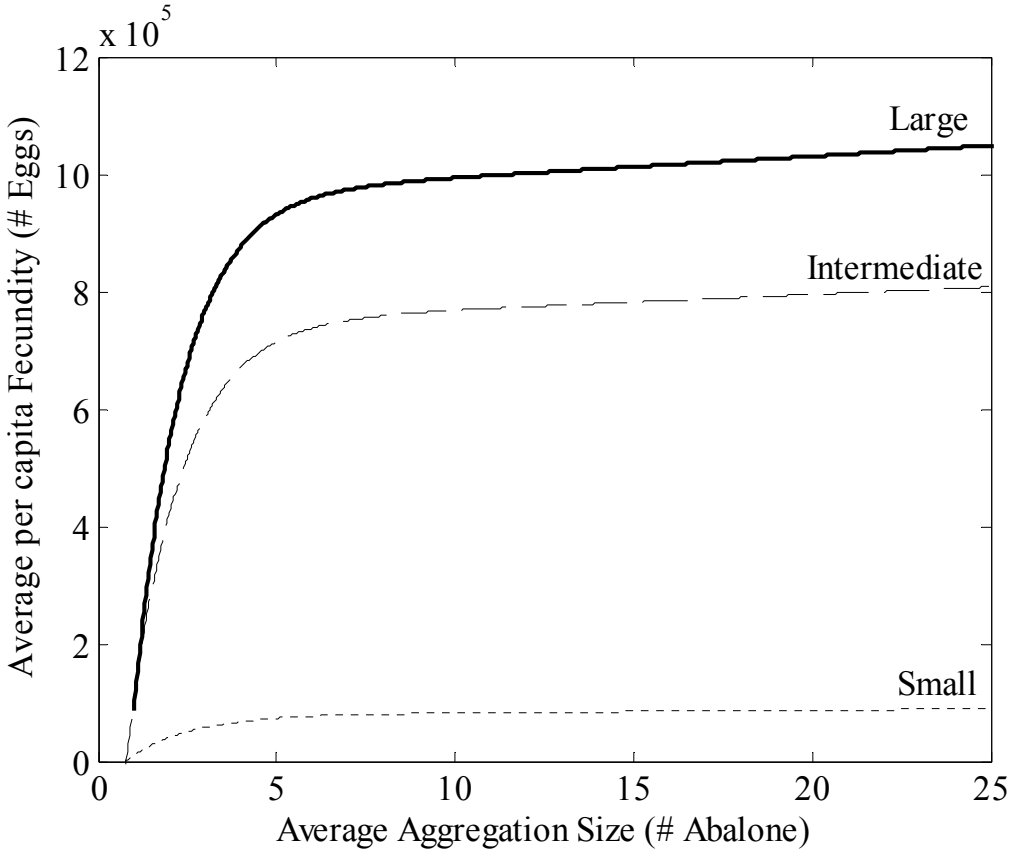

Figure 5.9 Mean per capita fecundity as a function of aggregation size calculated for three different size distributions. The large size distribution is the combined distributions of the San Miguel Island populations (μ = 184 mm). The intermediate size distribution is from the Ocean Cove population (μ = 172 mm). The small size distribution is from the Hopkins Marine Laboratory (μ = 100 mm). See Table 5.1 and Figure 5.4 for references to the size-frequency distribution. See Table 5.5 for parameter estimates and summary statistics of the relationships shown in this figure.

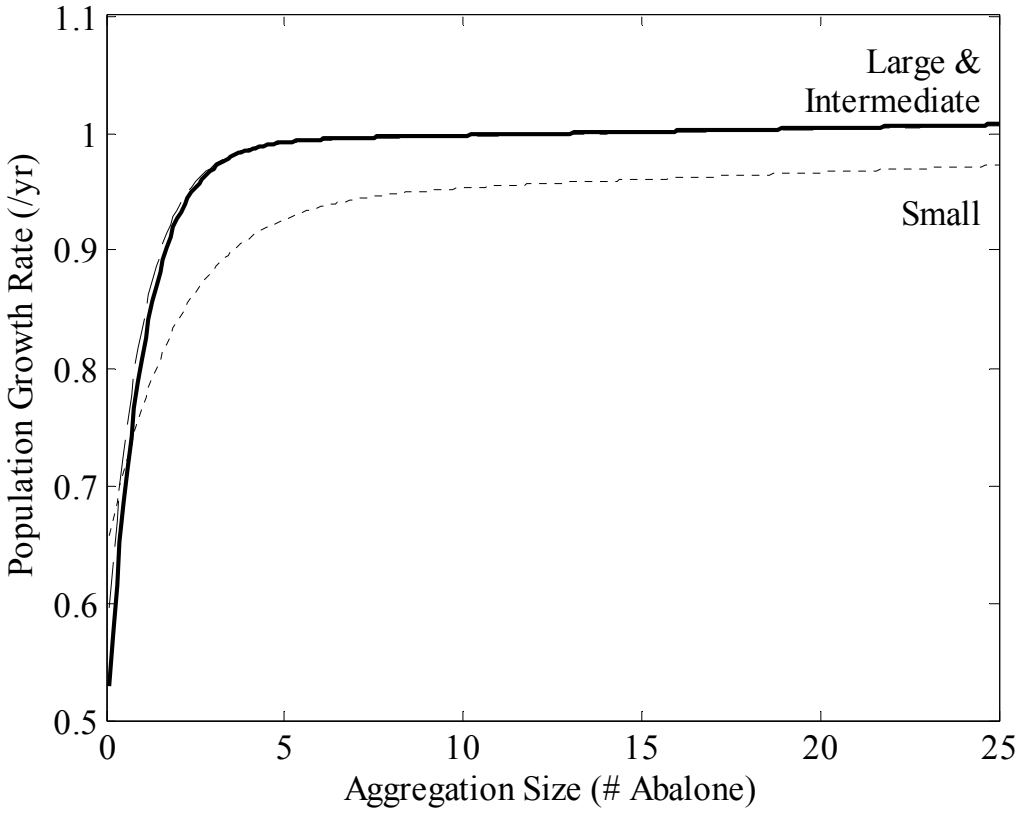

Figure 5.10 Population Growth as a function of aggregation size calculated for three different size distributions in the population. The large size distribution is the combined distributions of the San Miguel Island populations (μ = 184 mm). The intermediate size distribution is from the Ocean Cove population (μ = 172 mm). The small size distribution is from the Hopkins Marine Laboratory (μ = 100 mm). Note that the y-axis starts at 0.5 in the figure. See Table 5.1 and Figure 5.4 for references to the size-frequency distribution. See Table 5.6 for parameter estimates and summary statistics of the relationships shown in this figure.

Table 5.1 Summary statistics for the transect and aggregation surveys for the six red abalone populations listed in order from north to south. VDSP = Van Damme State Park; OC = Ocean Cove; FR = Fort Ross; HML = Hopkins Marine Laboratory; SMI – SW = San Miguel Island, southwest region; SMI – SE = San Miguel Island, southeast region. μ = mean; σ = standard deviation; n = sample size.

	Total Area	Transect Density (#/ha)			NN Distance (m)			Aggregation Size			Individual Size (mm)		
Population	(m^2)	μ	σ	n	μ	σ	n	μ	σ	n	μ	σ	n
VDSP	1080	6868	4923	18	0.86	1.25	20	12.2	9.1	20	175	24.4	453
OC	900	11100	7901	15	0.80	0.88	14	14.3	12.8	15	172	29.3	564
FR	395	7517	5986	10	1.00	0.84	28	8.7	11.7	28	174	29.3	333
HML	475	1406	1329	12	1.84	3.08	12	3.9	2.6	12	100	36.7	110
SMI - SW	4440	1061	870	20	1.88	1.40	22	3.9	4.0	22	189	29.0	557
SMI - SE	2040	1755	2458	9	1.46	1.45	9	4.1	4.5	9	185	25.2	264

Table 5.2 Parameter estimates for a generalized linear model describing the probability of maturity as a function of size (mm).

	Females		Males	
Parameter	μ	SE	μ	SE
β_0	-16.62	5.17	-12.26	4.01
β_1	0.14	0.04	0.15	0.05

Table 5.3 Summary of fecundity and estimated recruitment potentials for the six red abalone populations in order of increasing average density. Two measures of fecundity are provided – per capita fecundity (F_N) and fecundity per hectare (F_{ha}). The recruitment potential is calculated by converting F_{ha} to the number of eggs / m^2 and multiplying by an estimate of first-year survival (2.13×10^{-5}) (Rogers-Bennett and Leaf 2006). This estimate is meant to place the large fecundity values into a standard context that may be more intuitive to interpret, but is not meant to be a prediction of the actual recruitment to the populations. λ is the average deterministic population growth rate for the bootstrap matrix models for each of the six populations. These values were estimated with the assumption that vital rates do not differ among the populations and are meant to show only the relative influence of aggregation sizes and individual sizes on the population growth rates. μ is the mean value of 10,000 bootstrapped populations; σ is the standard deviation of the mean value. See Figures 5.5, 5.6, and 5.7 to view the relationship of these results to the average population density.

	F_N (# eggs / abalone)		F_{ha} (# eggs / ha)		Recruitment (# / m^2)		λ (yr^{-1})	
Population	μ	σ	μ	σ	μ	σ	μ	σ
HML	63,945	40,593	8.99×10^7	5.71×10^7	0.2	0.1	0.8947	0.0692
SMI - SW	852,660	141,440	1.37×10^9	2.26×10^8	2.9	0.5	0.9761	0.0286
SMI - SE	784,900	216,990	1.38×10^9	3.81×10^8	2.9	0.8	0.9748	0.0437
VDSP	836,530	68,122	5.75×10^9	4.68×10^8	12.2	1.0	0.9978	0.0099
FR	765,930	67,695	5.76×10^9	5.09×10^8	12.3	1.1	0.9937	0.0104
OC	784,320	71,730	8.71×10^9	7.96×10^8	18.5	1.7	1.0009	0.0103

Table 5.4 Comparing the effects of different size distributions on the relationship between average aggregation size and F_N, assuming the gender-specific size-at-maturity relationships described in the methods. The values in parentheses are calculated assuming no size-at-maturity limitations (i.e. 100% maturity in the population). The three size distributions represent three population histories – SMI (total) is the combined size distribution of the unfished populations at San Miguel Island, OC is a fished population at Ocean Cove in northern California, and HML is the population at Hopkins Marine Laboratory that is subject to sea otter predation. AS_C is the critical aggregation size defined by the point on the curve where the standardized derivative equals one. F_C is the average per capita egg production value for the critical aggregation size.

Size Distribution	Average Size (mm)	AS_C-F_N (# abalone)	F_C (# eggs)
SMI (total)	187	4.7 (4.8)	920,150 (922,680)
OC	172	4.8 (4.8)	705,900 (713,280)
HML	100	4.6 (4.3)	70,935 (86,221)

Table 5.5 Comparing the effects of different size distributions on the relationship between average aggregation size and F_N (per capita fecundity), assuming the gender-specific size-at-maturity relationships described in the methods. The three size distributions represent three population histories – SMI is the combined size distribution of the unfished populations at San Miguel Island, OC is a fished population at Ocean Cove in northern California, and HML is the population at Hopkins Marine Laboratory that is subject to sea otter predation. The four parameter estimates and the R^2 value for the function describing the relationship between the average aggregation size ($\bar{x}$) and the average per capita fecundity ($\overline{F_N}$) are given in the right-hand columns. μ is the average parameter estimate and L95 and U95 are the lower and upper 95% confidence intervals.

Size Distribution	Average Size (mm)	$F_N = ae^{b\bar{x}} + ce^{d\bar{x}}$ Parameter	μ	L95	U95	R^2
SMI	187	a	9.600×10^{5}	2.515×10^{5}	9.686×10^{5}	0.8804
		b	3.528×10^{-3}	2.911×10^{-3}	4.145×10^{-3}	
		c	-1.826×10^{6}	-1.948×10^{6}	-1.708×10^{6}	
		d	-0.7339	-0.7706	-0.6972	
OC	172	a	7.447×10^{5}	7.376×10^{5}	7.517×10^{5}	0.8796
		b	3.250×10^{-3}	2.603×10^{-3}	3.896×10^{-3}	
		c	-1.262×10^{6}	-1.344×10^{6}	-1.18×10^{6}	
		d	-0.6748	-0.7102	-0.6394	
HML	100	a	7.792×10^{4}	7.574×10^{4}	8.009×10^{4}	0.5884
		b	5.275×10^{-3}	3.441×10^{-3}	7.109×10^{-3}	
		c	-1.231×10^{5}	-1.408×10^{5}	-1.053×10^{5}	
		d	-0.5779	-0.6538	-0.5020	

Table 5.6 Comparing the effects of different size distributions on the relationship between average aggregation size and λ (population growth rate), assuming the gender-specific size-at-maturity relationships described in the methods. The three size distributions represent three population histories – SMI (total) is the combined size distribution of the unfished populations at San Miguel Island, OC is a fished population at Ocean Cove in northern California, and HML is the population at Hopkins Marine Laboratory that is subject to sea otter predation. AS_C is the critical aggregation size defined by the point on the curve where the standardized derivative equals one. λ_C is the average population growth rate value for the critical aggregation size. The four parameter estimates and the R^2 value for the function describing the relationship between the average aggregation size ($\bar{x}$) and the average population growth rate ($\bar{\lambda}$) are given in the right-hand columns. μ is the average parameter estimate and L95 and U95 are the lower and upper 95% confidence intervals.

Size Distribution	Average Size (mm)	AS_c-λ (# abalone)	λ_c (yr^{-1})	AS_c-λ=1 (# abalone)	$\bar{\lambda} = ae^{b\bar{x}} + ce^{d\bar{x}}$ Parameter	μ	L95	U95	R^2
SMI	187	2.6	0.9568	13.1	a	0.9922	0.9911	0.9934	0.8898
					b	0.0006	0.0005	0.0007	
					c	-0.5131	-0.5516	-0.4747	
					d	-1.0198	-1.0641	-0.9754	
OC	172	2.5	0.9544	14.1	a	0.9917	0.9907	0.9927	0.8816
					b	0.0006	0.0005	0.0007	
					c	-0.4374	-0.4736	-0.4012	
					d	-1.0096	-1.0573	-0.9619	
HML	100	2.9	0.8792	48.0	a	0.9432	0.9393	0.9471	0.8252
					b	0.0012	0.0010	0.0015	
					c	-0.3020	-0.3248	-0.2792	
					d	-0.5220	-0.5625	-0.4815	

REFERENCES

Alfaro, A.C., R.C. Carpenter (1999) Physical and biological processes influencing zonation patterns of a subtidal population of the marine snail, *Astraea* (*Lithopoma*) *undosa* Wood 1828. *Journal of Experimental Marine Biology & Ecology*, **240**(2), 259-283.

Allee, W.C. (1931). *Animal Aggregations*. The University of Chicago Press, Chicago: 431 pp.

Babcock, R., J. Keesing (1999) Fertilization biology of the abalone *Haliotis laevigata*: Laboratory and field studies. *Canadian Journal of Fisheries & Aquatic Sciences*, **56**(9), 1668-1678.

Babcock, R.C., C.N. Mundy, et al. (1994) Sperm diffusion models and in situ confirmation of long-distance fertilization in the free-spawning asteroid *Acanthaster planci*. *Biological Bulletin*, **186**(1), 17-28.

Benzie, J.A.H., P. Dixon (1994) The effects of sperm concentration, sperm:egg ratio, and gamete age on fertilization success in crown-of-thorns starfish (*Acanthaster planci*) in the laboratory. *Biological Bulletin (Woods Hole)*, **186**(2), 139-152.

California Department of Fish and Game (2002). *Draft Abalone Recovery and Management Plan*. California Department of Fish and Game, Marine Region, Sacramento, CA.

Claereboudt, M. (1999) Fertilization success in spatially distributed populations of benthic free-spawners: A simulation model. *Ecological Modelling* **121**(2-3), 221-233.
Coma, R., H.R. Lasker (1997) Effects of spatial distribution and reproductive biology on in situ fertilization rates of a broadcast-spawning invertebrate. *Biological Bulletin*, **193**(1), 20-29.

Cooper, J., M. Wieland, et al. (1977) Sub tidal abalone populations in an area inhabited by sea otters. *Veliger*, **20**(2), 163-167.

Cox, K. (1962) California abalones, Family Haliotidae. *Fish Bulletin*, **118**, 1-135.

Crouse, D.T., L.B. Crowder, et al. (1987) A stage-based population model for loggerhead sea turtles and implications for conservation. *Ecology*, **68**(5), 1412-1423.

Denny, M., J. Dairiki, et al. (1992) Biological consequences of topography on wave-swept rocky shores 1. Enhancement of external fertilization. *Biological Bulletin*, **183**(2), 220-232.

Denny, M.W., M.F. Shibata (1989) Consequences of surf-zone turbulence for settlement and external fertilization. *American Naturalist*, **134**(6), 859-889.

Dowling, N.A., S.J. Hall, et al. (2004) Assessing population sustainability and response to fishing in terms of aggregation structure for greenlip abalone (*Haliotis laevigata*) fishery management. *Canadian Journal of Fisheries and Aquatic Sciences*, **61**(2), 247-259.

Ebert, T.A. (1998) An analysis of the importance of Allee effects in management of the red sea urchin *Strongylocentrotus franciscanus*. In: R. Mooi & M. Telford (Eds). *Echinoderms: San Francisco*. A. A. Balkema International Publishers, Brookfield, Vermont: 619-627.

Fenberg, P.B., K. Roy (2008) Ecological and evolutionary consequences of size-selective harvesting: how much do we know? *Molecular Ecology*, **17**(1), 209-220.

Gotelli, N.J. (1991) Demographic models for *Leptogorgia virgulata*, a shallow-water gorgonian. *Ecology*, **72**(2), 457-467.

Haaker, P.L., D.O. Parker, et al. (1998) Growth of red abalone, *Haliotis rufescens* (Swainson), at Johnsons Lee, Santa Rosa Island, California. *Journal of Shellfish Research*, **17**(3), 747-753.

Heppell, S.S., H. Caswell, et al. (2000) Life histories and elasticity patterns: Perturbation analysis for species with minimal demographic data. *Ecology*, **81**(3), 654-665.

Hines, A.H., J.S. Pearse (1982) Abalones shells and sea otters: Dynamics of prey populations in central California USA. *Ecology*, **63**(5), 1547-1560.

Hobday, A.J., M.J. Tegner (2002) The warm and the cold: Influence of temperature and fishing on local population dynamics of red abalone. *California Cooperative Oceanic Fisheries Investigations Reports*, **43**, 74-95.

Hobday, A.J., M.J. Tegner, et al. (2001) Over-exploitation of a broadcast spawning marine invertebrate: Decline of the white abalone. *Reviews in Fish Biology and Fisheries*, **10**(4), 493-514.

Karpov, K.A., P.L. Haaker, et al. (1998) The red abalone, *Haliotis rufescens*, in California: Importance of depth refuge to abalone management. *Journal of Shellfish Research*, **17**(3), 863-870.

Karpov, K.A., P.L. Haaker, et al. (2000) Serial depletion and the collapse of the California abalone (*Haliotis* spp.) fishery. *Canadian Special Publication of Fisheries & Aquatic Sciences*, **130**, 11-24.

Leaf, R.T., L. Rogers-Bennett, et al. (2007) Spatial, temporal, and size-specific variation in mortality estimates of red abalone, *Haliotis rufescens*, from mark-recapture data in California. *Fisheries Research (Amsterdam)*, **83**(2-3), 341-350.

Levitan, D.R. (1991) Influence of body size and population density on fertilization success and reproductive output in a free-spawning invertebrate. *Biological Bulletin (Woods Hole)*, **181**(2), 261-268.

Levitan, D.R., M.A. Sewell, et al. (1992) How distribution and abundance influence fertilization success in the sea urchin *Strongylocentrotus franciscanus*. *Ecology*, **73**(1), 248-254.

Levitan, D.R., C.M. Young (1995) Reproductive success in large populations - Empirical measures and theoretical predictions of fertilization in the sea biscuit *Clypeaster rosaceus*. *Journal of Experimental Marine Biology and Ecology*, **190**(2), 221-241.

Lillie, F.R. (1915) Studies of Fertilization. VII. Analysis of variations in the fertilizing power of sperm suspensions of Arbacia. *Biological Bulletin*, **28**(4), 229-251.

Manly, B.F.J. (1997). *Randomization, bootstrap, and Monte Carlo methods in biology*. Chapman & Hall, London; New York.

McShane, P.E. (1996) Patch dynamics and effects of exploitation on abalone (*Haliotis iris*) populations. *Fisheries Research (Amsterdam)*, **25**(2), 191-199.

Metaxas, A., R.E. Scheibling, et al. (2002) Estimating fertilization success in marine benthic invertebrates: A case study with the tropical sea star *Oreaster reticulatus*. *Marine Ecology Progress Series*, **226**, 87-101.

Micheli, F., A.O. Shelton, et al. (2008) Persistence of depleted abalones in marine reserves of central California. *Biological Conservation*, **141**(4), 1078-1090.

Morris, W.F., D. Doak (2002). *Quantitative conservation biology: Theory and practice of population viability analysis*. Sinauer Associates, Inc., Sunderland, Massachusetts: 480 pp.

Myers, R.H., D.C. Montgomery, et al. (2002). *Generalized linear models : with applications in engineering and the sciences*. J. Wiley, New York.

Pennington, J.T. (1985) The ecology of fertilization of echinoid eggs: The consequences of sperm dilution, adult aggregation, and synchronous spawning. *Biological Bulletin (Woods Hole)*, **169**(2), 417-430.

Prince, J.D., T.L. Sellers, et al. (1988) Confirmation of a relationship between the localized abundance of breeding stock and recruitment for *Haliotis rubra* Leach Mollusca Gastropoda. *Journal of Experimental Marine Biology & Ecology*, **122**(2), 91-104.

Riffell, J.A. (2005) Establishing the biological and chemical processes regulating fertilization success in the red abalone, *Haliotis rufescens*. *Biology*. University of California, Los Angeles: 130.

Riffell, J.A., P.J. Krug, et al. (2004) The ecological and evolutionary consequences of sperm chemoattraction. *Proceedings of the National Academy of Sciences of the United States of America*, **101**(13), 4501-4506.

Rogers-Bennett, L., R.F. Dondanville, et al. (2004) Size specific fecundity of red abalone (*Haliotis rufescens*): Evidence for reproductive senescence? *Journal of Shellfish Research*, **23**(2), 553-560.

Rogers-Bennett, L., R.T. Leaf (2006) Elasticity analyses of size-based red and white abalone matrix models: Management and conservation. *Ecological Applications*, **16**(1), 213-224.

Rogers-Bennett, L., D.W. Rogers, et al. (2007) Modeling growth and mortality of red abalone (Haliotis rufescens) in Northern California. *Journal of Shellfish Research*, **26**(3), 719-727.

Shepherd, S.A. (1986) Studies on southern Australian abalone (Genus *Haliotis*) VII. Aggregative behavior of *Haliotis laevigata* in relation to spawning. *Marine Biology (Berlin)*, **90**(2), 231-236.

Shepherd, S.A., L.D. Brown (1993) What is an abalone stock: Implications for the role of refugia in conservation. *Canadian Journal of Fisheries & Aquatic Sciences*, **50**(9), 2001-2009.

Stokes, K., R. Law (2000) Fishing as an evolutionary force. *Marine Ecology Progress Series*, **208**, 307-309.

Tegner, M.J. (1993) Southern California abalones: Can stocks be rebuilt using marine harvest refugia? *Canadian Journal of Fisheries & Aquatic Sciences*, **50**(9), 2010-2018.

Tegner, M.J., P.K. Dayton (1999) Ecosystem effects of fishing. *International Council for the Exploration of the Sea; Scientific Committee for Oceanic Research*, **14(7)**, 261-262.

Tomascik, T., H. Holmes (2003) Distribution and abundance of *Haliotis kamtschatkana* in relation to habitat, competitors and predators in the Broken Group Islands, Pacific RIM National Park reserve of Canada. *Journal of Shellfish Research*, **22**(3), 831-838.

Vilchis, L.I., M.J. Tegner, et al. (2005) Ocean warming effects on growth, reproduction, and survivorship of Southern California abalone. *Ecological Applications*, **15**(2), 469-480.

CHAPTER 6.

Conclusions of the Dissertation

The work presented in this dissertation provides a combination of empirical and theoretical evidence describing the potential Allee effects influencing low-density populations of abalone and other benthic broadcast-spawning gastropods. The density-dependence of aggregation-level characteristics in the population initiates threshold behavior in the fertilization dynamics of low-density populations. The incorporation of aggregation-influenced fecundities into a demographic matrix model results in rapidly reduced population growth rates below a threshold aggregation size. These findings highlight the importance of continued monitoring of aggregation characteristics for both high- and low-density populations.

DENSITY-DEPENDENT FERTILIZATION SUCCESS

Per capita fecundity in broadcast-spawning species may be influenced by density-dependent aggregation characteristics regulating fertilization success rates. Nearest-neighbor distances are related to the density of the population by a negative power function such that distances increase rapidly below a threshold density (*Chapters 2 and 5*). Because fertilization success is related to the distance between spawning individuals by a negative exponential function (Babcock and Keesing 1999), the threshold effect of density on fertilization success is amplified. In addition, the probability of creating a mixed-gender aggregation in a population is partially related to the aggregation size by a two-part exponential function, such that the probability of mating decreases rapidly below a threshold aggregation size (*Chapters 2 and 5*).

DEMOGRAPHIC MATRIX MODEL

The matrix model described for the pink and red abalone populations (*Chapters 4 and 5*) provides an option for incorporating density-dependent fecundity in order to consider the potential Allee effect of reduced fertilization success on population growth rates at low population densities. By exploring the effect of a broad range of aggregation-influenced fecundities on the population growth rate, an estimate of the critical aggregation size may be obtained. The critical aggregation size for the population may be further influenced by the size distribution in the population and by the size-at-maturity probability function. Critical aggregation sizes used for managing a resource should consider the probability of obtaining a λ estimate greater than one given the variability in bootstrap results.

LONG-TERM MONITORING

Long-term monitoring of fished populations is important for defining the historic characteristics of a population and also to assess the trajectory of the population through time. For species that rely on aggregative behavior to persist at low densities, monitoring programs should also incorporate surveys of aggregation characteristics in order to establish management or recovery goals. In Chapter 2, I examined methods of measuring aggregation-level characteristics for monitoring both high- and low-density populations of benthic broadcast-spawning invertebrates. Neither of the distance-based methods of estimating density performed well in the high-density populations which also had higher levels of aggregation. A combination of transect- and distance-based surveys may prove to be the most informative option over time for aggregating species. The two survey methods are complementary to each other in terms of the amount of effort required to

accomplish each at different levels of population densities. By combining the two survey methods, a greater diversity of data may be obtained for the population with very little change in the effort over time as the population density changes. Only the allocation of the effort between the two methods will change. Both methods are also easily learned and executed by volunteers, as demonstrated by the diverse backgrounds of the surveyors participating in these surveys.

LOCALIZED MANAGEMENT

If populations of abalone in California are largely self-recruiting, then regional-scale management guidelines may be inappropriate. Because red abalone are subjected to very different fishing and predation pressures throughout their broad latitudinal range, the adult survival rates vary widely among populations (Leaf, Rogers-Bennett et al. 2007). Long-term reductions in adult survival, such as at Hopkins Marine Reserve, may select for slower-growing or earlier-maturing individuals in the population. The shape of the individual size-frequency distributions also differs among populations according to the influence of fishing or predation pressures (*see Chapter 5*). Additionally, environmental variables such as temperature and food quality can influence the number of eggs produced by a female abalone (Vilchis, Tegner et al. 2005). All of the demographic characteristics described above influence the predicted population growth rates and critical aggregation sizes for the populations. Establishing localized management guidelines would help to address the potentially different dynamics of these populations.

The localized management strategies may also need to adapt as demographic characteristics change through time. As management regulations change, or as the sea otter population continues to expand, individual size-frequency distributions within a

population may change dramatically. In addition, ocean temperatures may change, as a result of either global climate change or long-period regime shifts, which will influence the vital rates of individuals within the population (Vilchis, Tegner et al. 2005). The potential interaction between fishery management regulations and the increased susceptibility of individuals to withering foot syndrome in warmer temperatures should also be considered (Harley and Rogers-Bennett 2004). The potential for temporal variability in the demography of a population re-emphasizes the need for long-term monitoring of these populations.

RECRUITMENT VARIABILITY

The population models used in these studies assume that there is no external larval supply or variability in the recruitment success through time. The likelihood of external larval input to the population depends, in large part, on the distribution and abundance of the surrounding populations, the speed and direction of the current flow at the time of spawning, and the vertical migratory behavior of the larvae relative to the current flow (Sulkin 1984; Shepherd and Brown 1993; Levin 2006). Temporal variation in the abundance of predators may also influence the annual input of larvae to the population (Cushing 1974; Platt, Fuentes-Yaco et al. 2003).

ABALONE AGGREGATING BEHAVIOR

Little is currently known about abalone aggregating behavior as it relates to spawning events. Results from previous tag-recapture studies suggest that adults generally maintain a "home scar" on a particular rock or ledge, whereas juveniles travel longer distances (Clavier and Richard 1982; Blecha, Steinbeck et al. 1992; Dixon, Gorfine et al. 1998). Although very few abalone are seen travelling during the day,

anecdotal evidence indicates that individuals may engage in night-time foraging behaviors. Studies that only re-visit tagged animals during daylight hours may underestimate the home range of the abalone. In addition, aggregative behavior may increase during specific times of the year or the day, corresponding to spawning events (Breen and Adkins 1980). The intermittent view of abalone behavior obtained by traditional tag-recapture methods may be insufficient to detect rare behaviors associated with spawning events.

Thus, the aggregation-level characteristics measured during the my surveys may not represent the aggregation sizes or nearest-neighbor distances at the time of spawning. In addition, the relevant physical flow characteristics influencing fertilization dynamics at the time of spawning for the study species are unknown because of the lack of field data on natural spawning events. These are important issues that should be addressed by future research efforts before the growth and recovery potentials of the California abalone populations may be predicted. However, the limitations of the model assumptions do not detract from the overall conclusions of this research regarding the importance of aggregation characteristics to the low-density population dynamics of benthic broadcast-spawning gastropods. The results of the present work emphasize the critical need to consider aggregation characteristics in population models for species such as abalone that rely on aggregations for successful reproduction. In order to improve these population models and to compare future conditions of the populations with the present conditions, continued monitoring of aggregation characteristics is necessary.

REFERENCES

Babcock, R., J. Keesing (1999) Fertilization biology of the abalone *Haliotis laevigata*: Laboratory and field studies. *Canadian Journal of Fisheries & Aquatic Sciences*, **56**(9), 1668-1678.

Blecha, J.B., J.R. Steinbeck, et al. (1992) Aspects of the biology of the black abalone (*Haliotis cracherodii*) near Diablo Canyon, central California. In: S.A. Shepherd, M.J. Tegner & S.A. Guzman del Proo (Eds). *Abalone of the world: Biology, fisheries and culture*: 225-236.

Breen, P.A., B.E. Adkins (1980) Spawning in a British Columbia, Canada Population of Northern Abalone *Haliotis kamtschatkana*. *Veliger*, **23**(2), 177-179.

Clavier, J., O. Richard (1982) Experimental study of the movements of the ormer (*Haliotis tuberculata*) in nature. *Revue des Travaux de l'Institut des Pêches Maritimes*, **46**, 315-326.

Cushing, D.H. (1974) The natural regulation of fish populations. In: F.R. Harden Jones (Ed). *Sea fisheries research*. Paul Elek, London: 399-412.

Dixon, C.D., H.K. Gorfine, et al. (1998) Dispersal of tagged blacklip abalone, *Haliotis rubra*: Implications for stock assessment. *Journal of Shellfish Research*, **17**(3), 881-887.

Harley, C.D.G., L. Rogers-Bennett (2004) The potential synergistic effects of climate change and fishing pressure on exploited invertebrates on rocky intertidal shores. *California Cooperative Oceanic Fisheries Investigations Reports*, **45**, 98-110.

Leaf, R.T., L. Rogers-Bennett, et al. (2007) Spatial, temporal, and size-specific variation in mortality estimates of red abalone, *Haliotis rufescens*, from mark-recapture data in California. *Fisheries Research (Amsterdam)*, **83**(2-3), 341-350.

Levin, L.A. (2006) Recent progress in understanding larval dispersal: new directions and digressions. *Integrative and Comparative Biology*, **46**(3), 282-297.

Platt, T., C. Fuentes-Yaco, et al. (2003) Spring algal bloom and larval fish survival. *Nature*, **423**(6938), 398-399.

Shepherd, S.A., L.D. Brown (1993) What is an abalone stock: Implications for the role of refugia in conservation. *Canadian Journal of Fisheries & Aquatic Sciences*, **50**(9), 2001-2009.

Sulkin, S.D. (1984) Behavioral basis of depth regulation in the larvae of brachyuran crabs. *Marine Ecology Progress Series*, **15**(1-2), 181-206.

Vilchis, L.I., M.J. Tegner, et al. (2005) Ocean warming effects on growth, reproduction, and survivorship of Southern California abalone. *Ecological Applications*, **15**(2), 469-480.